CORRELATION OF GEOTECHNICAL PROPERTIES OF LIMESTONE WITH ULTRASONIC VELOCITY IN GAZİANTEP REGION

M.Sc. Thesis

in

Civil Engineering

University of Gaziantep

Supervisor

Assist. Prof. Dr. Hamza GÜLLÜ

By

Levent MARANGOZ

July 2005

ACKNOWLEDGEMENTS

I express my sincere appreciation to my superviser Assist. Prof. Dr. Hamza GÜLLÜ for his guidance and suggestions during the preparation of this thesis. My special thanks are extend to Assist. Prof. Dr. Hanifi ÇANAKCI for his support and his suggestions.

I especially thank my friend Teoman ERŞAN for his self-sacrificing, support and suggestions.

Thanks also go to my mother, my father, my sister for their endurance, reassurance and support.

ABSTRACT

CORRELATION OF GEOTECHNICAL PROPERTIES OF LIMESTONE WITH ULTRASONIC VELOCITY IN GAZİANTEP REGION

MARANGOZ, Levent

M.Sc. in Civil Eng.

Supervisor: Assist. Prof. Dr. Hamza GÜLLÜ

July 2005, 111 pages

Many engineering structures have recently been constructed on rock such as limestone around the world. Their properties and behaviour under different conditions are, however, not so well understood as those of other rocks or soils. It is necessary to study detailed testing programs on limestones and experimental data must be evaluated with engineering judgment. The aim of this thesis is to determine physical and mechanical properties of Gaziantep limestone. For this exactly 245 samples of limestone from different areas of Gaziantep were colleted and used in experiments. Ultrasonic Velocity, Brazillian Tensile, Direct Shear, Uniaxial Compressive Tests were performed and index properties such as dry-bulk-saturated densities, water absorbtion were determined on selected specimens in laboratory conditions. The tests were made according to International Society for Rock Mechanics ISRM (1981). The estimated ultrasonic velocity values were also correlated against the physical and mechanical properties of the Gaziantep limestone and a linear correlation coefficient ($R^2 \approx 0.85$) was obtained.

Key words: limestone, ultrasonic velocity, Brazillian tensile test, direct shear test, uniaxial compressive test.

ÖZET

GAZİANTEP BÖLGESİNDEKİ KİREÇTAŞLARININ GEOTEKNİK ÖZELLİKLERİYLE SONİK HIZ ARASINDA İLİŞKİNİN KURULMASI

MARANGOZ, Levent
Yüksek Lisans Tezi, İnş. Müh. Bölümü
Tez Yöneticisi: Yrd. Doç. Dr. Hamza GÜLLÜ
Temmuz 2005, 111 Sayfa

Dünyanın her tarafında birçok mühendislik yapıları son zamanlarda kireçtaşı gibi kayalar üzerine inşa edilmeye başlanmıştır. Bu kayaların değişik şartlardaki özellikleri ve davranışları diğer kayalar kadar bilinmemektedir. Bu bağlamda; kireçtaşlarının detaylı test dataları ve deney sonuçlarının mühendislik bakış açısıyla değerlendirilmesi kaçınılmazdır. Bu tezin amacı Gaziantep kireçtaşının fiziksel ve mekanik özelliklerinin belirlenmesidir. Bu amaçla Gaziantep'in değişik alanlarından toplanan 245 numune deneyler için kullanılmıştır. Laboratuar koşullarında, seçilen numuneler üzerinde sonik hız, Brazil çekme, direkt kesme, tek eksenli basınç testleri ve kuru, ıslak yoğunluklar, su emme gibi indeks özellikler tespit edildi. Tüm deneyler uluslararası kaya mekaniği deney standardı ISRM(1981)' ye uygun olarak yapılmıştır. Gaziantep kireçtaşının sonic hızı ile fiziksel ve mekanik özellikleri lineer korelasyonla ilişkilendirildiğinde korelasyon katsayısı ($R^2 \approx 0.85$) olarak elde edilmiştir.

Anahtar kelimeler: kireçtaşı, sonik hız, brazil çekme deneyi, direkt kesme deneyi, tek eksenli basınç deneyi.

TABLE OF CONTENTS

Page

LIST OF FIGURES

LIST OF SYMBOLS

Brz. = Brazillian tensile strength calculated with force divided by original area

$Brz.^{*}$ = Brazillian tensile strength calculated with force divided by fractured area

D. M. = Dry mass

Diam. = Diameter

L = Length

l_o = Original measured axial length

M_{sub} = Submerged mass of sample

M_{sat} = Saturated mass of sample

M_s = Dry mass of sample

N = Normal force

S. S. M. = Saturated – submerged – mass

S. S. D. M.= Saturated – surface – dried – mass

T = Shear force

Thick. = Thickness

Uni. Comp. Str. = Uniaxial Compressive Strength

V_p = Velocity of the longitudinal wave

V_s = Velocity of the shear wave

W_{abs} = Water absorbtion

Δ L = Change in measured axial length

LIST OF TABLES

CHAPTER 1

INTRODUCTION

1.1.General

Gaziantep limestone contains clayey limestone and chalky limestone. Clayey limestone is whitish, grey cream, dirty yellow colored and middle thin layered. Also it contains some cherts. Chalky limestone is grey, yellowish grey colored, middle thick layered. In some areas it contains fossils[1]. Limestone is used in road and building construction, as an agricultural fertiliser and in various industrial applications. It is an important building stone used as dimension stone, or more commonly as crushed stone, or aggregate, for general building purposes, roadbeds and railway track ballast. As dimension stone, its relatively soft nature is advantageous for decorative carving.

Limestones exsists in many parts of the Gaziantep. It was used as the major construction material for many years untill the arrival of concrete systems. Limestone is used as a construction material in urban areas. The chemical formula of limestone is $CaCO_3$. Limestone ores can be found in sedimentary and metamorphic rocks[1].

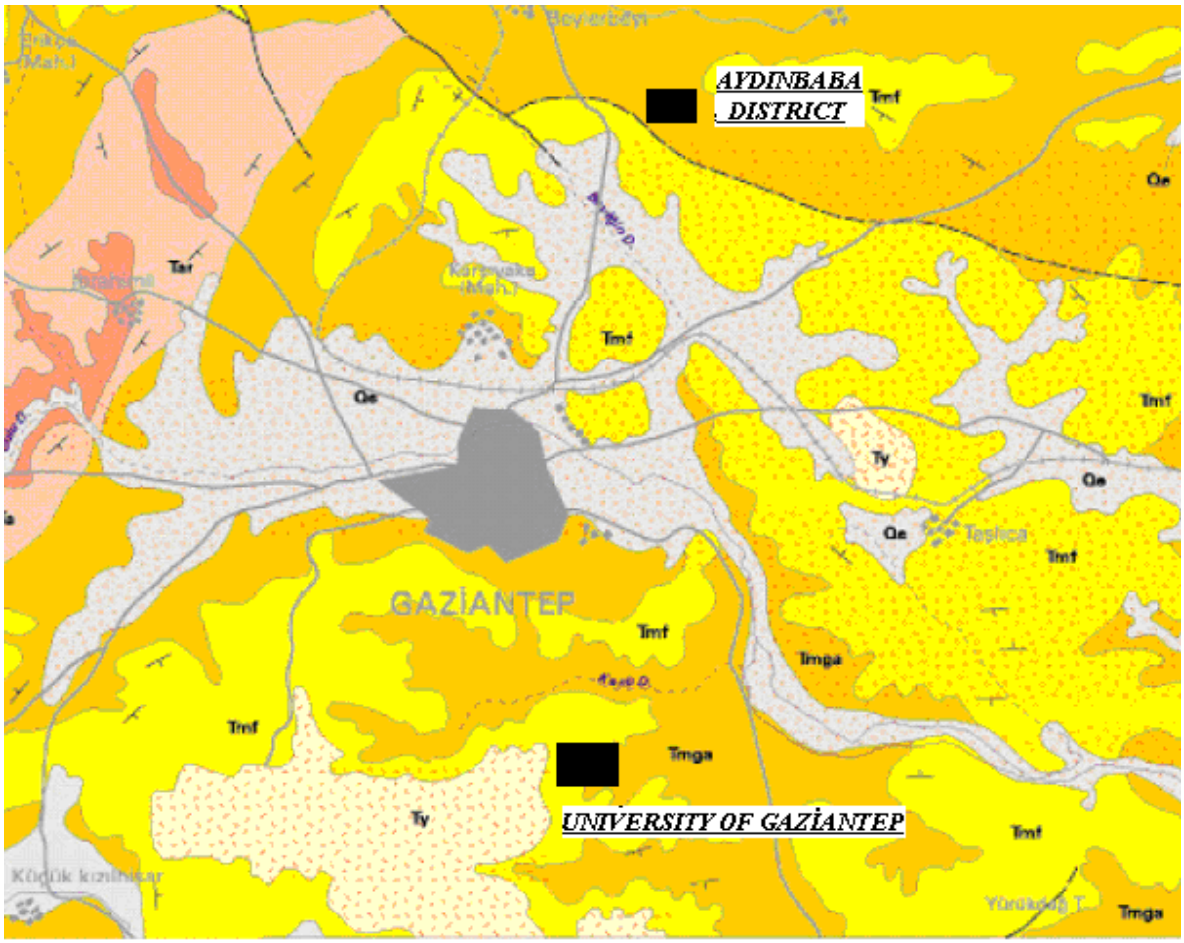

Figure 1.1a. Geologic map of the Gaziantep [54].

This thesis contains a regional study. Study was done in Gaziantep region. Figure 1.1a shows the geologic map of the Gaziantep and Figure 1.1b shows the description of map units. In this region a study like in this thesis has not done before. All experiments have one repetition number.

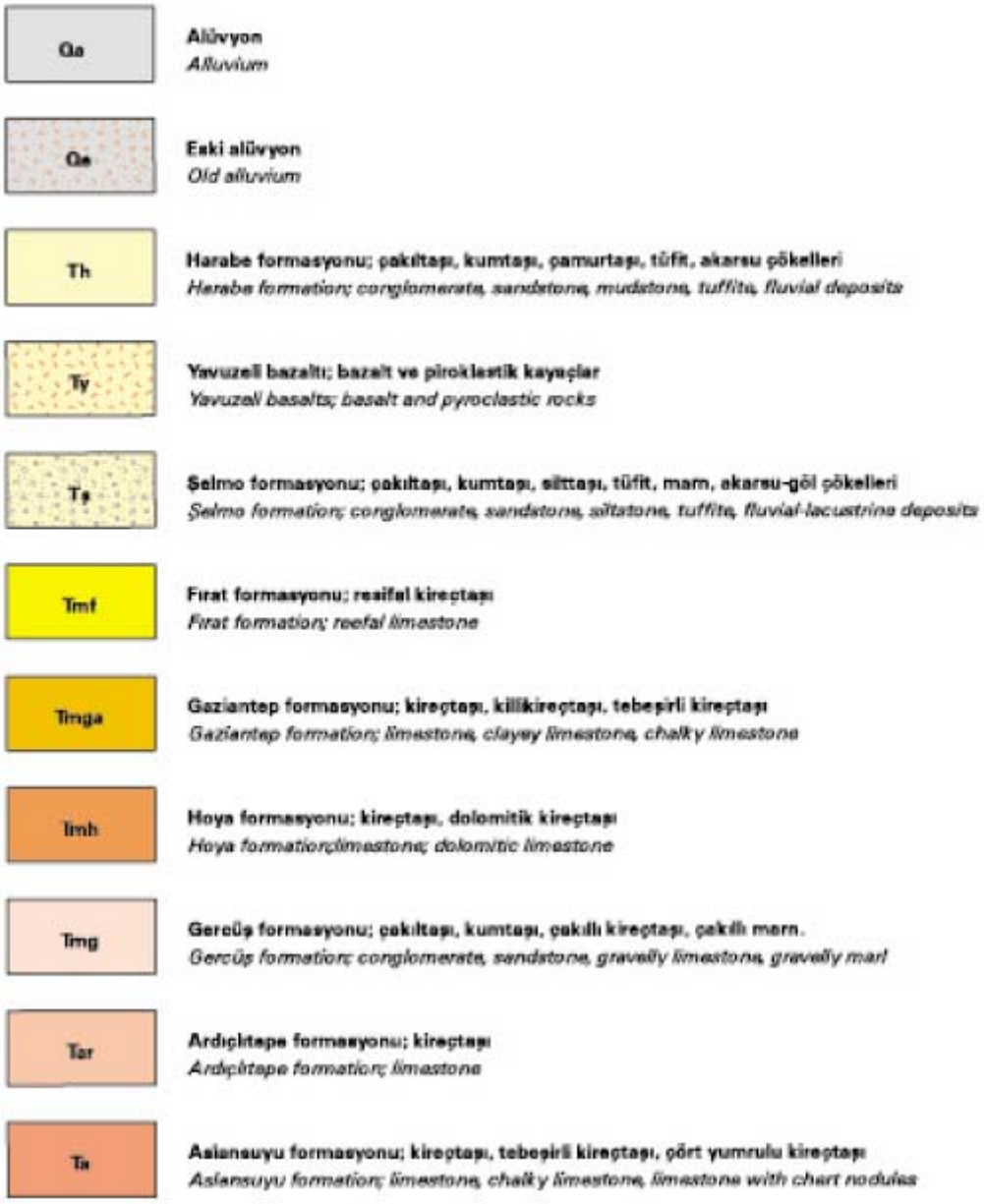

Figure 1.1b. Legend.[54].

The study aims to investigate the physical and mechanical properties of limestone present in Gaziantep with rock mechanics tests to correlate rock properties of limestones with ultrasonic velocity in Gaziantep region. This is done for evaluating the mechanical and physical properties of rock using nondestructive method (ultrasonic velocity test.). Because ultrasonic test machine is portable and rechargeable. Ultrasonic test equipment can be used everywhere you want. It can be achieved many physical and mechanical properties of rock only performing the ultrasonic velocity test to calculate the sonic velocity of the specimen easily. Because it is very easy to calculate the sonic velocity of the specimen.

Exactly 245 samples taken from Aydınbaba street, its neighborhood and University of Gaziantep Campus were used to determine the rock properties of limestone.

The experiments conducted are as follows:

Index properties :

- Dry and saturated densities
- Water absorption

Mechanical or strength properties :

- Ultrasonic velocity
- Uniaxial compressive
- Indirect tensile (Brazillian Test)
- Direct shear

1.2. Organization of The Thesis

The thesis is divided into 6 chapters, which are arranged as follows;

A literature review of the general properties of limestone is given in chapter 2.

In chapter 3, experimental studies are defined.

Chapter 4 includes the test results and correlations.

Chapter 5 includes the discussion.

Chapter 6 contains the conclusions drawn from this research work and the recommendations for future study are given.

CHAPTER 2

LITERATURE SURVEY

2.1. Introduction

Limestone is a extrusive sedimentary rock. In this section a general information is given about sedimentary rocks and limestone. Additionally preceding studies are have a part in.

2.2. Sedimentary Rocks

Sediments from a relatively thin surface layer of the earth's crust, covering the underlying igneous and metamorphic rocks.

This sedimentary cover is discontinuous and of varying thickness; it averages about 0.8 km in thickness but locally reaches over 12 km in long narrow belts, the sites of former geosynclines. It has been estimated that sediments constitute only about 5 per cent of the crustal rocks (to a depth of 16 km), in which the proportions of the three main types are approximately: shales and clays, 4 per cent; sandstones, 0.75 per cent; limestones, 0.25 per cent. Sedimentary rocks also include varieties which are composed of the remains of organisms, such as certain limestones and coals, and others which are formed by chemical deposition [9].

Accumulations of loose sand, for example, derived from the breakdown of older rocks in ways described earlier, and brought together and sorted by water and wind, have become hardened rocks such as sandstone and quartzite. Pore spaces in the original sands have been partly or completely filled with mineral matter brought by percolating water and deposited as coatings on the sand grains, thus acting as a

cement to bind them together. These processes are known as cementation. In muddy sediments, the very small particles of silt and clay of which they are mainly composed have been pressed together by the weight of sediment; interstitial water has been squeezed out and in course of time the mud has become a coherent mass of clay,shale,ormudstone.

Compaction of this kind of affects the muddy sediments to a greater degree than the sands, and during the compaction process much of the pore-contained water in an original mud is pressed out. Some of the water, with its dissolved salts, may remain in the sediment after its compaction, and is known as connate water. The general term diagenesis is used to denote the compaction of a sediment into a sedimentary rock, and includes the processes outlined above and also chemical processes such as re-crystallization and replacement.

When rock come again into the zone of weathering, after a long history, soluble substances are removed and insoluble matter is released, to begin a new cycle of sedimentation in rivers and the sea. The broad groupings used in the Table of Sedimentary Rocks are:

1) Detrital sediments(mechanically sorted), e.g. gravels, sandstones, clays and shales.

2) Chemical, and biochemical (organic), e.g. limestones,coals,centimeter [9].

2.3. Limestone

Limestones consist essentially of calcium carbonate, with which there is generally some magnesium carbonate, and siliceous matter such as quartz grains. The average of over 300 chemical analyses of limestones showed 92 per cent of $CaCO_3$ and $MgCO_3$ together, and 5 per cent of SiO_2 ; the proportion of magnesium carbonate is small except in dolomite and dolomitic limestones. Limestones are bedded rocks often containing many fossils; they are readily scratched with a knife, and effervesce on the addition of cold dilute hydrochloric acid. The distance between bedding-

planes in limestones is commonly 30 to 60 cm, but varies from a couple of centimeters or less in thin-bedded rocks to over 6 cm in some limestones [9].

Calcium carbonate is present in the from of crystals of calcite or aragonite, as amorphous calcium carbonate, and also as the hard parts of organisms(fossils) such as shells and calcareous skeletons, or their broken fragments. Thus, a consolidated shell-sand is a limestone by virtue of the calcium carbonate of which the shells are made. On the other hand, chemically deposited calcium carbonate builds limestones under conditions where water of high alkalinity has a restricted circulation, as in a shallow sea or lake. Non-calcareous constituents commonly present in limestones include clay, silica in colloidal from or as quartz grains or as parts of siliceous organisms, and other hard detrital grains. Though usually grey or white in colour, the rock may be tinted, e.g. by iron compounds or finely divided carbon, or by bitumen. The types listed in the table are now described [9].

Chalk is a soft white limestone largely made of finely divided calcium carbonate, much of which has been shown to consist of minute plates, 1 or 2 microns in diameter. These plates are derived from the external skeletons of calcareous algae, and are known as coccoliths. The Chalk also contains many foraminifera, which differ in king and abundance in different part of the formation; and other fossils, such as the shells of brachiopods and sea-urchins. The foraminifera are minute, very primitive jelly-like organisms (protozoa) with a hard globular covering of carbonate of lime; they float at the surface of the sea during life, and then sink and accumulate on the sea floor. Radiolaria are similar organisms which have siliceous frameworks, often of a complicated and beautiful pattern; these too are found in Chalk but are not so numerous as the foraminifera. Parts of the rock contain about 98 per cent $CaCO_3$ and it is thus almost a pure carbonate rock. It was probably formed at moderate depths (round about 180m) in clear water on the continental shelf [9].

2.4. Preceding Studies About Limestone

- Thermal decomposition study of crystalline limestone using P-wave velocity. [27].
- Surface strength and mineralogy of weathering crusts on limestone buildings in Budapest [48].
- Pore properties as indicators of breakdown mechanisms ın experimentally weathered limestones. [35].
- Physical deterioration of sedimentary rocks subjected to experimental freeze thaw weathering. [36].
- Design of anchorage and assessment of the stability of openings in silty, sandy limestone a case study in Turkey. [30].
- Pulse Velocity of Clay Shale and Limestone. [49].
- A correlation between P-wave velocity, number of joints and Schmidt hammer rebound number.[26].
- Determination of the elastic modulus set of foliated rocks from ultrasonic velocity measurements.[46].
- Empirical methods to estimate the strength of jointed rock masses.[43].
- Estimating the deformation modulus of rock masses: a comparative study.[28].
- Models to predict the uniaxial compressive strength and the modulus of elasticity for Ankara Agglomerate.[47].

CHAPTER 3

EXPERIMENTAL STUDY

3.1. Introduction

The experimental work is directed mainly towards an determination of rock properties of limestone and correlation of rock properties of limestone with ultrasonic velocity.

First the following physical properties are calculated :

- Dry density
- Saturated density
- Bulk density
- Water absorption

After calculating the main index properties the following tests are performed:

- Ultrasonic velocity
- Brazillian indirect tensile strength
- Uniaxial compressive strength
- Shear strength

All this tests were performed according to ISRM(1981).

3.1.1. Equipments

Specimens are obtained from the collected rocks using the core machine and drilling machine(see in figure 3.1a,3.1b). All tests were performed in the geotechnical laboratory of civil engineering department of university of Gaziantep. This laboratory have many specific apparatus for different goals. Some of them were used during the thesis. These are;

1. Brazillian test apparatus : The critical dimensions of the apparatus are the radius of the curvature of the jaws, the clearance and length of the guide pins coupling the two curved jaws and the width of the jaws. These are as follows: Radius of jaws – 1.5 × specimen radius; guide pin clearance – permit rotation of one jaws relative to the other by 4×10^{-3} rad out of plane of the apparatus (25 mm penetration of guide pin with 0.1 mm clearance); width of jaws – 1.1 × specimen thickness. The upper jaw contains a spherical seating conveniently formed by a 25-mm diameter half – ball bearing [8].

2. Uniaxial test machine : The auto test range of concrete and mortar compression testing machine is 3000 kN capacity and has been designed for consistent, reliable testing. The automatic cycle enables high throughput of samples making this machine particularly suitable for central or commercial testing organizations. Technical Features of the machines are:
   - Overall dimensions ……length * width * height
     Compression frame ……..590 * 510 * 1215 mm
   - Console ……520 * 430 * 1215 mm
   - Max. Vertical Clearance ……340 mm
   - Max. Vertical Clearance (block tester) ……...260 mm
   - Max. Horizontal Clearance ……310 mm
   - Maximum ram travel ……50 mm
   - Approx. Weight of Console ……..145 kg
   - Approx. Weight of Compressive frame ……1270 kg
   - Approx. Weight of compressive frame for Block Teste……..1370 kg

3. Direct Shear test machine (MATEST COMPANY):

- Length…….. 770mm
- Width …….. 235mm
- Height ……..615mm
- Mass ……46kg
- max. load ……50 kN
- Allowed temperature ……. from -10 Cº to + 80 Cº
- Allowed humidity ……..……. from 30% to %95%
- max. height over sea level ……1000m.

Calibration: The machine is controlled and calibration by the manufacturer, using sampling tools, which are periodically checked by Official Institutions. A copy of the Calibration Certificate is delivered together with this literature. The gauges for pressure measurement should normally work without any maintenance. Anyway the calibration of every gauge should be checked periodically. This procedure can be done by using a dead weight pressure tester or any similar instrument which could induce in the gauge a known hydraulic pressure. The value got by the gauge should then be compared with the one corresponding to the given pressure**.** In case the gauge is out of range, damage, out of calibration or doesn't return to zero at pressure release, we recommend its replacement.

4. Ultrasonic Velocity test machine : The Ultrasonic tester model C 368 is an instrument to measure material characteristics by using ultrasonic pulses. Technical features of the machine are:

- Maximum measurable time ……..9999 microsec.
- Resolution ……..0,16 microsec.
- Accuracy ……...-/+0,16 microsec.
- Feeding ……12 Volt D.C.
- Consumption ...……...0,30 A
- Autonomy ……...5 h with battery 12 V 1,9 Ah

Figure 3.1a. The core machine

Figure 3.1b. The drilling machine

3.2. Determination of Index Properties

Determination of index properties were done according to ISRM(1981). Exactly 245 of limestone samples index properties were determined this thesis.

3.2.1.Suggested method for density-water absorption and porositydetermination using saturation and buoyancy techniques

3.2.1.1. Scope

(a) The test is intended to measure the dry density and related properties of a rock sample in the from of lumps or aggregate of irregular geometry. It may also be applied to a sample in the from of specimens of regular geometry.

(b) The method should only be used for rocks that do not appreciably swell or disintegrate when oven dried and immersed in water [8].

3.2.1.2. Apparatus

(a) An oven capable of maintaining a temperature of 105 ^{o}C to within 3^{o}C for a period of at least 24 hr.

(b) A sample container of non-corrodible material, including an air-tight lid.

(c) A desiccator to hold sample containers during cooling.

(d) Vacuum saturation equipment such that the sample can be immersed in water under a vacuum of less than 800 Pa (6 torr) for a period of at least one hour.

(e) A balance of adequate capacity, capable of determining the mass of specimen to an accuracy of 0.01%.

(f) An immersion bath and a wire basket or perforated container, such that the sample immersed in water can be freely suspended from the stirrup of the balance to determine the saturated-submerged mass. The basket should be suspended from the balance by a fine wire so that only the wire intersects the water surface in the immersion bath.

3.2.1.3. Procedure

(a) A representative sample comprising at least 10 lumps of regular or irregular geometry, each having either a mass of at least 50g or a minimum dimension of at least 10 times the maximum grain size, whichever is the greater, is selected. The sample is washed in water to remove dust.

(b) The sample is saturated by water immersion in a vacuum of less than 800 Pa (6 torr) for a period of at least one hour, with periodic agitation to remove trapped air.

(c) The sample is then transferred under water to the basket in the immersion bath shown in figure 3.2. Its saturated-submerged mass M_{sub} is determined to an accuracy of 0.1 g from the difference between the saturated-submerged mass of the basket plus sample and that of the basket alone.

Figure 3.2. An apparatus used for calculating the volume
by using the archimed's law

(d) The sample is removed from the immersion bath and surface-dried with a moist cloth, care being taken to remove only surface water and to ensure that no rock fragments are lost. The mass M_{sat} of saturated-surface-dry sample determined.

(e) The sample dried to constant mass at a temperature of 105 ^{o}C then the sample allowed to cool for 30 min in a desiccator. The mass M_s of oven-dry sample is measured. An apparatus is shown in figure 3.3.

(f) V_v volume of voids can be determined by the subtraction dry mass from the saturated mass dry. V_d is a dimensional volume which is obtained from multiplying the dimensions each other.

Figure 3.3. A balance of adequate capacity, capable of determining the mass of specimen to an accuracy of 0.01%.

3.2.1.4. Calculations

- Saturated-surface dry mass M_{sat}
- Grain weight M_s
- Bulk volume $$V = \frac{M_{sat} - M_{sub}}{\rho_w} \quad (3.1)$$
- Pore volume $$V = \frac{M_{sat} - M_s}{\rho_w} \quad (3.2)$$
- Dry density $$\rho_d = \frac{M_s}{V} \quad (3.3)$$
- Saturated density $$\rho_{sat} = \frac{M_{sat}}{V} \quad (3.4)$$
- Water absorbtion $$W_{abs} = \frac{M_{sat} - M_s}{M_s} \times 100 \quad (3.5)$$
- Porosity $$n = \frac{V_v}{V_d} \text{ x } 100 \quad (3.6)$$

3.3. Determination of Strenght Properties

All test were done according to ISRM(1981). Exactly 245 of limestone samples used to perform this test in this thesis. Out of this 245 specimens ; 118 samples were used for Brazillian tensile strength, 12 samples were used for direct shear test, 115 samples were used for uniaxial compression test. Sample used for Brazillian test are core specimens which has a diameter of 60 mm and has a length 30 mm. Samples used for direct shear test are core specimens which has a diameter of 60 mm and has a length 100 mm. Samples used for uniaxial compression test are core specimens which has a diameter of 60 mm and has a length 150 mm.

3.3.1. Ultrasonic velocity test

The ultrasonic velocities are measured and calculated on dry samples.

3.3.1.1. Scope

This test is intended as a method to determine the velocity of propagation of elastic waves in laboratory rock testing. Three different variations of the method are given. Theese are the high frequency ultrasonic pulse technique, the low frequency ultrasonic pulse technique and the resonant method. In this thesis the low frequency ultrasonic pulse technique is used.

3.3.1.2. Apparatus

Although there are three different methods, the electronic components should, as far as possible, be chosen so as to be applicable to all three methods. The same rock or even the same sample can be used for all three methods. Consideration should of course be given to the respective frequencies used for the different methods. The electronic components should be impedance matched and have shielded leads to ensure efficient energy transfer. To prevent damage to the system allowable voltage inputs should not be exceeded. An apparatus used for determining the ultrasonic velocity is shown in figure 3.4.

Figure 3.4. Ultrasonic velocity test equipment.

(a) Pulse generator unit (e.g. function generator): Frequency range: 2-30 kHz (if the generator mentioned in the first method has a low frequency range it can obviously be used here); repetition frequency: 10-100 repetitions per second; pulse voltage: same as first method.

(b) Transducers:

(i) Transmitter: piezo-electric ceramics or magnetostrictive elements, which are capable to generate high amplitude pulses (depending on the rock type and specimen dimensions) in the frequency range 2-30 kHz.

(ii) Receivers: piezo-electric ceramics with flat frequency response in the frequency range 2-30 kHz or magneto-strictive elements.

(c) Filters, amplifiers, CRO, time-marker analog to first method with consideration of the low frequency range.

3.3.1.3. Procedure

Care should be exercised in core drilling, handling, sawing, grinding and lapping the test specimen to minimize mechanical damage. The surface area under each transducer shall be sufficiently plane to provide good coupling.

Drying of specimens may be carried out by using a desiccator. Saturated specimens shall remain submerged in water up to the time of testing. If the velocity is to be determined with the in-situ condition, care must be exercised during the preparation procedure. It is also suggested that both the sample where the specimen is taken from as well as the specimen, be stored in moisture-proof bags. Dry surface-preparation procedures may be employed.

This test is for the determination of the velocity of dilatational and torsional waves in bar or rod-like rock specimens (bar waves, one-dimensional wave propagation). This method is suitable for specimens which are long compared to the diameter (length to diameter ratio >3) and the wave length of the pulse should be long compared to the diameter (wave length to diameter ratio >5).

(a) Dimensions should be as stated above. For the pulse transmission technique and the resonant frequency technique both the end planes of the specimen should be flat and parallel to within 0.005mm/mm of the lateral dimension.

(b) Rock cores are positioned on the sample holder of an acoustical bench. The cores have at least a length to diameter ratio of >3. The transmitter, generating a sine wave of a wave-length >5 times the core diameter, is pressed to a saw-cut flat end plane (normal to the core axis) by a stress of approx 10N/cm^2 for V_p measurement.

(c) There are two possibilities in the positioning of the receiver (analog to (c) in first method):

(i) pulse transmission: the receiver is positioned at the opposite flat plane of the core is shown in figure 3.5a,3.5b,3.5c. Both end planes should be parallel to within about one degree: ball joints may be used

(ii) seismic profiling: the receiver is moved along the surface of the core parallel to the core axis.

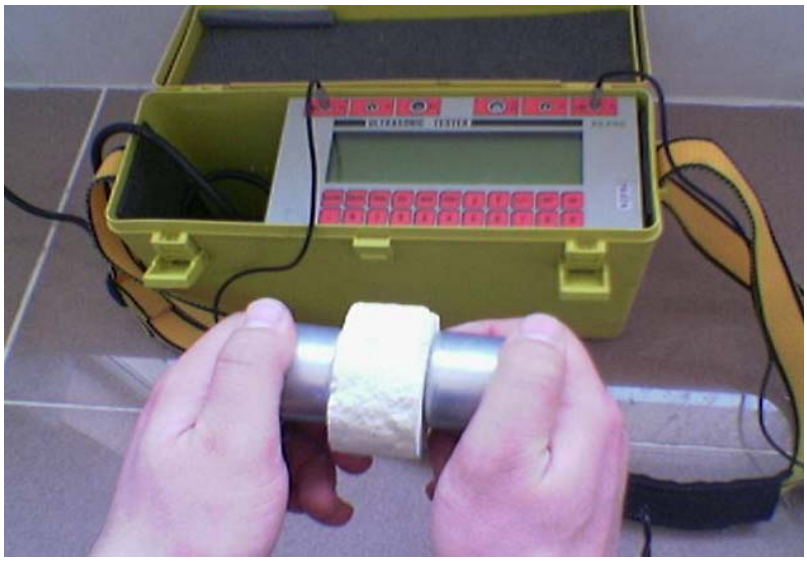

Figure 3.5a. The ultrasonic velocity test performed on core specimen for Brazillian test.

Figure 3.5b. The ultrasonic velocity test performed on core specimen for direct shear test.

Figure 3.5c. The ultrasonic velocity test performed on core specimen for uniaxial compression test

3.3.1.4. Calculation

One or three-dimensional equations of wave propagation are used.

(a) Velocities are calculated from travel times measured and the distance, d, between transmitter and receiver by using the equations:

$$V_p = d \times t_p^{-1} \quad (3.7)$$

$$V_s = d \times t_s^{-11} \quad (3.8)$$

where V_p is the velocity of the longitudinal wave, V_s is the velocity of the shear wave, t_p and t_s are the times which the P and S wave, respectively, took to travel the distance d.

(b) If seismic profiling technique was used the velocities are given by the slope of the curve travel time Vs distance d.

3.3.2. Brazil test

Brazillian tensile test was performed according to ISRM (1981). 118 samples were used for Brazillian tensile strength. Samples used for Brazillian test are core specimens which has a diameter of 60 mm and has a length 30 mm.

3.3.2.1. Scope

This test is intended to measure the uniaxial tensile strength of prepared rock specimens indirectly by the brazil test. The justification for the test is based on the experimental fact that most rocks in biaxial stress fields fail in tension at their uniaxial tensile strength when one principal stress is tensile and the other finite principal stress is compressive with a magnitude not exceeding three times that of the tensile principal stress [8].

3.3.2.2. Apparatus

(a) Two steel loading jaws designed so as to contact a disc-shaped rock sample at diametrically-opposed surfaces over an arc of contact of approx 10^0 at a failure. The suggested apparatus to achieve this is illustrated in figure 3.6a and figure 3.6b The critical dimensions of the apparatus are the radius of the curvature of the jaws, the clearance and length of the guide pins coupling the two curved jaws and the width of the jaws. These are as follows: Radius of jaws – 1.5 × specimen radius; guide pin clearance – permit rotation of one jaws relative to the other by 4×10^{-3} rad out of plane of the apparatus (25 mm penetration of guide pin with 0.1 mm clearance); width of jaws – 1.1 × specimen thickness. The upper jaw contains a spherical seating conveniently formed by a 25-mm diameter half – ball bearing.

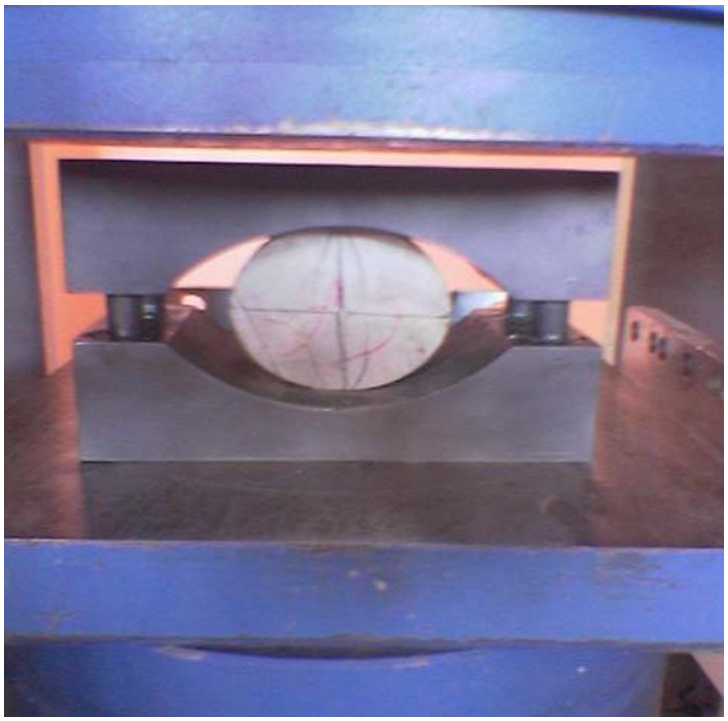

Figure 3.6a. The suggested apparatus for Brazil Test (ISRM 1981)

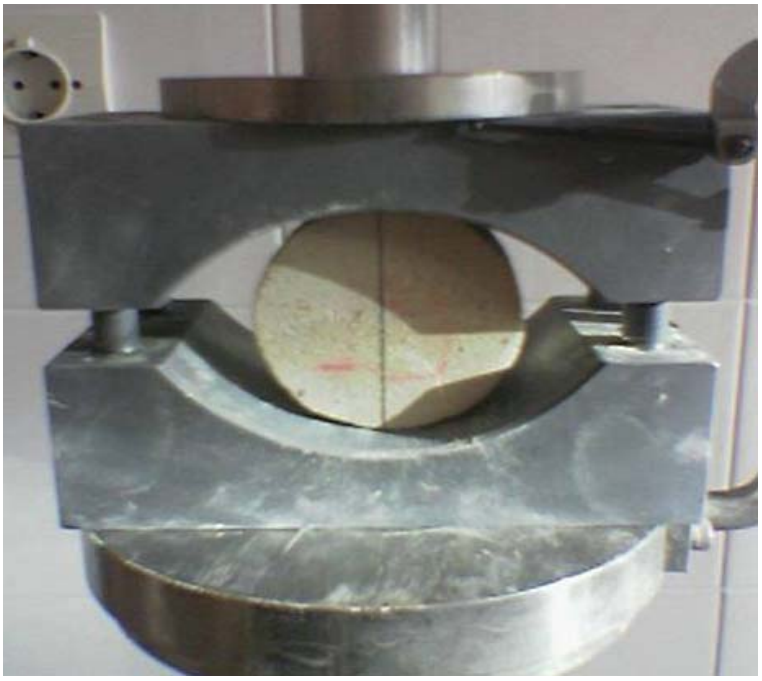

Figure 3.6b. The suggested apparatus for Brazil Test (ISRM 1981)

Double thickness (0.2 – 0.4 mm) adhesive paper strip (masking tape) with a width equal to or slightly greater than the specimen thickness.

(b) A suitable machine for applying and measuring compressive loads to the specimen can be seen in figure 3.7. It shall be of sufficient capacity and be capable of applying load at a rate conforming to the requirements set out in section 3.

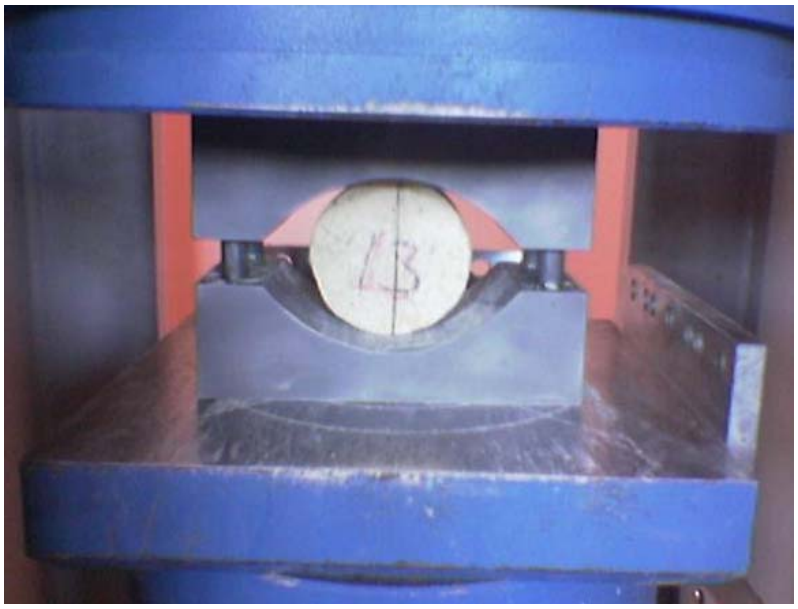

Figure 3.7. A suitable machine for applying and measuring compressive loads to the specimen

(c) A spherical seat, if any, of the testing machine crosshead shall be placed in a locked position, the two loading surfaces of the machine being parallel to each other.

(d) It is a preferable but not obligatory that the testing machine be fitted with a chart recorder to record load against displacement to aid in the measurement of the failure load.

3.3.2.3. Procedure

(a) The test specimens should be cut and prepared using clean water. The cylindrical surfaces should be free from obvious tool marks and any irregularities across the thickness of the specimen should not exceed 0.025

mm. End faces shall be flat to with 0.25 mm and square and parallel to within 0.25°.

(b) Specimen orientation shall be known and the water content controlled or measured and reported in accordance with the 'suggested method for the determination of the water content of rock sample.

(c) The specimen diameter shall not be less than NX core size, approximately 54 mm, and the thickness should be approximately equal to the specimen radius.

(d) The test specimen shall be wrapped around its periphery with one layer of the masking tape and mounted squarely in the test apparatus such that the curved platens load the specimen diametrally with the axes of rotation for specimen and apparatus coincident.

(e) Load on the specimen shall be applied continuously at a constant rate such that the failure in the weakest rocks occurs within 15-30s. A loading rate of 200 N / s is recommended.

3.3.2.4. Calculations

The tensile strength of the specimen σ_t, shall be calculated by the following formula:

$$\sigma_t = 0.636\ P / (D.t)\ \text{(MPa)} \qquad (3.9)$$

where P is the load at failure (kN), D is the diameter of the test specimen (mm), t is the thickness of the test specimen measured at the center (mm).

3.3.3. Uniaxial compression test and determination of young's modolus

Uniaxial compression test was performed according to ISRM(1981). 115 samples were used for uniaxial compression test. Samples used for uniaxial compression test are core specimens which has a diameter of 60 mm and has a length 150 mm.

3.3.3.1. Scope

This method of test is intended to determine stress-strain curves and young's modulus and Poisson's ratio in uniaxial compression of a rock specimen of regular geometry. The test is mainly intended for classification and characterization of intact rock.

3.3.3.2. Apparatus

(a) A suitable machine shall be used for applying and measuring axial load to the specimen which is shown in figure 3.8. It shall be of sufficient capacity and capable of applying load at a rate conforming to the requirements set in section 3.

Figure 3.8. A suitable machine shall be used for applying andmeasuring axial load to the specimen

(b) A spherical seat, if any, of the testing machine, if not complying with spesification 2(d) below, shall be removed or placed in a locked position, the two loading faces of the machine being parallel to each other.

(c) Steel platens in the form of discs and having a Rockwell hardness of not less than HRC58 shall be placed at the specimen ends. The diameter of the platens shall be between D and D + 2 mm where D is the diameter of the specimen. The thickness of the platens shall be at least 15 mm or D / 3. surfaces of the discs should be ground and their flatness should be better than 0.005 mm.

(d) One of the two platens shall incorporate a spherical seat. The spherical seat should be placed on the upper and of the specimen. It should be lightly lubricated with mineral oil so that it locks after the deadweight of the cross-head has been picked up. The specimen, the platens and spherical seat shall be accurately centered with respect to one another and to the loading machine. The curvature centre of the seat surface should coincide with the centre of the top end of the specimen.

(e) Electrical resistance strain gauges, linear variable differential transformers, compressometers, optical devices or other suitable measuring devices. Their design shall be such that the average of two circumferential and two axial strain measurements, equally spaced, can be determined for each increment of load. The devices should be robust and stable, with strain sensitivity of the order of $5x10^{-6}$.

Both axial and circumferential strains shall be determined within an accuracy of 2% of the reading and a precision of 0.2 percent of full scale.

If electrical resistance strain gauges are used, the length of gauges over which axial and circumferential strains are determined shall be at least ten grain diameters in magnitude and the gauges should not encroach within D/2 of the specimen ends, where D is diameter of the specimen.

If micrometers of LVDT's are used for measuring axial deformation due to loading, these devices should be graduated to read in 0.002mm units and accurate within 0.002mm in any 0.02mm range and within 0.005mm in any 0.25 range. The dial micrometer or LVDT's should not encroach within D/2 of the specimen ends.

(f) An apparatus for recording the loads and deformations; preferably an X-Y recorder capable of direct plotting of load-deformation curves.

3.3.3.3. Procedure

(a) Test specimens shall be right circular cylinders having a height to diameter ratio of 2.5 – 3 and a diameter preferably of not less than NX core size, approximately 54 mm . Figure 3.9. shows the specimens that can be used for calculating the uniaxial compressive strength. The diameter of the specimen should be related to the size of the largest grain in the rock by the ratio of at least 10 : 1.

Figure 3.9. Specimens for uniaxial compressive strength.

(b) The ends of the specimen shall be flat to 0.02 mm and shall not depart from perpendicularly to the axis of the specimen by more than 0.001 radian (about 3.5 min) or 0.05 mm in 50 mm.

(c) The sides of the specimen shall be smooth and free of abrupt irregularities and straight to within 0.3 mm over the full length of the specimen.

(d) The use of the capping materials or end surface treatments other than machining is not permitted.

(e) The diameter of the test specimen shall be measured to the nearest 0.1 mm by averaging two diameters measured at right angles to each other at about the upper height, the mid-height and the lower height of the specimen. The average diameter shall be used for calculating the cross-sectional area. The height of the specimen shall be determined to the nearest 1.0 mm.

(f) Moisture can have a significant effect on the deformability of the test specimen. When possible, in situ moisture conditions should be preserved until the time of the test. When the characteristic of the rock material under conditions varying from saturation to dry is required, proper note shall be made of moisture conditions so that correlation between deformability and moisture content can be made. Excess moisture can create a problem of adhesion of strain gauges which may require making a change in moisture content of the require making a change in moisture content of the sample. The moisture condition shall be reported in accordance with Suggested method for determination of the water content of a rock sample.

(g) Load on the specimen shall be applied continuously at a constant stress rate such that failure will occur within 5-10 min of loading, alternatively the stress rate shall be within the limits of 0.5-10 MPa/s.

(h) Load and axial and circumferential strains or deformations shall be recorded at evenly spaced load intervals during the test, if not continually recorded. At least ten readings should be taken over the load range to define the axial and diametric stress-strain curves.

(i) It is sometimes advisable for a few cycles of loading and unloading to be performed.

(j) The number of specimens instrumented and tested under a specified set of conditions shall be governed by practical considerations but at least five are preferred.

3.3.3.4. Calculations

(a) Axial strain, ε_a, and diametric strain, ε_d, may be recorded directly from strain indicating equipment or may be calculated from strain indicating equipment or may be calculated from deformation readings depending upon the type of instrumentation such as discussed in 3.3.3.2. apparatus (e).

(b) Axial strain is calculated from the equation

$$\varepsilon_a = \frac{\Delta l}{l_0} \tag{3.10}$$

Where

l_0 = original measured axial length

Δl = change in measured axial length (defined to be positive for a decrease in length)

(c) Diametric strain may be determined either by measuring the changes in specimen diameter or by measuring the circumferential strain. In the case of measuring the changes in diameter, the diametric strain is calculated from the equation.

$$\varepsilon_d = \frac{\Delta d}{d_0} \tag{3.11}$$

Where

d_0 = original undeformed diameter of the specimen

Δd = change in diameter (defined to be negative for an increase in diameter)

In the case of measuring the circumferential strain ε_d, the circumference is $C = \pi d$, thus the change in circumference is $\Delta C = \pi \Delta d$. Consequently, the circumferential strain, ε_c, is related to diametric strain, ε_d, by

$$\varepsilon_c = \frac{\Delta C}{C_0} = \frac{\Delta d}{d_0} \tag{3.12}$$

So that

$$\varepsilon_c = \varepsilon_d$$

Where C_0 and d_0 are original specimen circumference and diameter, respectively.

(d) The compressive stress in the test specimen, σ, is calculated by dividing the compressive load P on the specimen by the initial cross-sectional area, A_0.

Thus

$$\sigma = \frac{P}{A_0} \tag{3.13}$$

where in this test procedure, compressive stresses and strains are considered positive.

(e) Figure 3.10 illustrates typical plot of axial stress versus axial and diametric strains. These curves show typical behaviour of rock materials from zero stress up to ultimate strength, σ_u, The complete curves give the best description of the deformation behaviour of rocks having non-linear stress-strain behaviour at low and high stress levels.

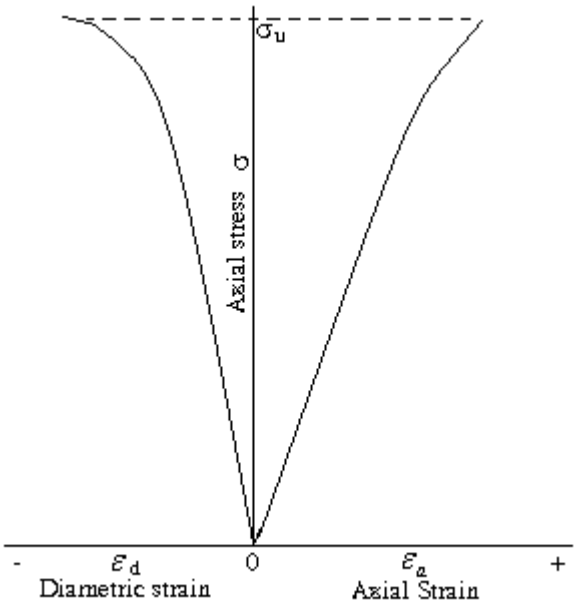

Figure 3.10. Format for graphical presentation of axial and diametric stress-strain curves.

(f) Axial Young's modulus, E (defined as the ratio of the axial stress change to axial strain produced by the stress change) of the specimen may be calculated using any one of several methods(in this thesis tangent modulus is used) employed in accepted engineering practice. The most common methods, listed in figure 3.10 are as follows:

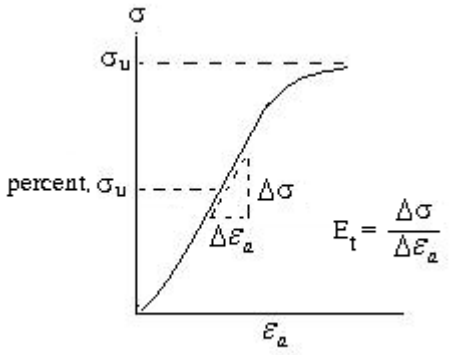

Figure 3.11a. tangent modulus measured at a fixed percentage of ultimate strength

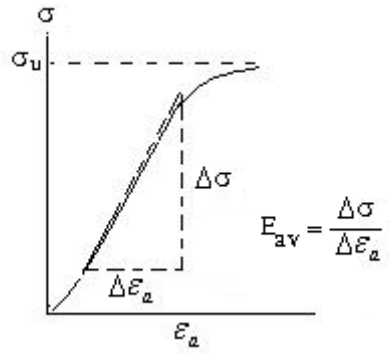

Figure 3.11b. Average modulus of linear portion of the stress-strain curve

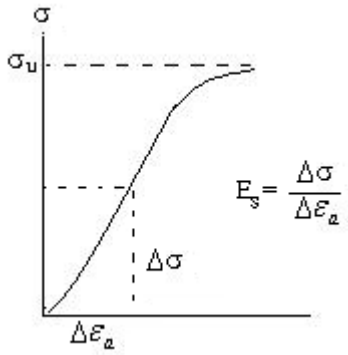

Figure 3.11c. Secant modulus measured up to a fixed percentage of ultimate strength

(1) Tangent Young's modulus, E_t, is measured at a stress level which is some fixed percentage of the ultimate strength (figure 3.11a). It is generally taken at a stress level equal to 50% of the ultimate uniaxial compressive strength [8].

(2) Average Young's modulus, E_{av}, is determined from the average slopes of the more-or-less straight line portion of the axial stress-axial strain curve (figure 3.11b).

(3) Secant Young's modulus, E_t, is usually measured from zero stress to some fixed percentage of the ultimate strength (figure 3.11c), generally at 50%.

Axial Young's modulus E is expressed in units of stress i.e. pascal (Pa) but the most appropriate multiple is the gigapascal (GPa = 10^9 Pa).

(g) Poisson's ratio, ν, may be calculated from the equation.(ISRM 1981)

$$\nu = - \frac{\text{slope of axial stress - strain curve}}{\text{slope of diametric stress - strain curve}} \tag{3.14}$$

$$= - \frac{\text{E}}{\text{slope of diametric curve}} \tag{3.15}$$

where the slope of the diametric curve is calculated in the same manner for either of the three ways discussed for Young's modulus in paragraph 3.3.3.4.(f). Note that Poisson's ratio in this equation has a positive value, since the slope of the diametric curve is negative by the conventions used in this procedure.

(h) The volumetric strain, ε_v, for a given stress level is calculated from the equation.

$$\varepsilon_v = \varepsilon_a + 2\varepsilon_d \tag{3.16}$$

3.3.4. Direct shear test

Direct shear test was performed according to ISRM(1981). 12 samples were used for direct shear test.Samples used for direct shear test are core specimens which has a diameter of 60 mm and has a length 100 mm.

3.3.4.1. Scope

(a) This test measures peak and residual direct shear strength as a function of stress normal to the sheared plane. Results are employed, for example, in the limiting equilibrium analysis of slope stability problems or for the stability analysis of dam foundations [8].

(b) The inclination of the test specimen with respect to the rock mass, and its direction of mounting in the testing machine are usually selected so that the sheared plane coincides with a plane of weakness in the rock, for example a joint, plane of bedding, schistosity or cleavage, or with the interface between soil and rock or concrete and rock.

(c) A shear strength determination should preferably comprise at least five tests on the same test horizon with each specimen tested at a different but constant normal stress.

(d) In applying the results of the test, the pore-water pressure conditions and the possibility of progressive failure must be assessed for the design case as they may differ from the test conditions.

3.3.4.2. Apparatus

Equipment for taking specimens of rock, including:

(a) Equipment for cutting the specimen; for example a large-diameter core drill, percussive drills, rock saws or hammers and chisels, also equipment for

measuring the dip, dip direction, roughness and other characteristic features of the test horizon.

(b) Materials for holding the specimen together, for example binding wire or metal bands.

(c) Materials to protect the specimen against mechanical damage and change in water content both during cutting and transit to the laboratory, example protective packing and wax or similar waterproofing material.

Equipment for mounting the specimen including:

(a) Specimen carriers, forming a dismountable part of the test equipment.

(b) Cement, plaster, resin or similar strong encapsulating materials together with appropriate mixing utensils.

Testing equipment (a shear box, for example Figure 3.12) incorporating:

(a) A means of applying the normal load, typically a hydraulic, pneumatic or dead-weight mechanical system, designed to ensure that the load is uniformly distributed over the plane to be tested. The resultant force should act normal to the shear plane, passing through its centre of area. The system should have a travel greater than the amount of dilation or consolidation to be expected, and should be capable of maintaining normal load to within 2% of a selected value throughout the test.

Figure 3.12. Arrangement for laboratory direct shear test.

(b) A means of applying the shear force, typically a hydraulic jack or a mechanical gear-drive system, designed so that the load is distributed uniformly along one half-face of the specimen with the resultant applied shear force acting in the plane of shearing. The equipment should be designed for a shear travel greater than 10% of the specimen length. It should include rollers, cables or a similar low friction device to ensure that resistance of the equipment to shear displacement is less than 1% of the maximum shear force applied in the test.

(c) Equipment for independent measurement of the applied shear and normal forces, with an accuracy better than +-2% of the maximum forces reached in the test. Recent calibration data applicable to the range of testing should be appended to the test report.

(d) Equipment for measuring shear, normal and lateral displacement, for example micrometer dial gauges or electric transducers or the four normal displacement gauges may be replaced by a single gauge mounted centrally. The shear displacement measuring system should have a travel greater than 10% of the specimen length and an accuracy better 0.1 mm. The normal and lateral displacement measuring systems should have a travel greater than 20 mm and an accuracy better than 0.05 mm. Resetting of gauges during the test

should if possible be avoided. If electric calibration should be included in the report.

3.3.4.3. Procedure

Preparation:

(a) The test horizon is selected and dip, dip direction and other relevant geological characteristic are recorded. Block or core specimens containing the test horizon are collected using methods selected to minimize disturbance, if possible in such a way as to retain natural water content. The specimen dimensions and the location of the test horizon within the block or core should if possible allow mounting without further trimming in the laboratory, and with sufficient clearance for adequate encapsulation. The test plane should preferable be square with a minimum area of 2500mm^2. The mechanical integrity with wire or tape which is to be left in position until immediately before testing [8].

(b) Specimens that are not encapsulated immediately for testing should be given a waterproof coating, labeled and packaged to avoid damage in transit to the laboratory. Fragile specimens require special treatment, for example packaging in polyurethane foam [8].

(c) The protective packaging, with the exception of the steel wire, is removed and the block supported in one of the carriers so that the horizon to be tested is secured in the correct position and orientation. The encapsulating material is poured and, after this has set, the other half-specimen is encapsulated in a similar manner (see in figure 3.13). A zone at least 5mm either side of the shear horizon should be free from encapsulating material.

Figure 3.13. shows the encapsulating material as concrete

Shearing:

(a) The propose of shearing is to establish values for the peak and residual direct shear strengths of the test horizon.

(b) The shear force may be applied in increments but is usually applied continuously in such a way as to control the rate of shear displacement.

(c) Approximately 10 sets of readings should be taken before reaching peak strength. The rate of shear displacement should be less than 0.1 mm/min in the 10-minute period before taking a set of readings. This rate may be increased to not more than 0.5 mm/min between sets of readings provided that the peak strength itself is adequately recorded. For a 'drained' test particularly when testing clay-filled discontinuities, the total time to reach peak strength should exceed $6t_{100}$ as determined from the consolidation curve. If necessary the rate of the shear should be reduced or the application of later shear force increments delayed to meet this requirement.

(d) After reaching peak strength, readings should be taken at increments of from 0.5 to 5 mm shear displacement as required to adequately define the force-

displacement curves. The rate of the shear displacement should be 0.002-0.2 mm/min in the 10-minute period before a set o readings is taken, and may be increased to not more than 1 mm/min between sets of readings.

(e) It may be possible to establish a residual strength value when the sample is sheared at constant normal stress and at least four consecutive sets of readings are obtained which show not more than 5% variation in shear stress over a shear displacement of 1 cm.

(f) Having established a residual strength the normal stress may be increased or reduced and shearing continued to obtain additional residual strength values. The specimen should be reconsolidated under each new normal stress.

(g) After the test the shear plane should be exposed and fully described. The area of the shear surface is measured and photographs may be also be required. Samples of rock, infilling and shear debris should be taken for index testing.

3.3.4.4. Calculations

(a) Shear and normal stress are computed as follows:

$$\text{Normal stress } \tau = \frac{Ps}{A} \tag{3.17}$$

$$\text{Shear stress } \sigma_n = \frac{Pn}{A} \tag{3.18}$$

Where

P_s = Total shear force;

P_n =Total normal force;

A = Area of shear surface overlap (corrected to account for shear displacement).

(b) For each test specimen graphs of shear stress (or shear force) and normal displacement vs. shear displacement are plotted. Annotated to show the nominal normal stress and any change in normal stress during shearing. Values of peak and residual shear strength and the normal stresses, shear and normal displacement at which these occur are abstracted from these graphs.

(c) Graphs of peak and residual shear strength vs. normal stress are plotted from the combined results for all test specimens. Shear strength parameters Ø, $Ø_r$, and c are abstracted from figure 3.14. [8].

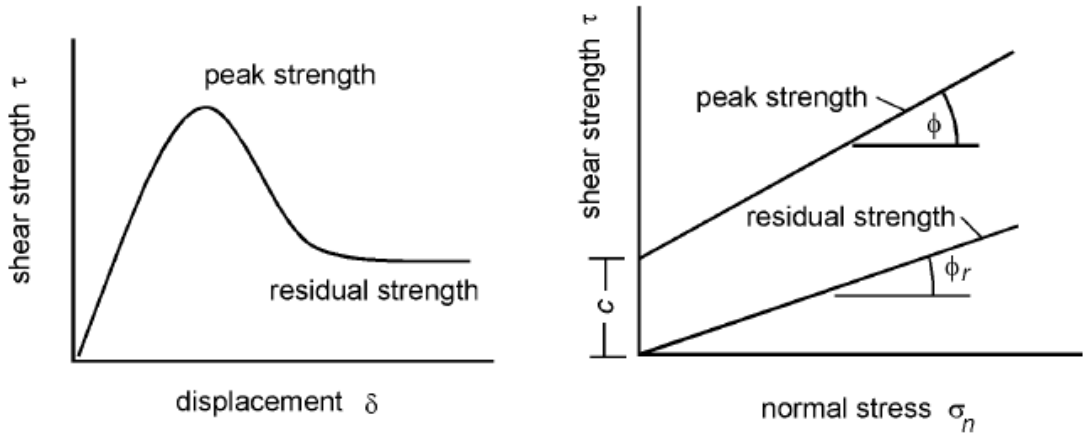

Figure 3.14. Shear testing of discontinuities [50].

3.4. Sources of Error in Strength Tests

In assessing the scope and method of testing appropriate for a particular project it is important that the likely errors be properly taken into account. These come from two sources, namely: (i) bias in sample selection; and (ii) errors resulting from inappropriate sample preparation, test apparatus or test procedure.

The substantial variability which is usually found in rocks in engineering projects means that critical appraisal must be made of errors which may occur in testing but which may have an effect substantially less than the inherent variability. This does not mean that a casual attitude to laboratory testing should be condoned, but it does mean that there is little point in spending time and money in chasing a 1% error in

the laboratory tests when there is a 40% variability in the results due to natural variability, sample selection bias, etc. [20].

3.5. Factors Influencing The Measurement of Strength

Many factors influence the measurement and determination of rock strength such as uniaxial compressive strength shear strength etc. The most important factors are briefly reviewed here.

The rock specimen tested in the laboratory is considered to be an element of the field and to contain properties that are representative of the rock mass from which it is taken. However, depending on a number of factors to which the specimen is exposed in the laboratory test, the specimen may not yield properties that are directly applicable to the field. An appreciation of the limitations of the laboratory tests may provide guidance in selecting appropriate properties for use in analyses of rock structures [23].

3.5.1. Specimen shape

The rock specimens tested in uniaxial and triaxial compression are most often cylindrical The height : diameter ratio of the specimen influences the measured strength. Typically the strength decreases with increasing height : diameter ratio , but it tends to become constant for ratios in the order of 2:1 to 3: [21,37]. For higher ratios the specimen strength may be influenced by buckling.

3.5.2. Specimen size

The specimen size may influence the measured strength. According to Weibull [51] a large specimen contains more flaws than a small specimen. The large specimen therefore also has more flaws with critical orientation relative to the applied shear stresses than the small specimen. A large specimen with a given shape is therefore likely to fail and exhibit lower strength than a small specimen with the same shape.

This type of behaviour is observed for most brittle materials, including many rocks [5, 14, 24].

3.5.3. Platen friction

The end of platens through which the specimen is loaded may apply frictional forces directed towards the center of the specimen as it begins to expand laterally during axial compression. This results in apparent higher confining pressure near the ends of the specimen, and it will consequently exhibit higher strength. This effect is more pronounced and is directly responsible for the higher strength observed in shorter specimens as discussed above [37]. Procedures involving brush platens or fluid cushions may be employed to reduce the platen friction and improve the test results significantly [3, 4, 7, 16, 29, 34].

3.5.4. Rate of loading

Experimental observations show that the strength decreases with decreasing rate of loading or strain rate [3, 4, 7, 14, 16, 24, 29, 34, 45]. This is due to effects of creep that are present in all materials. Longer times to peak failure allow greater amounts of creep to occur, and this plays a role in the measured strength. Some rock types are known to creep more (e.g. rock salt) than others (e.g. granite), and the creep behaviour has a dominant influence on the design of structures in such rocks [10].

3.5.5. Presence of water

Water may have two effects on the behaviour: (i) chemical or physical effects that will cause the rock to be altered simply due to the presence of moisture; and (ii) a mechanical effect when the water is under pressure. Some rocks may be weaker by addition of water, either by deterioration of cementing agents or by swelling and consequent reduction in strength [18, 41]. The effects of water under pressure can be accounted for by Terzaghi's effective stress principle [6, 13, 18, 41].

The presence of moisture in a rock body can influence the rupture behaviour of the rock in two important ways:

a) The moisture can reduce the strenght of the rock by chemical or physical alteration of its inherent properties. This strength reduction can be very important.

b) If the moisture is present under pressure, the strength of rock is further reduced [44].

3.5.6. Temperature

Increasing temperature will cause a reduction in strength [11, 12, 25]. This strength reduction may not be pronounced until the rock begins to recrystallize or melt at relatively high temperatures. Experiments at increasingly high temperatures indicate reductions in both tensile and compressive strengths, as well in the overall three-dimensional strength properties of rocks.

3.5.7. Stiffness of the testing

The stiffness of the testing machine controls the measured stress-strain-strength behaviour, especially in the softeing portion of the curve for brittle rocks[14, 22, 24]. Stiff testing machines prevent a sudden release of energy and consequent rapid, uncontrolled decline in the stress-strain relation past peak failure. This may not affect the peak failure value substantially, but it may have an effect on the residual strength of the rock.

CHAPTER 4

TEST RESULTS AND CORRELATIONS

4.1.Introduction

This chapter contains the test results and correlations obtained from the test results. All physical and mechanical properties of Gaziantep limestones are correlated with ultrasonic velocity. In addition, Some physical and mechanical properties of Gaziantep limestones are correlated with each other. This correlations were done by linear correlation method (Least square method). The accuracy of correlations were checked by correlation coefficient of R^2 since higher correlation coefficients.

R^2 was calculated by

$$R^2 = SSR / SST \tag{4.1}$$

- SSR : Sum of square regression
- SST : Sum of square total

4.2. Brazil Test

Brazillian tensile test was performed according to ISRM (1981). 118 samples were used for Brazillian tensile strength. Samples used for Brazillian test are core specimens which has a diameter of 60 mm and has a length 30 mm.

4.2.1. Results

Result obtained from Brazillian tensile test were plotted on graphics.

4.2.1.1. Dry density versus ultrasonic velocity for samples of Brazil test

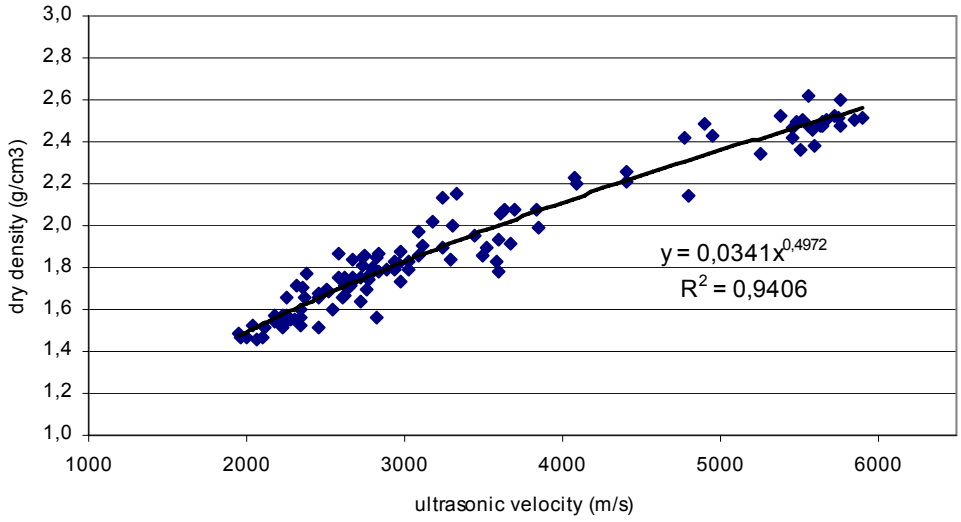

Figure 4.1.Ultrasonic Velocity – Dry density diagram

Table 4.1. Equation and R^2 values for Ultrasonic Velocity – Dry density

TRENDLINE TYPE	R^2	EQUATION
LINEAR	$R^2 = 0,9383$	$y = 0,0003x + 1,0076$
POWER	$R^2 = 0,9406$	$y = 0,0341x^{0,4972}$
EXPONENTIAL	$R^2 = 0,9173$	$y = 1,2019e^{0,0001x}$

Figure 4.1 shows the highest R^2 for test results of the dry density of limestones versus ultrasonic velocity. Other trends of correlation are also given in table 4.1. 118 specimens are used to perform this test. It can be seen clearly from figure 4.1, dry density of limestone increases as ultrasonic velocity increase. Dry density of limestones reach the maximum value at 5909,1 m/s ultrasonic velocity and it reaches the minimum value at 1946,7 m/s ultrasonic velocity. Maximum and minimum dry density values are 2,62 g/cm^3 and 1,46 g/cm^3.

Rock samples were selected different from each other much possible. However, rock samples are concentrated dense between 1960,0 m/s and 3085,1 m/s ultrasonic velocities. If the rock samples were selected between maximum and minimum ultrasonic velocity values equally, it would be seen clearer increase in the figure 4.1. In this graphic the relationship follows a power law with a reasonable squared regression coefficient R-square is 0,9406 and equation is $y = 0,0341x^{0,4972}$.

4.2.1.2. Bulk density versus ultrasonic velocity for samples of Brazil test

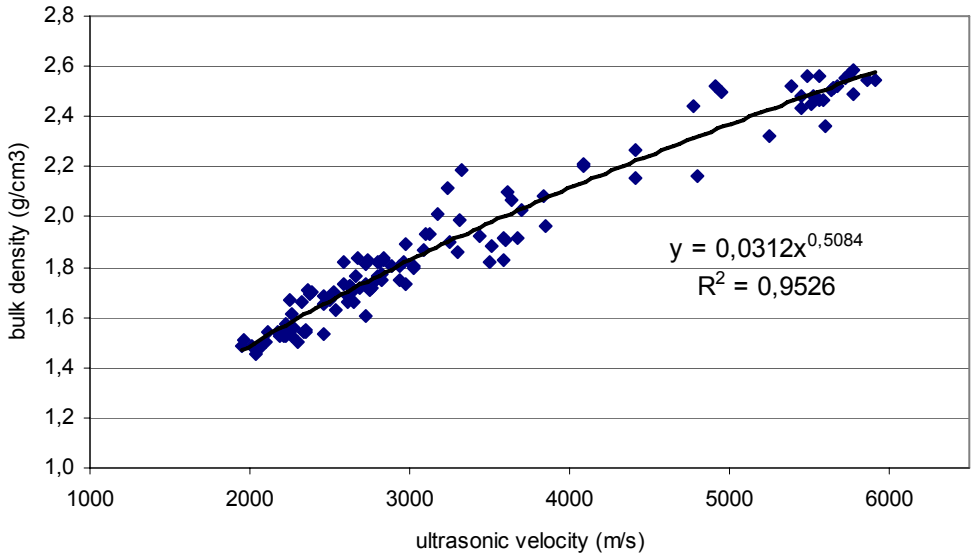

Figure 4.2. Ultrasonic Velocity – Bulk density diagram

Table 4.2. Equation and R^2 values for Ultrasonic Velocity – Bulk density diagram

TRENDLINE TYPE	R^2	EQUATION
LINEAR	$R^2 = 0,9493$	$y = 0,0003x + 0,9836$
POWER	$R^2 = 0,9526$	$y = 0,0312x^{0,5084}$
EXPONENTIAL	$R^2 = 0,9315$	$y = 1,1887e^{0,0001x}$

Figure 4.2 shows the highest R^2 for test results of the bulk density of limestones versus ultrasonic velocity. Other trends of correlation are also given in table 4.2. 118 specimens are used to perform this test. It can be seen clearly from figure 4.2, bulk density of limestone increases as ultrasonic velocity increase. Bulk density of limestones reach the maximum value at 5909,1 m/s ultrasonic velocity and it reaches the minimum value at 1946,7 m/s ultrasonic velocity. Maximum and minimum bulk density values are 2,59 g/cm^3 and 1,45 g/cm^3.

Rock samples were selected different from each other much possible. However, rock samples are concentrated between 1946,7 m/s and 3085,1 m/s ultrasonic velocities. If the rock samples were selected between maximum and minimum ultrasonic velocity values equally, it would be seen clearer increase in the figure 4.2. In this

graphic the relationship follows a power law with a reasonable squared regression coefficient R-square is 0,9526 and equation is $y = 0{,}0312x^{0{,}5084}$.

4.2.1.3. Saturated density versus ultrasonic velocity for samples of Brazil test

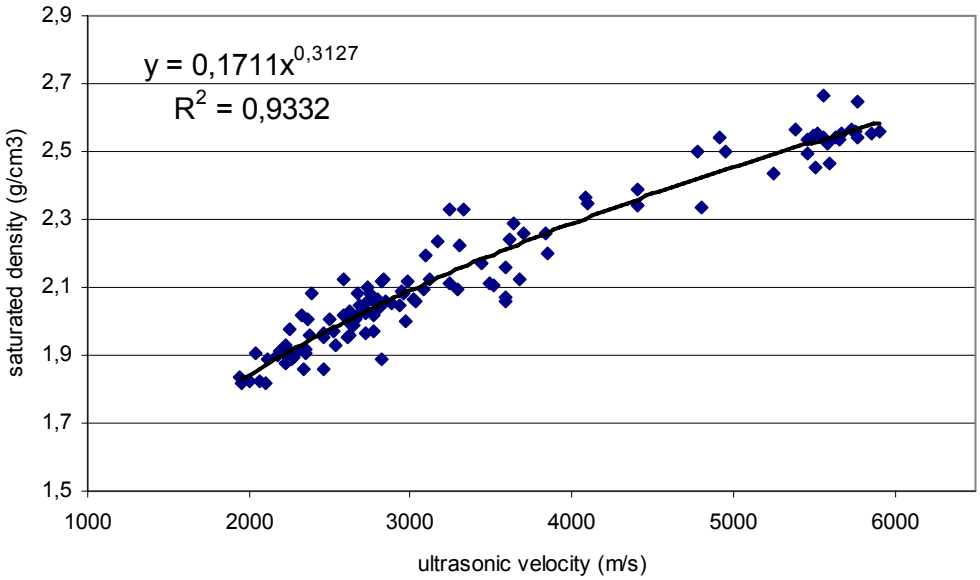

Figure 4.3. Ultrasonic Velocity – Saturated density diagram

Table 4.3. Equation and R^2 values for Ultrasonic Velocity – Saturated density

TRENDLINE TYPE	R^2	EQUATION
LINEAR	$R^2 = 0{,}9296$	$y = 0{,}0002x + 1{,}5124$
POWER	$R^2 = 0{,}9332$	$y = 0{,}1711x^{0{,}3127}$
EXPONENTIAL	$R^2 = 0{,}9315$	$y = 1{,}6042e^{8E\text{-}05x}$

Figure 4.3 shows the highest R^2 for test results of the saturated density of limestones versus ultrasonic velocity. Other trends of correlation are also given in table 4.3. 118 specimens are used to perform this test. It can be seen clearly from figure 4.3, saturated density of limestone increases as ultrasonic velocity increase. Saturated density of limestones reach the maximum value at 5909,1 m/s ultrasonic velocity and it reaches the minimum value at 1946,7 m/s ultrasonic velocity. Maximum and minimum saturated density values are 2,66 g/cm^3 and 1,82 g/cm^3.

Rock samples were selected different from each other much possible. However, rock samples are concentrated between 1960,0 m/s and 3085,1 m/s ultrasonic velocities. If the rock samples were selected between maximum and minimum ultrasonic velocity values equally, it would be seen clearer increase in the figure 4.3. In this graphic the relationship follows a power law with a reasonable squared regression coefficient R-square is 0,9332 and equation is $y = 0,1711x^{0,3127}$.

4.2.1.4. Water absorption versus ultrasonic velocity for samples of Brazil test

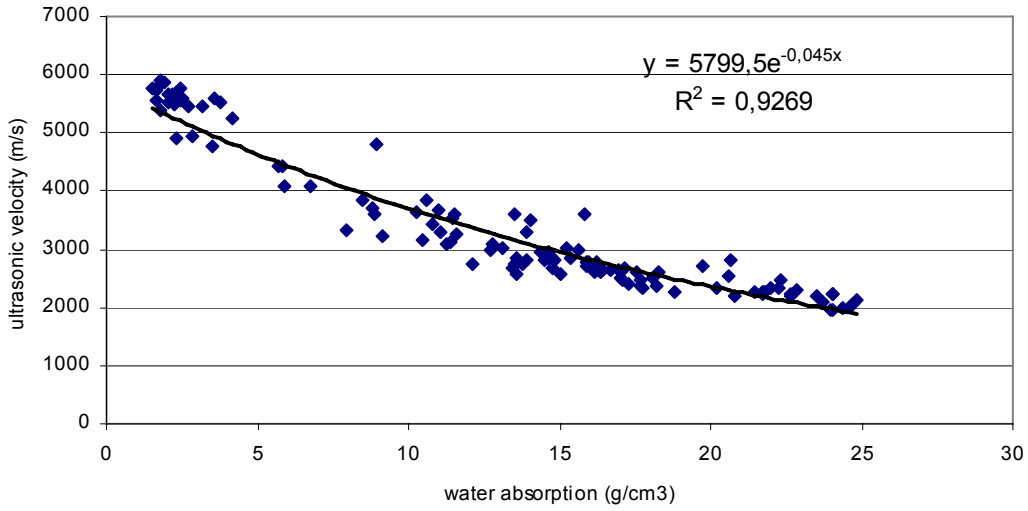

Figure 4.4. Ultrasonic Velocity – Water absorption diagram

Table 4.4. Equation and R^2 values for Ultrasonic Velocity – Water absorption

TRENDLINE TYPE	R^2	EQUATION
LINEAR	$R^2 = 0,8841$	$y = -161,8x + 5526,4$
POWER	$R^2 = 0,9172$	$y = 7834,3x^{0,3835}$
EXPONENTIAL	$R^2 = 0,9269$	$y = 5799,5e^{-0,045x}$

Figure 4.4 shows the highest R^2 for test results of the water absorption of limestones versus ultrasonic velocity. Other trends of correlation are also given in table 4.4. 118 specimens are used to perform this test. It can be seen clearly from figure 4.4, water absorption of limestone decreases as ultrasonic velocity increase. Water absorption of limestones reach the maximum value at 5909,1 m/s ultrasonic velocity and it reaches the minimum value at 1946,7 m/s ultrasonic velocity. Maximum and minimum water absorption values are 24,81 % and 1,54 %.

Rock samples were selected different from each other much possible. However, rock samples are concentrated between 2114,3 m/s and 2837,8 m/s ultrasonic velocities. If the rock samples were selected between maximum and minimum ultrasonic velocity values equally, it would be seen clearer increase in the figure 4.4. In this graphic the relationship follows an exponential law with a reasonable squared regression coefficient R-square is 0,9269 and equation is $y = 5799{,}5e^{-0{,}045x}$.

4.2.1.5. Porosity versus ultrasonic velocity for samples of Brazil test

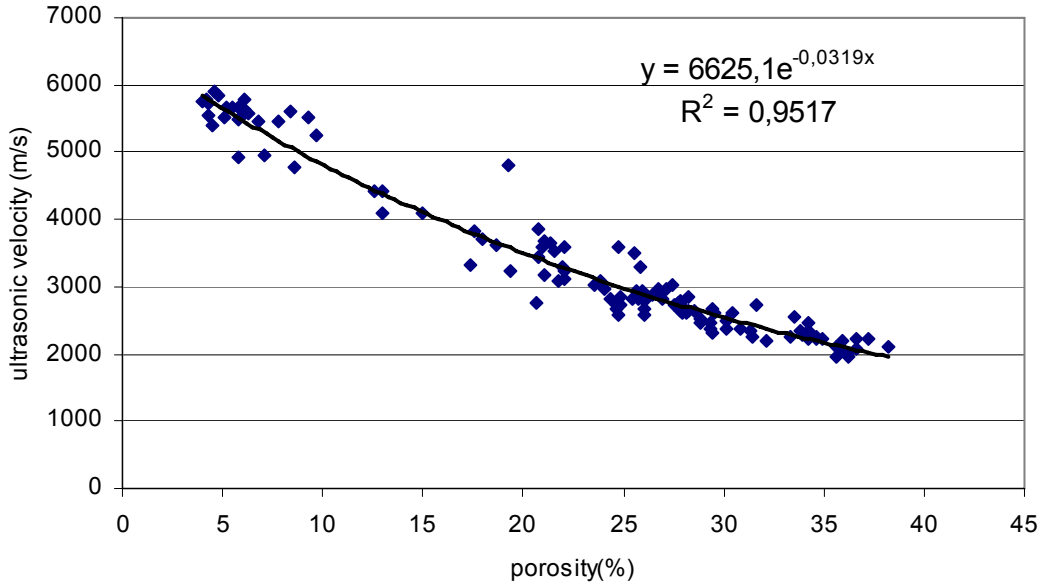

Figure 4.5. Ultrasonic Velocity – porosity diagram

Table 4.5. Equation and R^2 values for Ultrasonic Velocity – porosity

TRENDLINE TYPE	R^2	EQUATION
LINEAR	$R^2 = 0{,}9381$	$y = -116{,}66x + 6048{,}5$
POWER	$R^2 = 0{,}8976$	$y = 13143x^{-0{,}4766}$
EXPONENTIAL	$R^2 = 0{,}9517$	$y = 6625{,}1e^{-0{,}0319x}$

Figure 4.5 shows the highest R^2 for test results of the porosity of limestones versus ultrasonic velocity. Other trends of correlation are also given in table 4.5. 118 specimens are used to perform this test. It can be seen clearly from figure 4.5, porosity of limestone decreases as ultrasonic velocity increase. Porosity of limestones reach the maximum value at 5909,1 m/s ultrasonic velocity and it reaches

the minimum value at 1946,7 m/s ultrasonic velocity. Maximum and minimum porosity values are 38,2 % and 4 %.

Rock samples were selected different from each other much possible. However, rock samples are concentrated between 2114,3 m/s and 2837,8 m/s ultrasonic velocities. If the rock samples were selected between maximum and minimum ultrasonic velocity values equally, it would be seen clearer increase in the figure 4.5. In this graphic the relationship follows an exponential law with a reasonable squared regression coefficient R-square is 0,9517 and equation is $y = 6625{,}1e^{-0{,}0319x}$.

4.2.1.6.Brazillian tensile strength versus ultrasonic velocity for samples of Brazil test

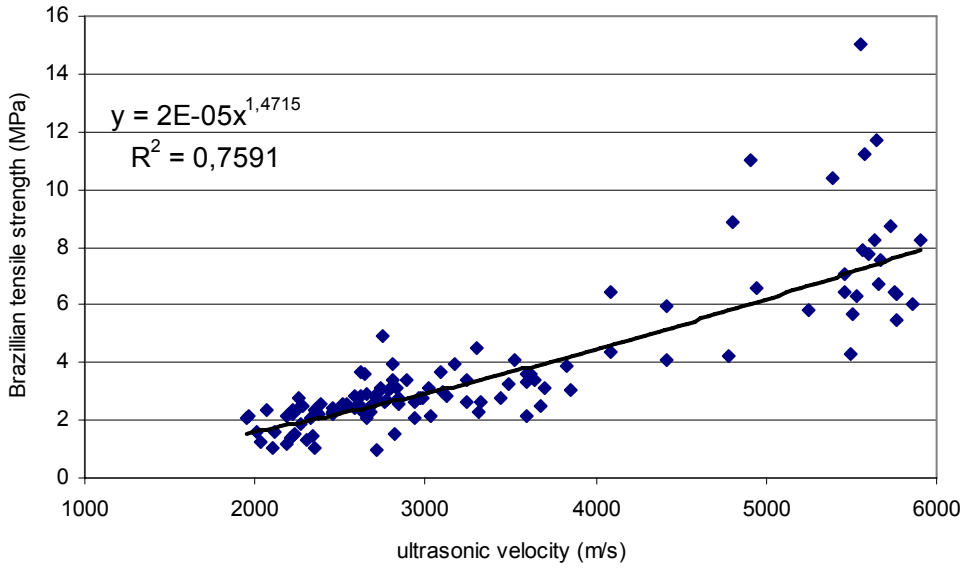

Figure 4.6. Ultrasonic Velocity – Brazillian tensile strength diagram

Table 4.6.Equation and R^2 values for Ultrasonic Velocity – Brazillian tensile strength

TRENDLINE TYPE	R^2	EQUATION
LINEAR	$R^2 = 0{,}7140$	$y = 0{,}0018x - 2{,}1318$
POWER	$R^2 = 0{,}7591$	$y = 2E\text{-}05x^{1{,}4715}$
EXPONENTIAL	$R^2 = 0{,}7556$	$y = 0{,}8317e^{0{,}0004x}$

Figure 4.6 shows the highest R^2 for test results of the brazillian tensile strength of limestones versus ultrasonic velocity. Other trends of correlation are also given in table 4.6. 118 specimens are used to perform this test. It can be seen clearly from

figure 4.6, brazillian tensile strength of limestone increases as ultrasonic velocity increase. Brazillian tensile strength of limestones reach the maximum value at 5909,1 m/s ultrasonic velocity and it reaches the minimum value at 1946,7 m/s ultrasonic velocity. Maximum and minimum brazillian tensile strength values are 8,224 MPa and 0,991 MPa.

Rock samples were selected different from each other much possible. However, rock samples are concentrated between 2007,1 m/s and 3642,0 m/s ultrasonic velocities. If the rock samples were selected between maximum and minimum ultrasonic velocity values equally, it would be seen clearer increase in the figure 4.6. In this graphic the relationship follows a power law with a reasonable squared regression coefficient R-square is 0,7591 and equation is $y = 2E - 0,5x^{1,4716}$.

4.2.1.7. Dry density versus Brazillian tensile strength

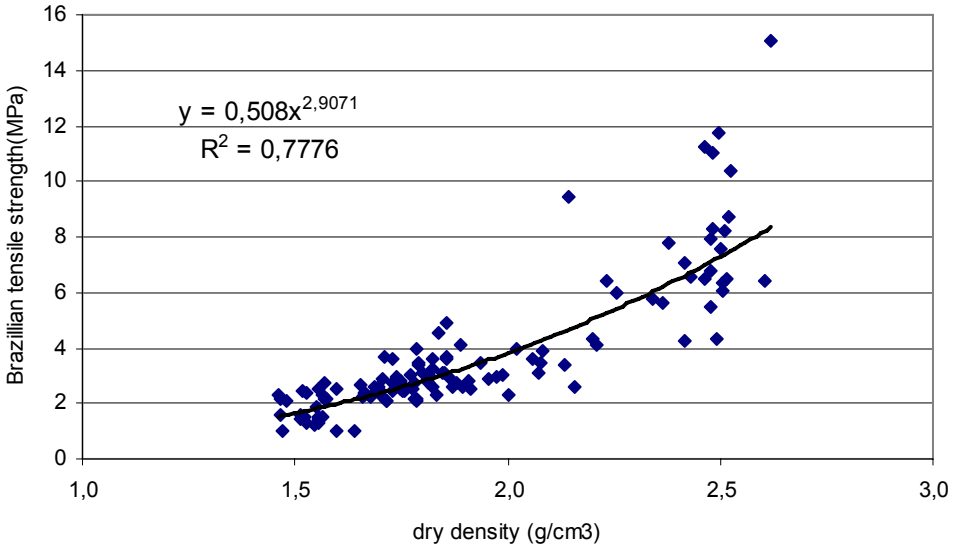

Figure 4.7. Dry density - Brazillian tensile strength diagram

Table 4.7. Equitment and R^2 values for Dry density - Brazillian tensile strength

TRENDLINE TYPE	R^2	EQUATION
LINEAR	$R^2 = 0,7086$	$y = 0,1122x + 1,4875$
POWER	$R^2 = 0,7776$	$y = 1,3803x^{0,2675}$
EXPONENTIAL	$R^2 = 0,6820$	$y = 1,5284e^{0,0554x}$

Figure 4.7 shows the highest R^2 for test results of the dry density of limestones versus brazillian tensile strength. Other trends of correlation are also given in table 4.7. 118 specimens are used to perform this test. It can be seen clearly from figure 4.7, dry density of limestone increases as Brazillian tensile strength increase. Dry density of limestones reach the maximum value at 15,06 MPa Brazillian tensile strength and it reaches the minimum value at 0,99 MPa Brazillian tensile strength. Maximum and minimum dry density values are 2,62 g/cm^3 and 1,46 g/cm^3.

Rock samples were selected different from each other much possible. However, rock samples are concentrated dense between 0,99 MPa and 3,90 MPa Brazillian tensile strengths. If the rock samples were selected between maximum and minimum Brazillian tensile strength values equally, it would be seen clearer increase in the figure 4.7.In this graphic the relationship follows a power law with a reasonable squared regression coefficient R-square is 0,7776 and equation is $y = 1{,}3803x^{0{,}2675}$.

4.2.1.8. Bulk density versus Brazillian tensile strength

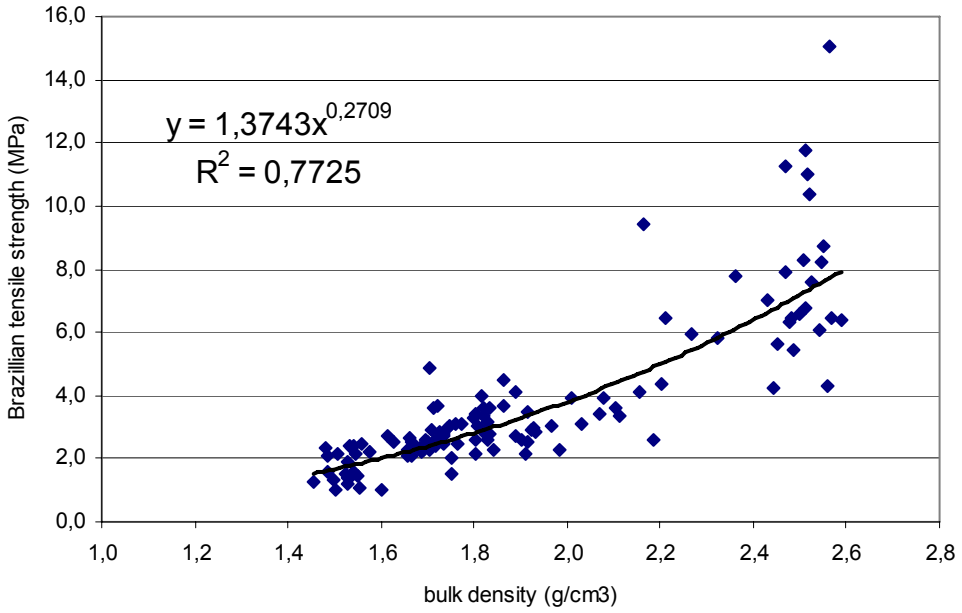

Figure 4.8. Bulk density - Brazillian tensile strength diagram

Table 4.8. Equitment and R^2 values for Bulk density - Brazillian tensile strength

TRENDLINE TYPE	R^2	EQUATION
LINEAR	$R^2 = 0,6980$	$y = 0,1137x + 1,4822$
POWER	$R^2 = 0,7725$	$y = 1,3743x^{0,2709}$
EXPONENTIAL	$R^2 = 0,6761$	$y = 1,5242e^{0,056x}$

Figure 4.8 shows the highest R^2 for test results of the bulk density of limestones versus brazillian tensile strength. Other trends of correlation are also given in table 4.8. 118 specimens are used to perform this test. It can be seen clearly from figure 4.8, bulk density of limestone increases as Brazillian tensile strength increase. Bulk density of limestones reach the maximum value at 15,06 MPa Brazillian tensile strength and it reaches the minimum value at 0,99 MPa Brazillian tensile strength . Maximum and minimum bulk density values are 2,59 g/cm^3 and 1,45 g/cm^3.

Rock samples were selected different from each other much possible. However, rock samples are concentrated between 0,99 MPa and 3,90 MPa Brazillian tensile strengths. If the rock samples were selected between maximum and minimum Brazillian tensile strength values equally, it would be seen clearer increase in the figure 4.8. In this graphic the relationship follows a power law with a reasonable squared regression coefficient R-square is 0,7725 and equation is $y = 1,3743x^{0,2709}$.

4.2.1.9. Saturated density versus Brazillian tensile strength

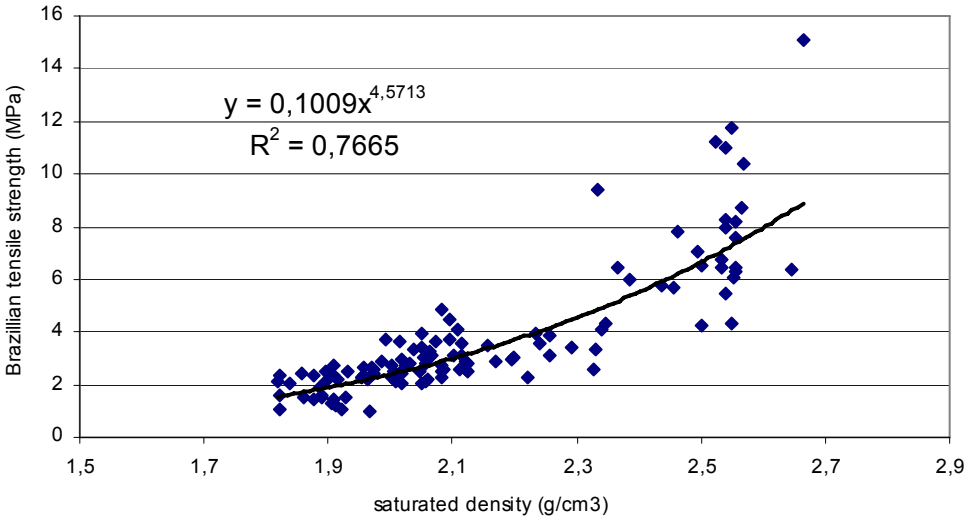

Figure 4.9. Saturated density - Brazillian tensile strength diagram

Table 4.9. Equitment and R^2 values for Saturated density - Brazillian tensile strength

TRENDLINE TYPE	R^2	EQUATION
LINEAR	$R^2 = 0,7054$	$y = 0,0785x + 1,8465$
POWER	$R^2 = 0,7665$	$y = 1,7533x^{0,1677}$
EXPONENTIAL	$R^2 = 0,6885$	$y = 1,866e^{0,0351x}$

Figure 4.9 shows the highest R^2 for test results of the saturated density of limestones versus brazillian tensile strength. Other trends of correlation are also given in table 4.9. 118 specimens are used to perform this test. It can be seen clearly from figure 4.9, saturated density of limestone increases as Brazillian tensile strength increase. Saturated density of limestones reach the maximum value at 15,06 MPa Brazillian tensile strength and it reaches the minimum value at 0,99 MPa Brazillian tensile strength . Maximum and minimum saturated density values are 2,66 g/cm^3 and 1,82 g/cm^3.

Rock samples were selected different from each other much possible. However, rock samples are concentrated between 0,99 MPa and 3,90 MPa Brazillian tensile strengths. If the rock samples were selected between maximum and minimum Brazillian tensile strength values equally, it would be seen clearer increase in the

figure 4.9. In this graphic the relationship follows a power law with a reasonable squared regression coefficient R-square is 0,7665. and equation is $y = 1{,}7533x^{0{,}1677}$.

4.2.1.10. Water absorption versus Brazillian tensile strength

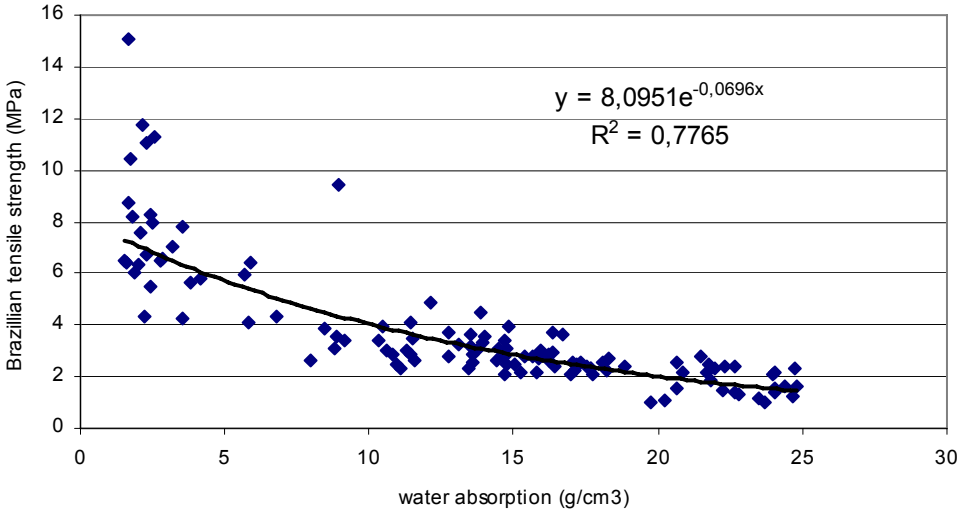

Figure 4.10. Water absorption - Brazillian tensile strength diagram

Table 4.10.Equitment and R^2 values for Water absorption - Brazillian tensile strength

TRENDLINE TYPE	R^2	EQUATION
LINEAR	$R^2 = 0{,}6446$	$y = -0{,}2869x + 7{,}605$
POWER	$R^2 = 0{,}7645$	$y = 12{,}845x^{-0{,}5917}$
EXPONENTIAL	$R^2 = 0{,}7765$	$y = 8{,}0951e^{-0{,}0696x}$

Figure 4.10 shows the highest R^2 for test results of the water absorption of limestones versus brazillian tensile strength. Other trends of correlation are also given in table 4.10. 118 specimens are used to perform this test. It can be seen clearly from figure 4.10, water absorption of limestone decreases as Brazillian tensile strength increase. Water absorption of limestones reach the maximum value at 15,06 MPa Brazillian tensile strength and it reaches the minimum value at 0,99 MPa Brazillian tensile strength . Maximum and minimum water absorption values are 24,81 % and 1,54 %.

Rock samples were selected different from each other much possible. However, rock samples are concentrated between 0,99 MPa and 3,90 MPa Brazillian tensile strengths. If the rock samples were selected between maximum and minimum Brazillian tensile strength values equally, it would be seen clearer increase in the figure 4.10. In this graphic the relationship follows an exponential law with a reasonable squared regression coefficient R-square is 0,7765 and equation is $y = 8{,}0951e^{-0{,}0696x}$.

4.2.1.11. Porosity versus Brazillian tensile strength

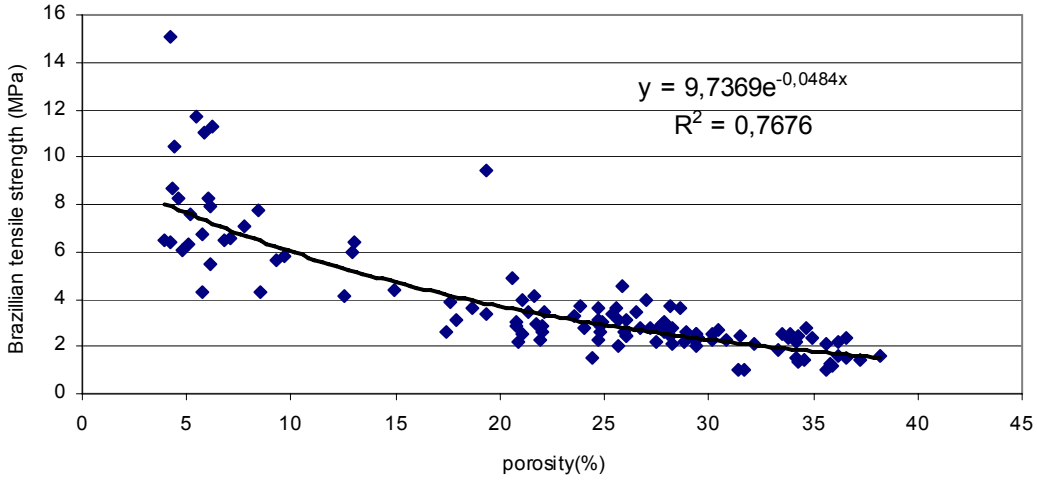

Figure 4.11. Porosity - Brazillian tensile strength diagram

Table 4.11. Equitment and R^2 values for Porosity - Brazillian tensile strength

TRENDLINE TYPE	R^2	EQUATION
LINEAR	$R^2 = 0{,}6861$	$y = -0{,}2072x + 8{,}539$
POWER	$R^2 = 0{,}7366$	$y = 28{,}057x^{-0{,}7297}$
EXPONENTIAL	$R^2 = 0{,}7676$	$y = 9{,}7369e^{-0{,}0484x}$

Figure 4.11 shows the highest R^2 for test results of the porosity of limestones versus brazillian tensile strength. Other trends of correlation are also given in table 4.11. 118 specimens are used to perform this test. It can be seen clearly from figure 4.11, porosity of limestone decreases as Brazillian tensile strength increase. porosity of limestones reach the maximum value at 15,06 MPa Brazillian tensile strength and it

reaches the minimum value at 0,99 MPa Brazillian tensile strength . Maximum and minimum porosity values are 38,2 % and 4 %.

Rock samples were selected different from each other much possible. However, rock samples are concentrated between 0,99 MPa and 3,90 MPa Brazillian tensile strengths. If the rock samples were selected between maximum and minimum Brazillian tensile strength values equally, it would be seen clearer increase in the figure 4.11. In this graphic the relationship follows an exponential law with a reasonable squared regression coefficient R-square is 0,7676 and equation is $y = 9{,}7369e^{-0{,}0484x}$.

4.3. Direct Shear Test

Direct shear test was performed according to ISRM (1981). 12 samples were used for direct shear test.Samples used for direct shear test are core specimens which has a diameter of 60 mm and has a length 100 mm. This test is not confidental because of the lack of the specimen friction between the concretes after the sample was broken.

4.3.1. Results

Result obtained from Direct shear test were plotted on graphics.

4.3.1.1. Dry density versus ultrasonic velocity for samples of direct shear test

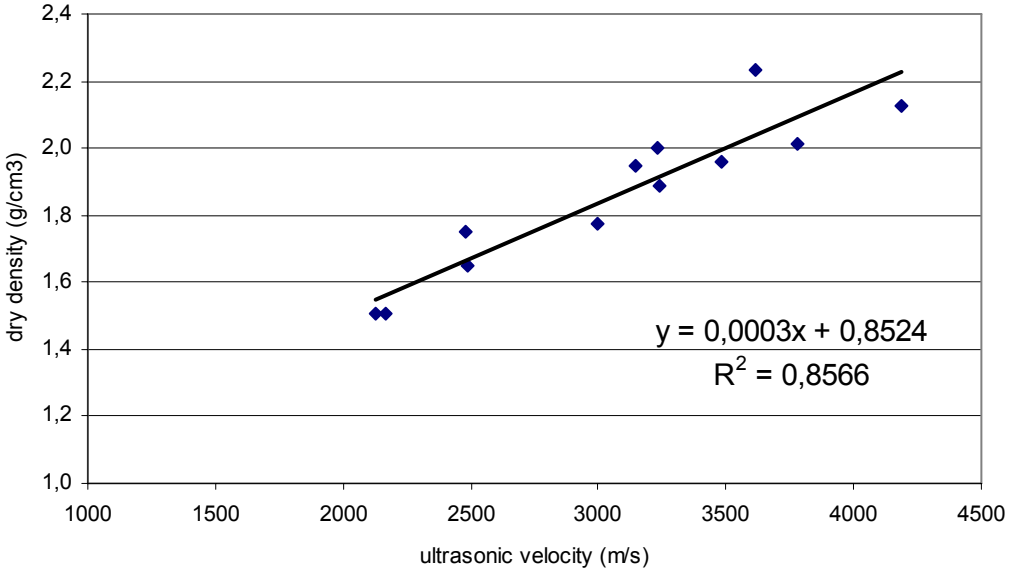

Figure 4.12. Ultrasonic Velocity – Dry density diagram

Table 4.12. Equitment and R^2 values for Ultrasonic Velocity – Dry density

TRENDLINE TYPE	R^2	EQUATION
LINEAR	$R^2 = 0,8566$	$y = 0,0003x + 0,8524$
POWER	$R^2 = 0,8911$	$y = 0,0233x^{0,5458}$
EXPONENTIAL	$R^2 = 0,8619$	$y = 1,0596e^{0,0002x}$

Figure 4.12 shows the highest R^2 for test results of the dry density of limestones versus ultrasonic velocity. Other trends of correlation are also given in table 4.12. 12 specimens are used to perform this test. It can be seen clearly from figure 4.12, dry density of limestone increases as ultrasonic velocity increase. Dry density of limestones reach the maximum value at 4186,9 m/s ultrasonic velocity and it reaches the minimum value at 2129,9 m/s ultrasonic velocity. Maximum and minimum dry density values are 2,23 g/cm^3 and 1,51 g/cm^3.

In this graphic the relationship follows a linear law with a reasonable squared regression coefficient R-square is 0,8566 and equation is y = 0,0003x + 0,8524.

4.3.1.2. Bulk density versus ultrasonic velocity for samples of direct shear test

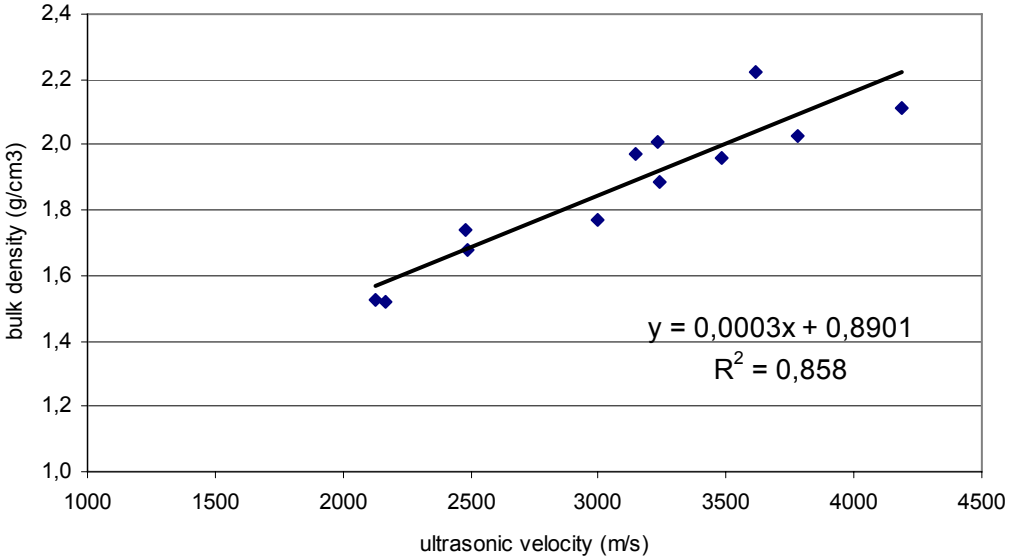

Figure 4.13. Ultrasonic Velocity – Bulk density diagram

Table 4.13. Equitment and R^2 values for Ultrasonic Velocity – Bulk density

TRENDLINE TYPE	R^2	EQUATION
LINEAR	$R^2 = 0,8580$	$y = 0,0003x + 0,8901$
POWER	$R^2 = 0,8928$	$y = 0,0272x^{0,5271}$
EXPONENTIAL	$R^2 = 0,8624$	$y = 1,0844e^{0,0002x}$

Figure 4.13 shows the highest R^2 for test results of the bulk density of limestones versus ultrasonic velocity. Other trends of correlation are also given in table 4.13. 12 specimens are used to perform this test. It can be seen clearly from figure 4.13, bulk density of limestone increases as ultrasonic velocity increase. Bulk density of limestones reach the maximum value at 4186,2 m/s ultrasonic velocity and it reaches the minimum value at 2129,9 m/s ultrasonic velocity. Maximum and minimum bulk density values are 2,22 g/cm^3 and 1,52 g/cm^3.

In this graphic the relationship follows a linear law with a reasonable squared regression coefficient R-square is 0,858 and equation is y = 0,0003x + 0,8901.

4.3.1.3. Saturated density versus ultrasonic velocity for samples of direct shear test

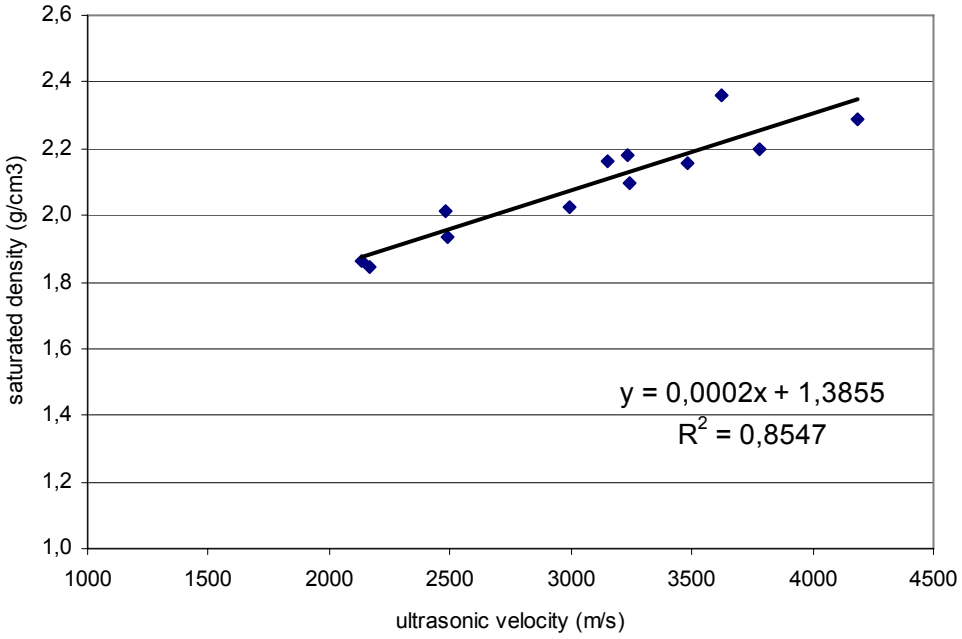

Figure 4.14. Ultrasonic Velocity – Saturated density

Table 4.14. Equitment and R^2 values for Ultrasonic Velocity – Saturated density

TRENDLINE TYPE	R^2	EQUATION
LINEAR	$R^2 = 0,8547$	$y = 0,0002x + 1,3855$
POWER	$R^2 = 0,8801$	$y = 0,1444x^{0,3334}$
EXPONENTIAL	$R^2 = 0,8610$	$y = 1,483e^{0,0001x}$

Figure 4.14 shows the highest R^2 for test results of the saturated density of limestones versus ultrasonic velocity. Other trends of correlation are also given in table 4.14. 12 specimens are used to perform this test. It can be seen clearly from figure 4.14, saturated density of limestone increases as ultrasonic velocity increase. Saturated density of limestones reach the maximum value at 4186,2 m/s ultrasonic velocity and it reaches the minimum value at 2129,9 m/s ultrasonic velocity. Maximum and minimum saturated density values are 2,36 g/cm^3 and 1,84 g/cm^3.

In this graphic the relationship follows a linear law with a reasonable squared regression coefficient R-square is 0,8547 and equation is y = 0,0002x + 1,3855.

4.3.1.4. Water absorption versus ultrasonic velocity for samples of direct shear test

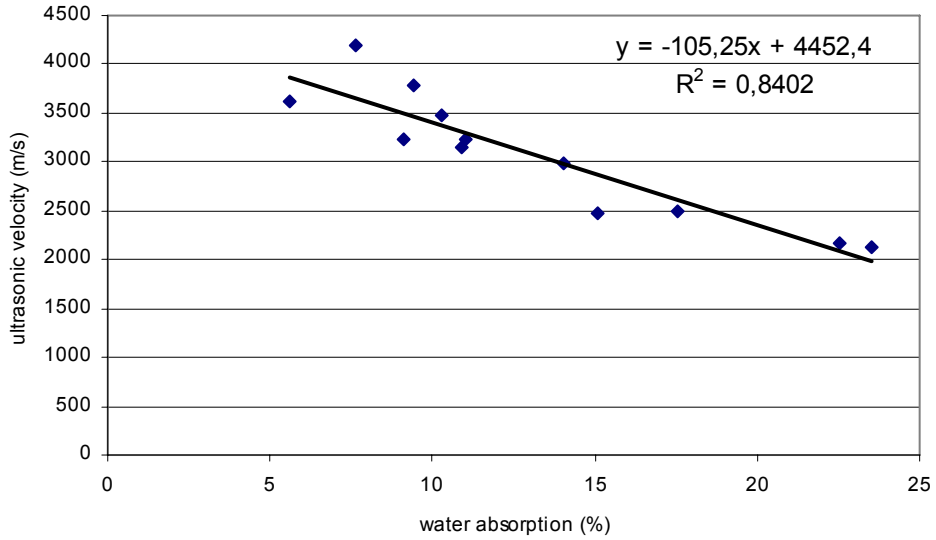

Figure 4.15. Ultrasonic Velocity – Water absorption

Table 4.15. Equitment and R^2 values for Ultrasonic Velocity – Water absorption

TRENDLINE TYPE	R^2	EQUATION
LINEAR	$R^2 = 0,8402$	$y = -105,25x + 4452,4$
POWER	$R^2 = 0,8474$	$y = 9688,7x^{-0,4701}$
EXPONENTIAL	$R^2 = 0,8874$	$y = 4847,4e^{-0,0364x}$

Figure 4.15 shows the highest R^2 for test results of the water absorption of limestones versus ultrasonic velocity. Other trends of correlation are also given in table 4.15. 12 specimens are used to perform this test. It can be seen clearly from figure 4.15, water absorption of limestone decreases as ultrasonic velocity increase. Water absorption of limestones reach the maximum value at 4186,2 m/s ultrasonic velocity and it reaches the minimum value at 2129,9 m/s ultrasonic velocity. Maximum and minimum water absorption values are 23,50 % and 5,60 %.

In this graphic the relationship follows a linear law with a reasonable squared regression coefficient R-square is 0,8402 and equation is y = -105,25x + 4452,4 the

4.3.2. Determination of friction angle and cohesion of limestone samples by direct shear test

In this part friction angle and cohesion of limestone samples were determined. limestone samples were divided into four groups according to their ultrasonic velocity values. Four different samples selected out of variety of limestone samples that represent each group. Results are found out and represented as figures and tables.

- Hard limestone
- Medium limestone
- Soft limestone
- Very soft limestone

4.3.2.1. Hard limestone

Table 4.16. Direct Shear Test Results (Hard limestone)

Sample no	N (kN)	T (kN)	Diameter (mm)	Area (m2)	shear strength (kPa)	normal stress (kPa)
62	2,5	10,5	62	0,00302	3479,66	828,49
25	5	14	61,1	0,00293	4777,23	1706,15
1	5	13	62	0,00302	4308,15	1656,98
57	7,5	18	60,8	0,00290	6202,91	2584,55

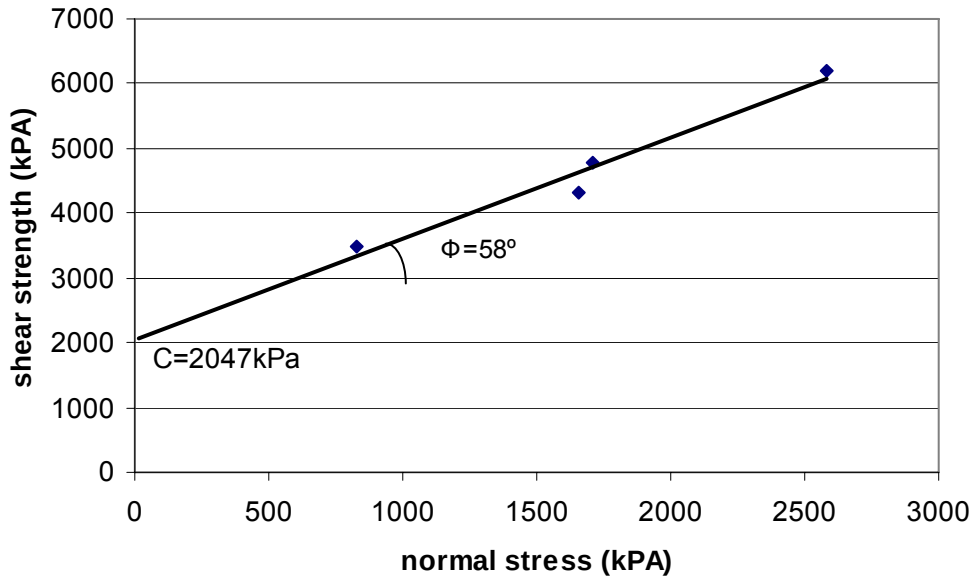

Figure 4.16. Shear Strength – Normal stress diagram (hard limestone)

Figure 4.16 shows the shear strength – normal stress diagram of the hard limestone samples. Other values which was obtained from the test is given in table 4.16. Four specimens are used to performe this test. As can be seen from figure 4.16, shear strength increases as normal strength increase. From this figure friction angle and cohesion can be determined. The cohesion of this group determined from the graphic is 2047 kPa and the friction angle is 58°.

4.3.2.2. Medium limestone

Table 4.17. Direct Shear Test Results (Medium limestone)

Sample no	N (kN)	T (kN)	Diameter (mm)	Area (m2)	shear strength (kPa)	normal stress (kPa)
70	2,5	4	61,1	0,00293	1364,92	853,08
37	5	7	60,2	0,00284	2460,57	1757,55
8	7,5	11	60,7	0,00289	3803,17	2593,07
79	8,5	12	60,6	0,002883	4162,62	2948,52

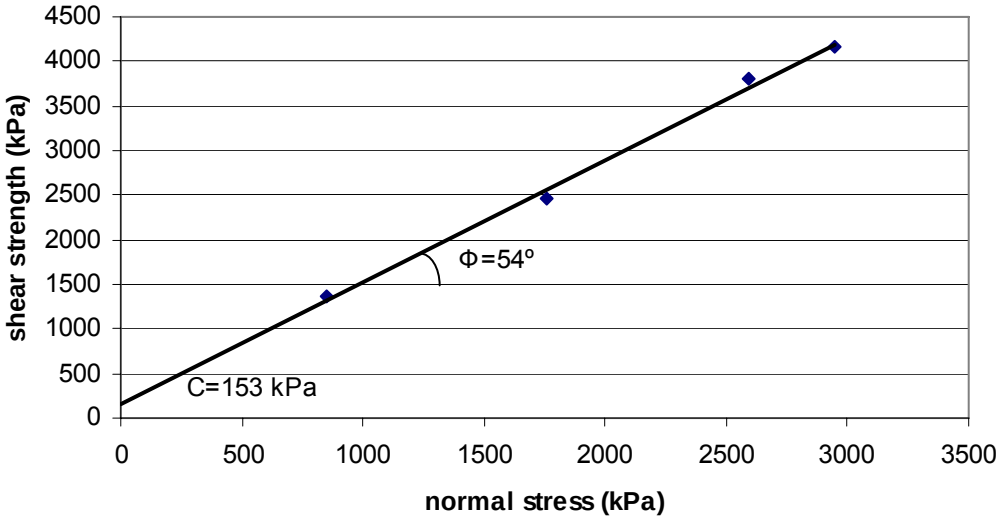

Figure 4.17. Shear Strength – Normal stress diagram (Medium limestone)

Figure 4.17 shows the shear strength – normal stress diagram of the medium limestone samples. Other values which was obtained from the test is given in table 4.17. Four specimens are used to performe this test. As can be seen from figure 4.17, shear strength increases as normal strength increase. From this figure friction angle and cohesion can be determined. The cohesion of this group determined from the graphic is 153 kPa and the friction angle is 54^0.

4.3.2.3. Soft limestone

Table 4.18. Direct Shear Test Results (soft limestone)

Sample no	N (kN)	T (kN)	Diameter mm	Area (m2)	shear strength (kPa)	normal stress (kPa)
41	2,5	5,5	61,4	0,00296	1858,47	844,76
32	5	7,5	60,2	0,00285	2636,32	1757,55

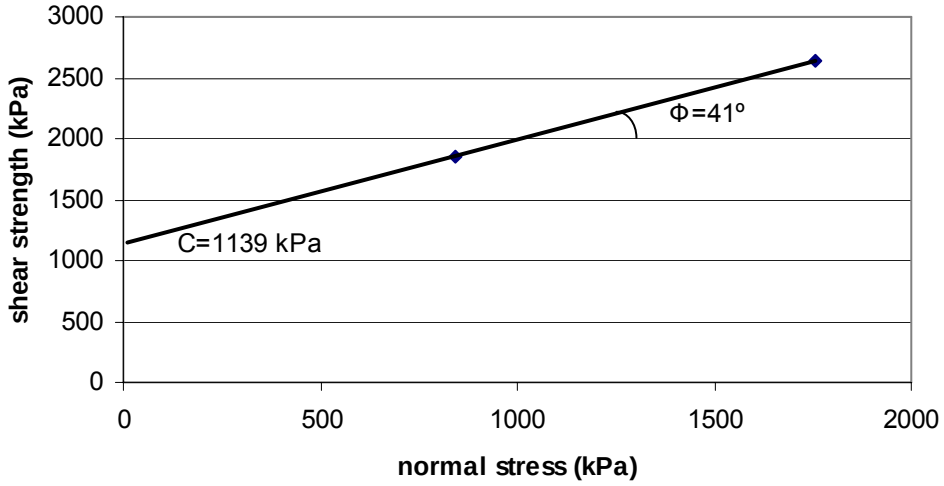

Figure 4.18. Shear Strength – Normal stress diagram (soft limestone)

Figure 4.18 shows the shear strength – normal stress diagram of the soft limestone samples. Other values which was obtained from the test is given in table 4.18. Two specimens are used to performe this test. As can be seen from figure 4.18, shear strength increases as normal strength increase. From this figure friction angle and cohesion can be determined. The cohesion of this group determined from the graphic is 1139 kPa and the friction angle is 41^0.

4.3.2.4. Very soft limestone

Table 4.19. Direct Shear Test Results (Very soft limestone)

Sample no	N (kN)	T (kN)	Diameter Mm	Area (m2)	shear strength (kPa)	normal stress (kPa)
71	2,5	3,5	60	0,00283	1238,50	884,64
17	5	6,5	59,5	0,00278	2338,89	1799,15

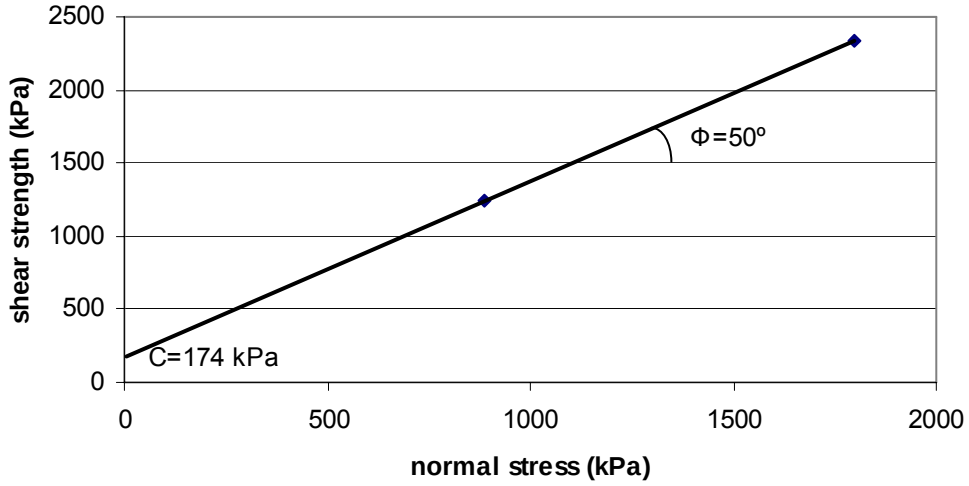

Figure 4.19. Shear Strength – Normal stress diagram (Very soft limestone)

Figure 4.19 shows the shear strength – normal stress diagram of the very soft limestone samples. Other values which was obtained from the test is given in table 4.19.Two specimens are used to performe this test. As can be seen from figure 4.19, shear strength increases as normal strength increase. From this figure friction angle and cohesion can be determined. The cohesion of this group determined from the graphic is 174 kPa and the friction angle is 50^0.

4.3.2.5. Graphics ultrasonic velocity versus friction angle and cohesion.

Table 4.20. Friction angle and cohesion values for each group

Sample No	Cohesion (kPa)	Angle Φ	Average Velocity (m/s)
70-37-8-79	153	54	3154,239
62-25-1-57	2047	58	3766,266
32-41	1139	41	2486,683
17-71	174	50	2146,516

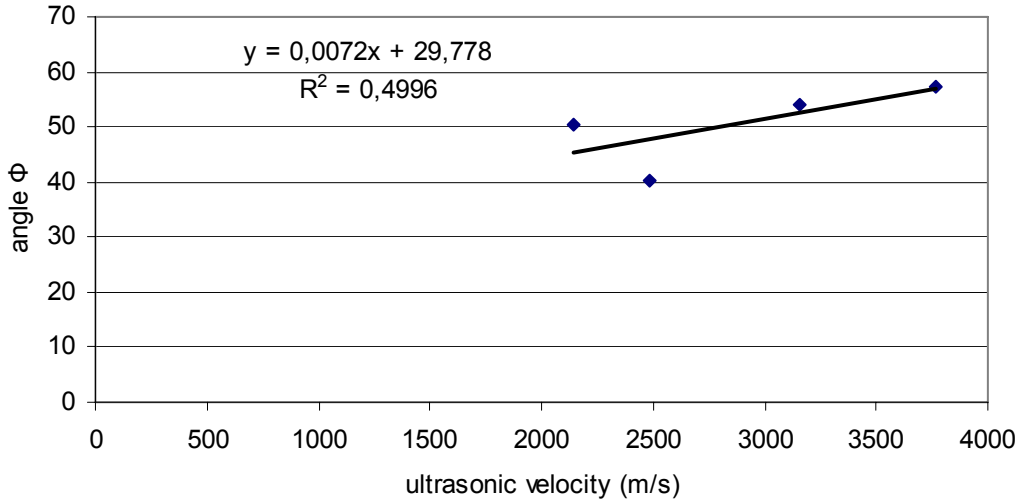

Figure 4.20. Friction angle – Ultrasonic velocity diagram

Table 4.21. Equitment and R^2 values for Ultrasonic Velocity – Friction angle

TRENDLINE TYPE	R^2	EQUATION
LINEAR	$R^2 = 0,4996$	$y = 0,0072x + 29,778$
POWER	$R^2 = 0,4148$	$y = 2,201x^{0,3933}$
EXPONENTIAL	$R^2 = 0,4553$	$y = 33,148e^{0,0001x}$

Figure 4.20 shows the highest R^2 for test results of the friction angle of limestones versus ultrasonic velocity. Other trends of correlation are also given in table 4.21 and table 4.20 shows the friction angle, cohesion and ultrasonic velocity values for each group. 12 specimens are used to perform this test. As can be seen from the figure 4.20 friction angle increases as ultrasonic velocity inceases.

In this graphic the relationship follows a linear law with a reasonable squared regression coefficient R-square is 0,4996 and equation is y = 0,0072x+29,778.

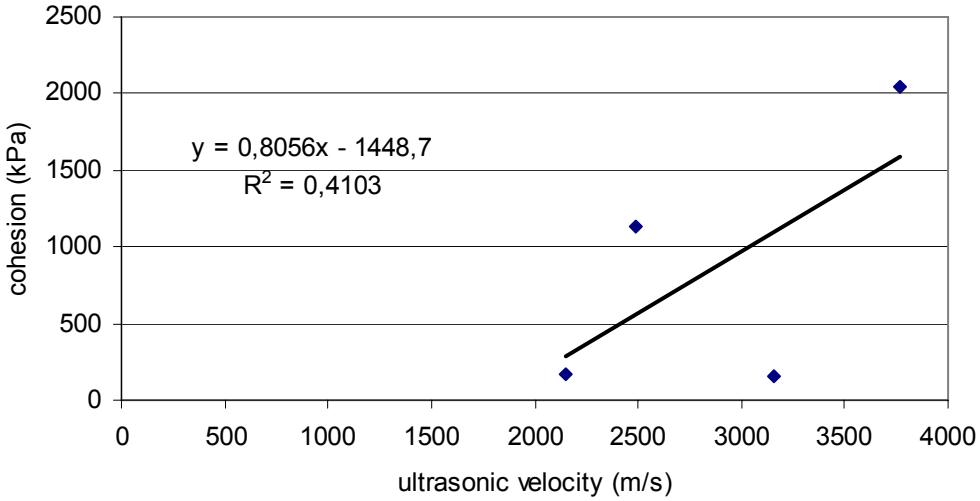

Figure 4.21. Cohesion – Ultrasonic velocity diagram

Table 4.22. Equitment and R^2 values for Ultrasonic Velocity – Cohesion

TRENDLINE TYPE	R^2	EQUATION
LINEAR	$R^2 = 0,4103$	$y = 0,8056x-1448,7$
POWER	$R^2 = 0,2182$	$y = 2E-06x^{2,4626}$
EXPONENTIAL	$R^2 = 0,2345$	$y = 38,717e^{0,0009x}$

Figure 4.21 shows the highest R^2 for test results of the cohesion of limestones versus ultrasonic velocity. Other trends of correlation are also given in table 4.22. 12 specimens are used to this test. As can be seen from the figure cohesion increases as ultrasonic velocity increases.

In this graphic the relationship follows a linear law with a reasonable squared regression coefficient R-square is 0,4103 and equation is y = 0,8056x-1448,7.

4.3.3. Determination of residual friction angle and cohesion of limestone samples by direct shear test

In this part residual friction angle and cohesion of limestone samples were determined. limestone samples were divided into four groups according to their ultrasonic velocity values. And four samples selected out of variety of limestone

samples that represent each group. Results are found out and represented as figures and tables.

- Hard limestone
- Medium limestone
- Soft limestone
- Very soft limestone

4.3.3.1. Hard limestone

Table 4.23. Direct Shear Test Results obtained for residual strength (hard limestone)

Sample no	N (kN)	T (kN)	Diameter (mm)	Area (m2)	shear strength (kPa)	normal stress (kPa)
62	2,5	3	62	0,00302	994,19	828,49
25	5	7,5	61,1	0,00293	2559,23	1706,15
1	5	7,5	62	0,00302	2485,47	1656,98
57	7,5	10	60,8	0,00290	3446,06	2584,55

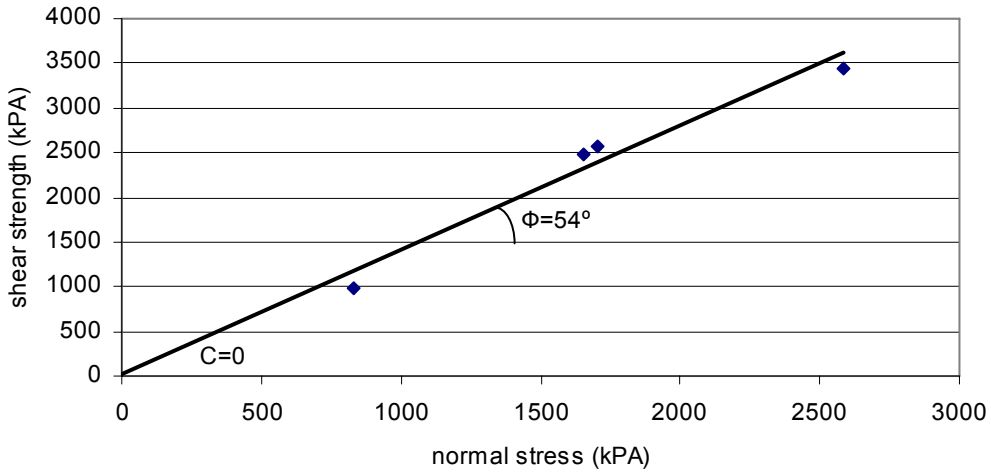

Figure 4.22. Shear Strength – Normal stress diagram for residual strength (hard limestone)

Figure 4.22 shows the shear strength – normal stress diagram of the hard limestone samples. Other values which was obtained from the test is given in table 4.23. Four specimens are used to performe this test. As can be seen from figure 4.22, shear

strength increases as normal strength increase. From this figure friction angle and cohesion can be determined. The cohesion of this group determined from the graphic is 0 kPa and the friction angle is 54^0.

4.3.3.2. Medium limestone

Table 4.24. Direct Shear Test Results obtained for residual strength (Medium limestone)

Sample no	N (kN)	T (kN)	Diameter (mm)	Area (m2)	shear strength (kPa)	normal stress (kPa)
70	2,5	2,5	61,1	0,00293	853,08	853,08
37	5	6	60,2	0,00284	2109,06	1757,55
8	7,5	7,5	60,7	0,00289	2593,07	2593,07
79	8,5	9,5	60,6	0,00288	3295,40	2948,52

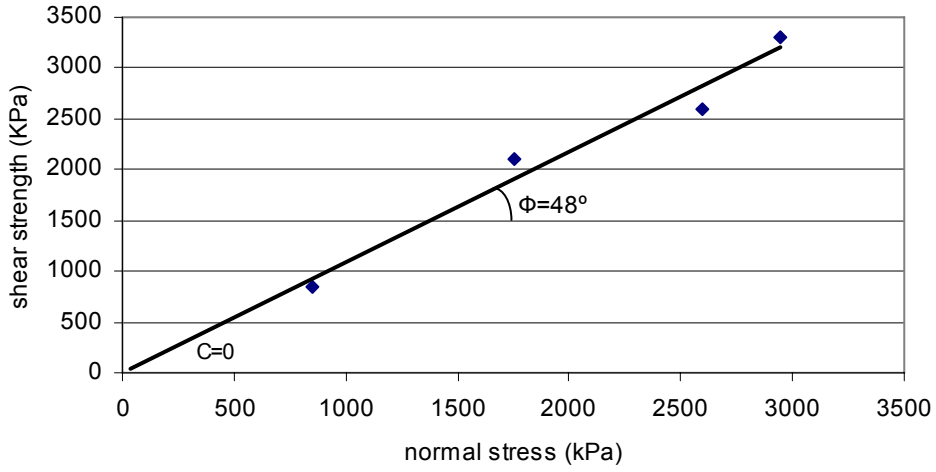

Figure 4.23. Shear Strength – Normal stress diagram for residual strength (Medium limestone)

Figure 4.23 shows the shear strength – normal stress diagram of the medium limestone samples. Other values which was obtained from the test is given in table 4.24. Four specimens are used to performe this test. As can be seen from figure 4.23, shear strength increases as normal strength increase. From this figure friction angle and cohesion can be determined. The cohesion of this group determined from the graphic is 0 kPa and the friction angle is 48^0.

4.3.3.3. Soft limestone

Table 4.25. Direct Shear Test Results obtained for residual strength (soft limestone)

Sample no	N (kN)	T (kN)	Diameter mm	Area (m2)	shear strength (kPa)	normal stress (kPa)
41	2,5	3	61,4	0,00296	1013,71	844,761
32	5,0	6	60,2	0,00285	2109,06	1757,55

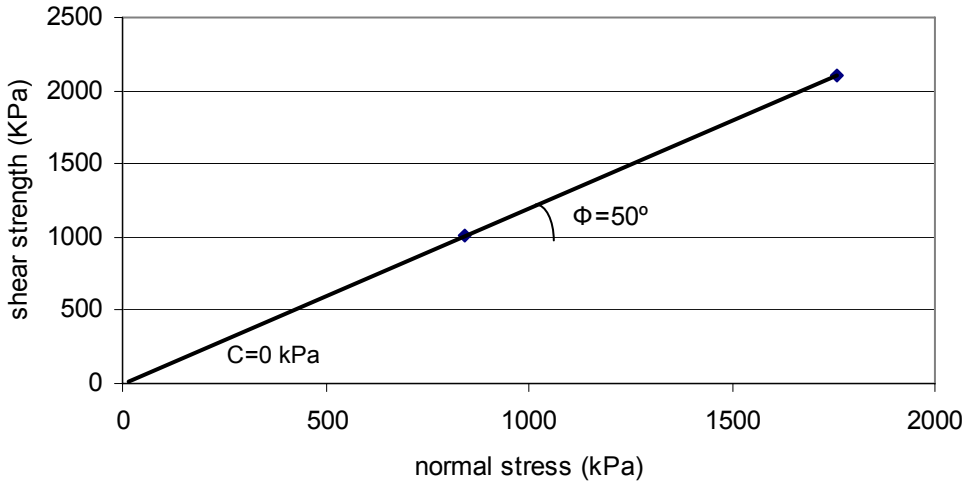

Figure 4.24. Shear Strength – Normal stress diagram for residual strength (soft limestone)

Figure 4.24 shows the shear strength – normal stress diagram of the soft limestone samples. Other values which was obtained from the test is given in table 4.25. Four specimens are used to performe this test. As can be seen from figure 4.24, shear strength increases as normal strength increase. From this figure friction angle and cohesion can be determined. The cohesion of this group determined from the graphic is 0 kPa and the friction angle is 50^0.

4.3.3.4 Very soft limestone

Table 4.26. Direct Shear Test Results obtained for residual strength (Very soft limestone)

Sample no	N (kN)	T (kN)	Diameter mm	Area (m2)	shear strength (kPa)	normal stress (kPa)
71	2,5	2	60	0,00283	707,71	884,64
17	5	4	59,5	0,00278	1439,32	1799,15

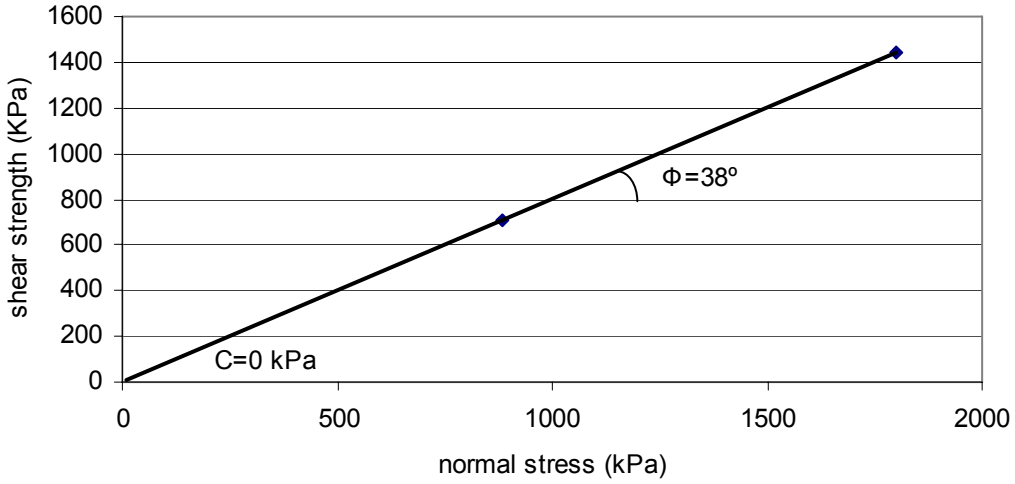

Figure 4.25. Shear Strength – Normal stress diagram for residual strength (Very soft limestone)

Figure 4.25 shows the shear strength – normal stress diagram of the very soft limestone samples. Other values which was obtained from the test is given in table 4.26. Four specimens are used to performe this test. As can be seen from figure 4.25, shear strength increases as normal strength increase. From this figure friction angle and cohesion can be determined. The cohesion of this group determined from the graphic is 0 kPa and the friction angle is 38^0.

4.3.3.5. Graphics ultrasonic velocity versus residual friction angle and cohesion.

Table 4.27. Friction angle and cohesion values for each group obtained for residual shear strength

Sample No	Cohesion (kPa)	Angle Φ	Average Velocity (m/s)
70-37-8-79	0	48	3154,239
62-25-1-57	0	54	3766,266
32-41	0	50	2486,683
17-71	0	38	2146,516

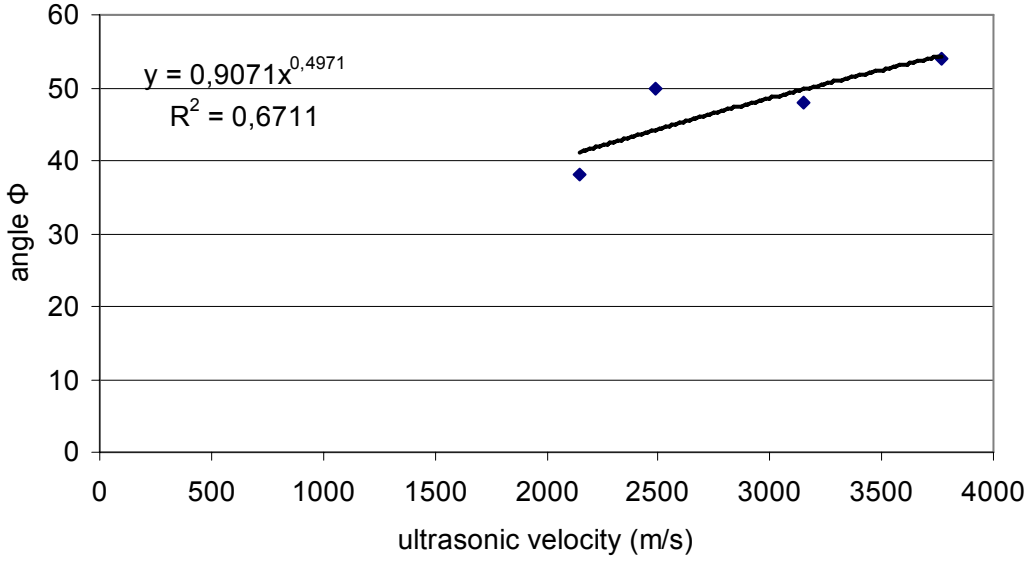

Figure 4.26. Residual friction angle – Ultrasonic velocity diagram

Table 4.28.Equitment and R^2 values for Ultrasonic Velocity – Residual friction angle

TRENDLINE TYPE	R^2	EQUATION
LINEAR	$R^2 = 0,6541$	$y = 0,0077x+25,401$
POWER	$R^2 = 0,6711$	$y = 0,9071x^{0,4971}$
EXPONENTIAL	$R^2 = 0,6350$	$y = 29,03e^{0,0002x}$

Figure 4.26 shows the highest R^2 for test results of the residual friction angle of limestones versus ultrasonic velocity. Other trends of correlation are also given in table 4.28 and table 4.27 shows the residual friction angle, residual cohesion and

ultrasonic velocity values for each group. 12 specimens are used to perform this test. As can be seen from the figure 4.26 friction angle is increases as ultrasonic velocity increases. But one of the residual friction angle is bigger than the normal friction angle, but not. Because of the friction between the concretes after the sample was broken.

In this graphic the relationship follows a power law with a reasonable squared regression coefficient R-square is 0,6711 and equation is $y = 0{,}9071x^{0{,}4971}$.

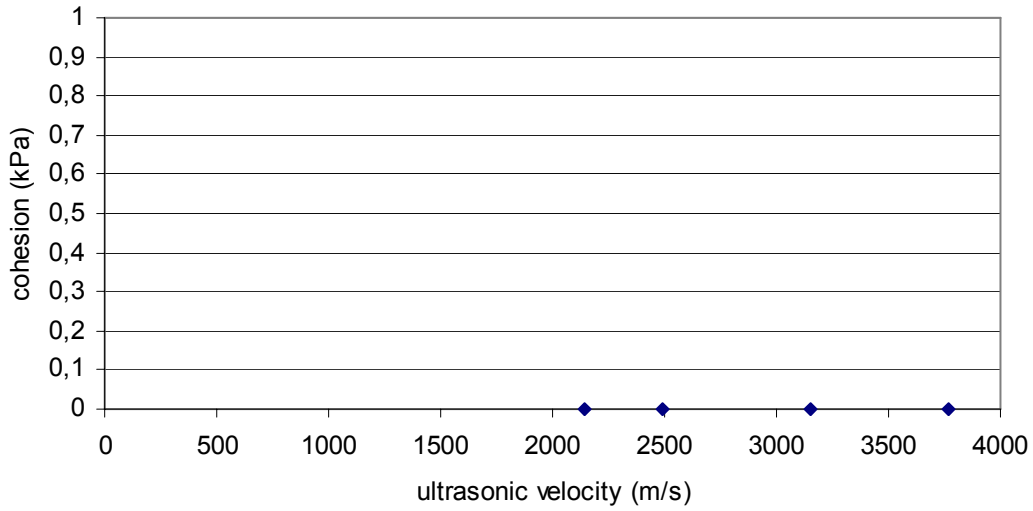

Figure 4.27. Residual cohesion – Ultrasonic velocity diagram

Figure 4.27 shows the ultrasonic velocity – residual cohesion diagram. 12 specimens are used to perform this test. In the case of the residual strength, the cohesion *c* has dropped to zero and the relationship between Φr and σn can be represented by:
τr =σn tanΦr, where Φr is the residual angle of friction [45].

As can be seen from the figure; the cohesion of the samples aproximate zero.

4.4. Uniaxial Compression Test

Uniaxial compression test was performed according to ISRM(1981). 115 samples were used for uniaxial compression test. Samples used for uniaxial compression test are core specimens which has a diameter of 60 mm and has a length 150 mm.

4.4.1. Results

Result obtained from Uniaxial compression test were plotted on graphics.

4.4.1.1. Dry density versus ultrasonic velocity for samples of uniaxial compression test

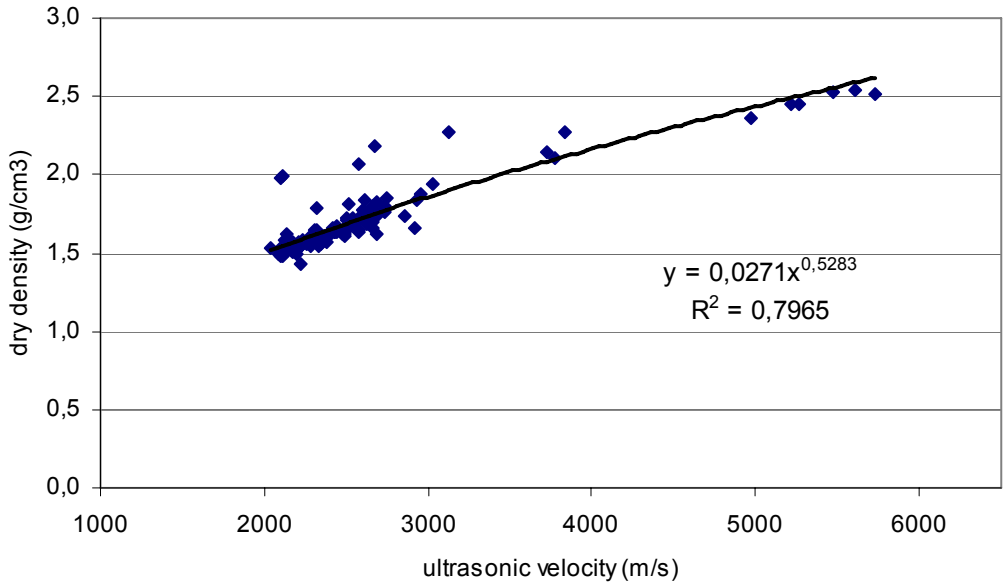

Figure 4.28. Ultrasonic Velocity – Dry density diagram

Table 4.29.Equitment and R^2 values for Ultrasonic Velocity – Dry density

TRENDLINE TYPE	R^2	EQUATION
LINEAR	$R^2 = 0,8044$	$y = 0,0003x+0,9476$
POWER	$R^2 = 0,7965$	$y = 0,0271x^{0,5283}$
EXPONENTIAL	$R^2 = 0,7631$	$y = 1,1511e^{0,0002x}$

Figure 4.28 shows the highest R^2 for test results of the dry density of limestones versus ultrasonic velocity. Other trends of correlation are also given in table 4.29. 115 specimens are used to perform this test. It can be seen clearly from figure 4.28, dry density of limestone increases as ultrasonic velocity increase. Dry density of limestones reach the maximum value at 5735,3 m/s ultrasonic velocity and it reaches the minimum value at 2040,8 m/s ultrasonic velocity. Maximum and minimum dry density values are 2,54 g/cm^3 and 1,42 g/cm^3.

Rock samples were selected different from each other much possible. However, rock samples are concentrated dense between 2040,8 m/s and 2746,4 m/s ultrasonic velocities. If the rock samples were selected between maximum and minimum ultrasonic velocity values equally, it would be seen clearer increase in the figure 4.28. In this graphic the relationship follows a power law with a reasonable squared regression coefficient R-square is 0,7965 and equation is $y = 0{,}0271x^{0{,}5283}$.

4.4.1.2. Bulk density versus ultrasonic velocity for samples of uniaxial compression test

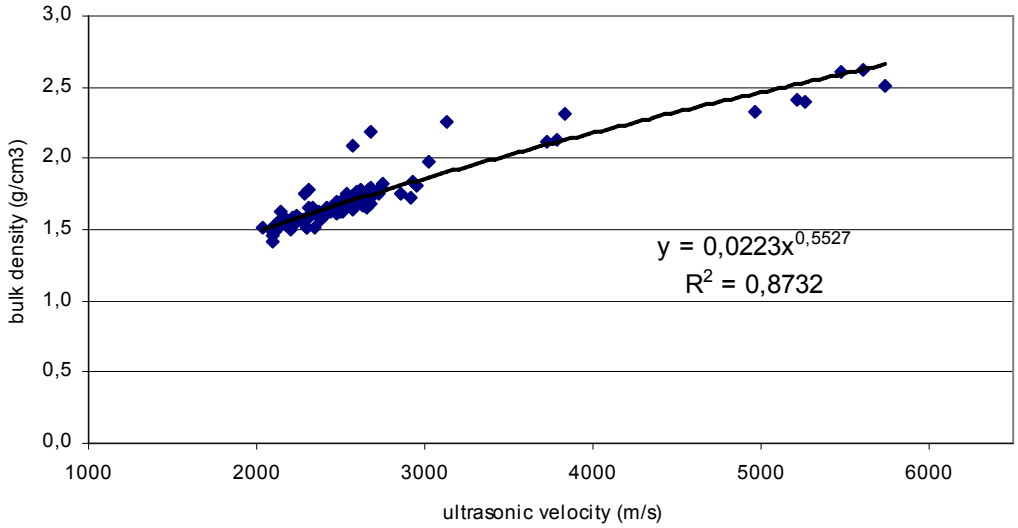

Figure 4.29. Ultrasonic Velocity – Bulk density diagram

Table 4.30.Equitment and R^2 values for Ultrasonic Velocity – Bulk density

TRENDLINE TYPE	R^2	EQUATION
LINEAR	$R^2 = 0{,}8601$	$y = 0{,}0003x+0{,}9103$
POWER	$R^2 = 0{,}8732$	$y = 0{,}0223x^{0{,}5527}$
EXPONENTIAL	$R^2 = 0{,}8247$	$y = 1{,}1283e^{0{,}0002x}$

Figure 4.29 shows the highest R^2 for test results of the bulk density of limestones versus ultrasonic velocity. Other trends of correlation are also given in table 4.30. 115 specimens are used to perform this test. It can be seen clearly from figure 4.29, bulk density of limestone increases as ultrasonic velocity increase. Bulk density of

limestones reach the maximum value at 5735,3 m/s ultrasonic velocity and it reaches the minimum value at 2040,8 m/s ultrasonic velocity. Maximum and minimum bulk density values are 2,62 g/cm^3 and 1,42 g/cm^3.

Rock samples were selected different from each other much possible. However, rock samples are concentrated between 2084,9 m/s and 2746,4 m/s ultrasonic velocities. If the rock samples were selected between maximum and minimum ultrasonic velocity values equally, it would be seen clearer increase in the figure 4.29. In this graphic the relationship follows a power law with a reasonable squared regression coefficient R-square is 0,8732 and equation is y = 0,0223x^{0,5527}.

4.4.1.3.Saturated density versus ultrasonic velocity for samples of uniaxial compression test

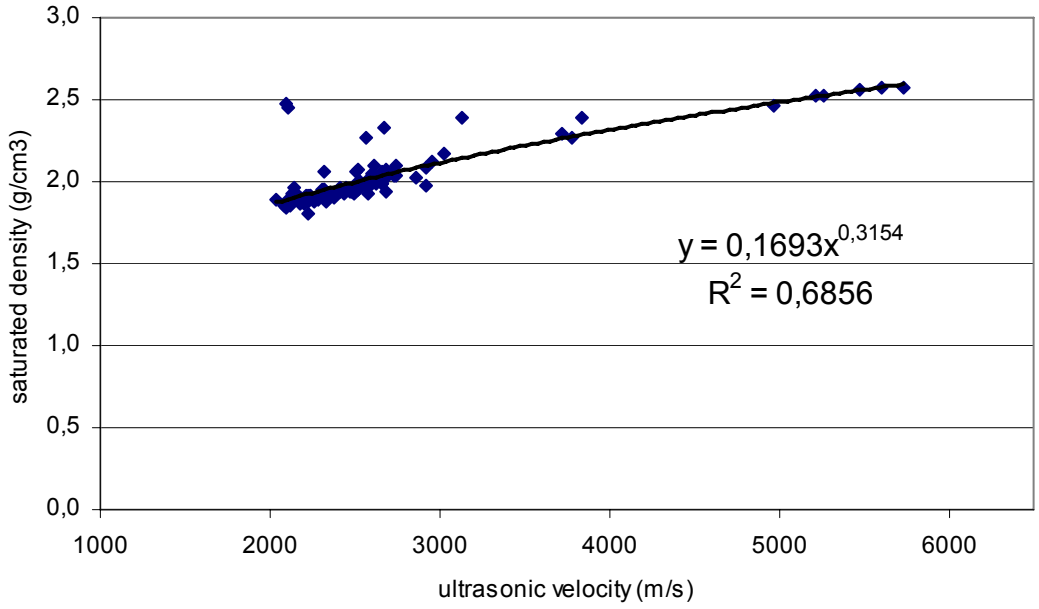

Figure 4.30. Ultrasonic Velocity – Saturated density diagram

Table 4.31.Equitment and R^2 values for Ultrasonic Velocity – Saturated density

TRENDLINE TYPE	R^2	EQUATION
LINEAR	R^2 = 0,6902	y = 0,0002x+1,494
POWER	R^2 = 0,6856	y = 0,1693x^{0,3154}
EXPONENTIAL	R^2 = 0,6754	y = 1,5828e^{9E-05x}

Figure 4.30 shows the highest R^2 for test results of the saturated density of limestones versus ultrasonic velocity. Other trends of correlation are also given in table 4.31. 115 specimens are used to perform this test. It can be seen clearly from figure 4.30, saturated density of limestone increases as ultrasonic velocity increase. Saturated density of limestones reach the maximum value at 5735,3 m/s ultrasonic velocity and it reaches the minimum value at 2040,8 m/s ultrasonic velocity. Maximum and minimum saturated density values are 2,57 g/cm^3 and 1,81 g/cm^3.

Rock samples were selected different from each other much possible. However, rock samples are concentrated between 2084,9 m/s and 2746,4 m/s ultrasonic velocities. If the rock samples were selected between maximum and minimum ultrasonic velocity values equally, it would be seen clearer increase in the figure 4.30. In this graphic the relationship follows a power law with a reasonable squared regression coefficient R-square is 0,6856 and equation is $y = 0,1693x^{0,8164}$.

4.4.1.4.Water absorption versus ultrasonic velocity for samples of uniaxial compression test

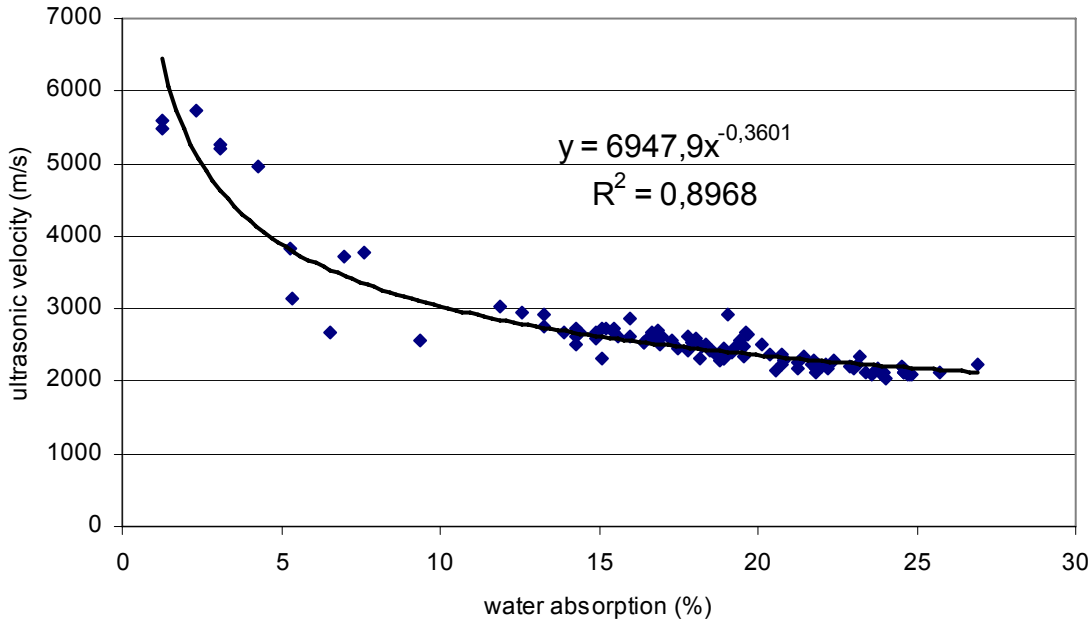

Figure 4.31. Ultrasonic Velocity – Water absorption

Table 4.32.Equitment and R^2 values for Ultrasonic Velocity – Water absorption

TRENDLINE TYPE	R^2	EQUATION
LINEAR	$R^2 = 0,7555$	$y = -113,03x+4639,8$
POWER	$R^2 = 0,8968$	$y = 6947,9x^{-0,3601}$
EXPONENTIAL	$R^2 = 0,8305$	$y = 4724,8e^{-0,0345x}$

Figure 4.31 shows the highest R^2 for test results of the water absorption density of limestones versus ultrasonic velocity. Other trends of correlation are also given in table 4.32. 115 specimens are used to perform this test. It can be seen clearly from figure 4.31, water absorption of limestone decreases as ultrasonic velocity increase. Water absorption of limestones reach the maximum value at 5735,3 m/s ultrasonic velocity and it reaches the minimum value at 2040,8 m/s ultrasonic velocity. Maximum and minimum water absorption values are 26,89 % and 1,24 %.

Rock samples were selected different from each other much possible. However, rock samples are concentrated between 2097,1 m/s and 2735,3 m/s ultrasonic velocities. If the rock samples were selected between maximum and minimum ultrasonic velocity values equally, it would be seen clearer increase in the figure 4.31. In this graphic the relationship follows a power law with a reasonable squared regression coefficient R-square is 0,8968 and equation is $y = 6947,9x^{0,3601}$.

4.4.1.5.Porosity versus ultrasonic velocity for samples of uniaxial compression test

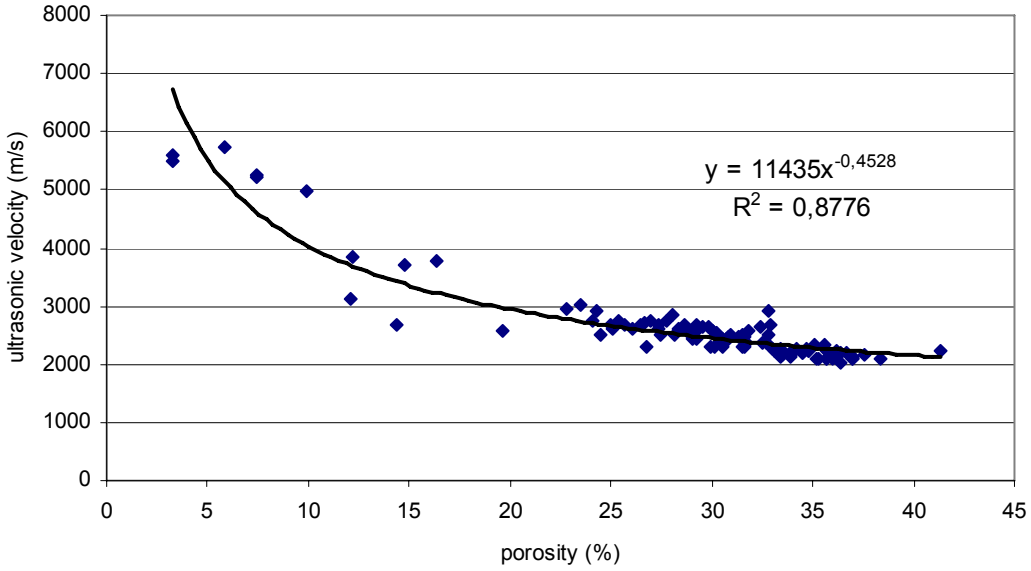

Figure 4.32. Ultrasonic Velocity – porosity

Table 4.33.Equitment and R^2 values for Ultrasonic Velocity – porosity

TRENDLINE TYPE	R^2	EQUATION
LINEAR	$R^2 = 0,8239$	$y = -87,466x+5181,6$
POWER	$R^2 = 0,8776$	$y = 11435x^{-0,4528}$
EXPONENTIAL	$R^2 = 0,8666$	$y = 5480,8e^{-0,0261x}$

Figure 4.32 shows the highest R^2 for test results of the porosity of limestones versus ultrasonic velocity. Other trends of correlation are also given in table 4.33. 115 specimens are used to perform this test. It can be seen clearly from figure 4.32, porosity of limestone decreases as ultrasonic velocity increase. porosity of limestones reach the maximum value at 5735,3 m/s ultrasonic velocity and it reaches the minimum value at 2040,8 m/s ultrasonic velocity. Maximum and minimum porosity are 41,29 % and 3,24 %.

Rock samples were selected different from each other much possible. However, rock samples are concentrated between 2097,1 m/s and 2735,3 m/s ultrasonic velocities. If the rock samples were selected between maximum and minimum ultrasonic velocity values equally, it would be seen clearer increase in the figure 4.32. In this

graphic the relationship follows a power law with a reasonable squared regression coefficient R-square is 0,8776 and equation is $y = 11435x^{-0,4528}$.

4.4.1.6. Uniaxial compressive strength versus ultrasonic velocity for samples of uniaxial compression test

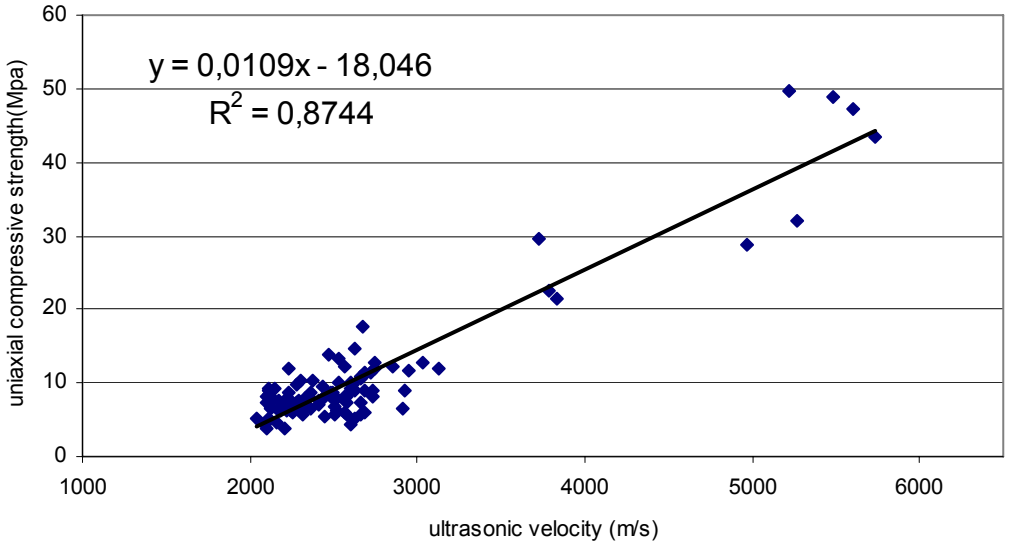

Figure 4.33. Ultrasonic Velocity – Uniaxial compressive strength

Table 4.34.Equitment and R^2 values for Ultrasonic Velocity –Uniaxial compressive strength

TRENDLINE TYPE	R^2	EQUATION
LINEAR	$R^2 = 0,8744$	$y = 0,0109x-18,046$
POWER	$R^2 = 0,7373$	$y = 1E-06x^{2,0057}$
EXPONENTIAL	$R^2 = 0,7386$	$y = 1,9068e^{0,0006x}$

Figure 4.33 shows the highest R^2 for test results of the ultrasonic velocity of limestones versus uniaxial compressive strength. Other trends of correlation are also given in table 4.34. 115 specimens are used to perform this test. It can be seen clearly from figure 4.33, uniaxial compressive strength of limestone increases as ultrasonic velocity increase. Uniaxial compressive strength of limestones reach the maximum value at 5735,3 m/s ultrasonic velocity and it reaches the minimum value at

2040,8 m/s ultrasonic velocity. Maximum and minimum uniaxial compressive strength values are 49,786 MPa and 3,746 MPa.

Rock samples were selected different from each other much possible. However, rock samples are concentrated between 2097,1 m/s and 2746,4 m/s ultrasonic velocities. If the rock samples were selected between maximum and minimum ultrasonic velocity values equally, it would be seen clearer increase in the figure 4.33. In this graphic the relationship follows a linear law with a reasonable squared regression coefficient R-square is 0,8744 and equation is y = 0,0109x – 18,046.

4.4.1.7. Dry density versus uniaxial compressive strength

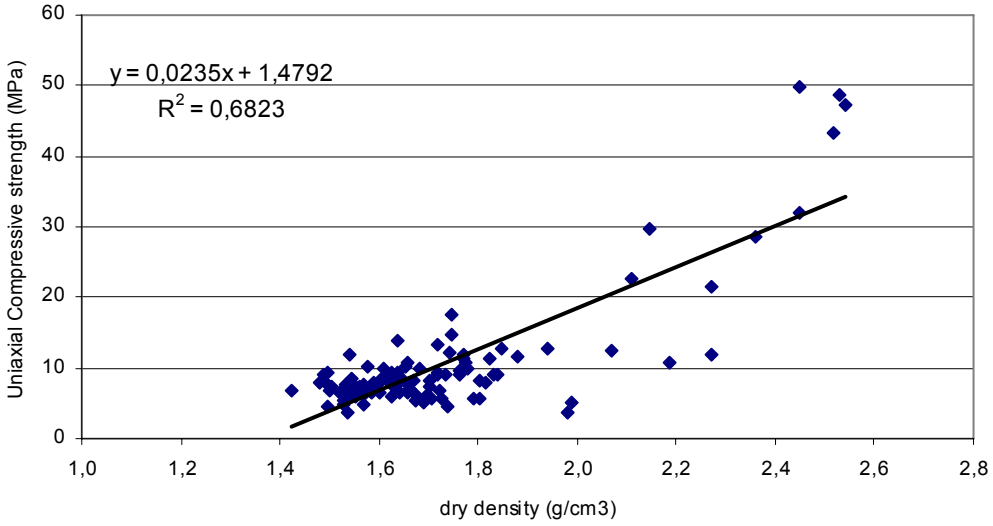

Figure 4.34. Dry density - Uniaxial Compressive strength diagram

Table 4.35.Equitment and R^2 values for Dry density - Uniaxial Compressive strength

TRENDLINE TYPE	R^2	EQUATION
LINEAR	$R^2 = 0,6823$	$y = 0,0235x+1,4792$
POWER	$R^2 = 0,5742$	$y = 1,125x^{0,192}$
EXPONENTIAL	$R^2 = 0,6301$	$y = 1,5114e^{0,0118x}$

Figure 4.34 shows the highest R^2 for test results of the dry density of limestones versus uniaxial compressive strength. Other trends of correlation are also given in table 4.35.115 specimens are used to perform this test. It can be seen clearly from

figure 4.34, dry density of limestone increases as Uniaxial compressive strength increase. Dry density of limestones reach the maximum value at 49,79 MPa Uniaxial compressive strength and it reaches the minimum value at 3,76 MPa Uniaxial compressive strength . Maximum and minimum dry density values are 2,54 g/cm^3 and 1,42 g/cm^3.

Rock samples were selected different from each other much possible. However, rock samples are concentrated dense between 3,76 MPa and 12,82 MPa Uniaxial compressive strengths. If the rock samples were selected between maximum and minimum Uniaxial compressive strength values equally, it would be seen clearer increase in the figure 4.34. In this graphic the relationship follows a linear law with a reasonable squared regression coefficient R-square is 0,6823 and equation is y = 0,0235x + 1,4792.

4.4.1.8. Bulk density versus uniaxial compressive strength

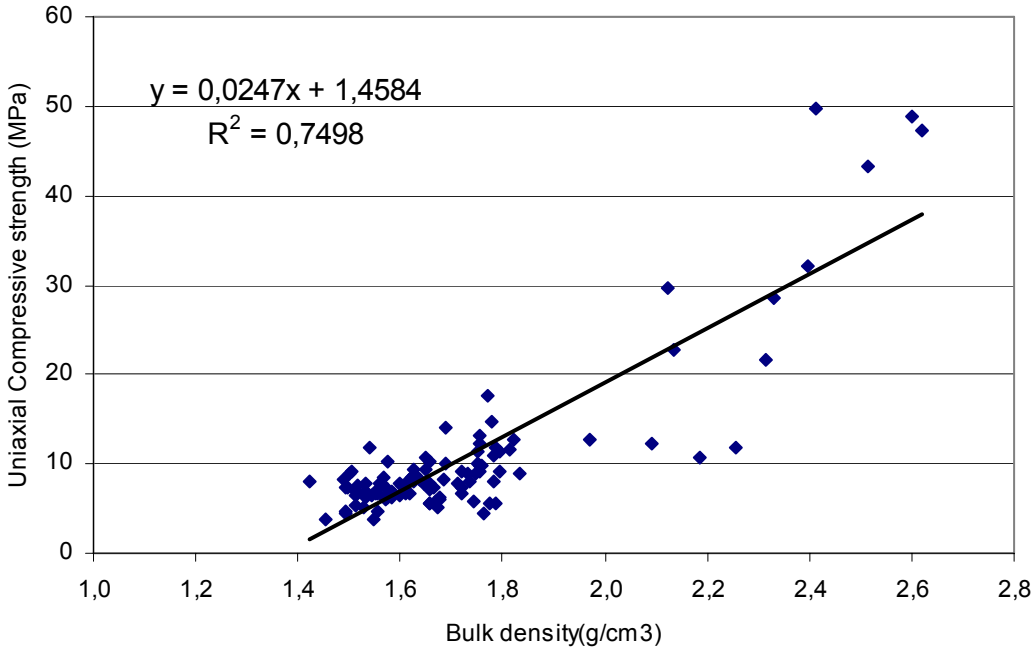

Figure 4.35. Bulk density - Uniaxial Compressive strength diagram

Table 4.36.Equitment and R^2 values for Bulk density - Uniaxial Compressive strength

TRENDLINE TYPE	R^2	EQUATION
LINEAR	$R^2 = 0,7498$	$y = 0,0247x+1,4584$
POWER	$R^2 = 0,6955$	$y = 1,0739x^{0,2112}$
EXPONENTIAL	$R^2 = 0,7011$	$y = 1,4944e^{0,0124x}$

Figure 4.35 shows the highest R^2 for test results of the bulk density of limestones versus uniaxial compressive strength. Other trends of correlation are also given in table 4.36. 115 specimens are used to perform this test. It can be seen clearly from figure 4.35, bulk density of limestone increases as Uniaxial compressive strength increase. Bulk density of limestones reach the maximum value at 49,79 MPa Uniaxial compressive strength and it reaches the minimum value at 3,76 MPa Uniaxial compressive strength . Maximum and minimum bulk density values are 2,62 g/cm^3 and 1,42 g/cm^3.

Rock samples were selected different from each other much possible. However, rock samples are concentrated between 3,76 MPa and 12,82 MPa Uniaxial compressive strengths. If the rock samples were selected between maximum and minimum Uniaxial compressive strength values equally, it would be seen clearer increase in the figure 4.35. In this graphic the relationship follows a linear law with a reasonable squared regression coefficient R-square is 0,7498 and equation is y = 0,0247x+1,4584.

4.4.1.9.Saturated density versus uniaxial compressive strength

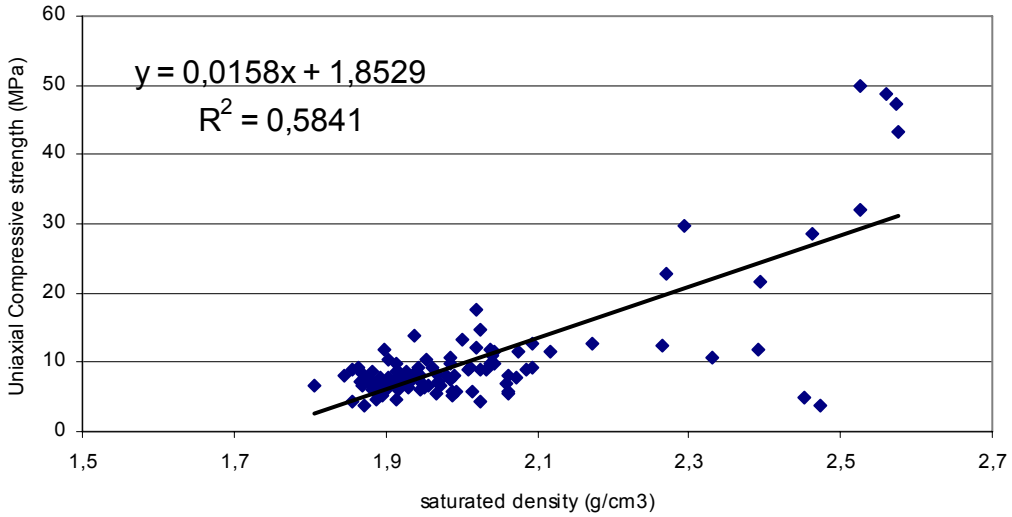

Figure 4.36. Saturated density - Uniaxial Compressive strength diagram

Table 4.37.Equitment and R^2 values for Saturated density - Uniaxial Compressive strength

TRENDLINE TYPE	R^2	EQUATION
LINEAR	$R^2 = 0,5841$	$y = 0,0247x+1,8529$
POWER	$R^2 = 0,4758$	$y = 1,5739x^{0,1125}$
EXPONENTIAL	$R^2 = 0,5630$	$y = 1,8659e^{0,0072x}$

Figure 4.36 shows the highest R^2 for test results of the saturated density of limestones versus uniaxial compressive strength. Other trends of correlation are also given in table 4.37. 115 specimens are used to perform this test. It can be seen clearly from figure 4.36, saturated density of limestone increases as Uniaxial compressive strength increase. Saturated density of limestones reach the maximum value at 49,79 MPa Uniaxial compressive strength and it reaches the minimum value at 3,76 MPa Uniaxial compressive strength . Maximum and minimum saturated density values are 2,57 g/cm^3 and 1,81 g/cm^3.

Rock samples were selected different from each other much possible. However, rock samples are concentrated between 3,76 MPa and 12,82 MPa Uniaxial compressive strengths. If the rock samples were selected between maximum and minimum Uniaxial compressive strength values equally, it would be seen clearer increase in

the figure 4.36. In this graphic the relationship follows a linear law with a reasonable squared regression coefficient R-square is 0,5841 and equation is y = 0,0247x+1,8529.

4.4.1.10.Water absorption versus uniaxial compressive strength

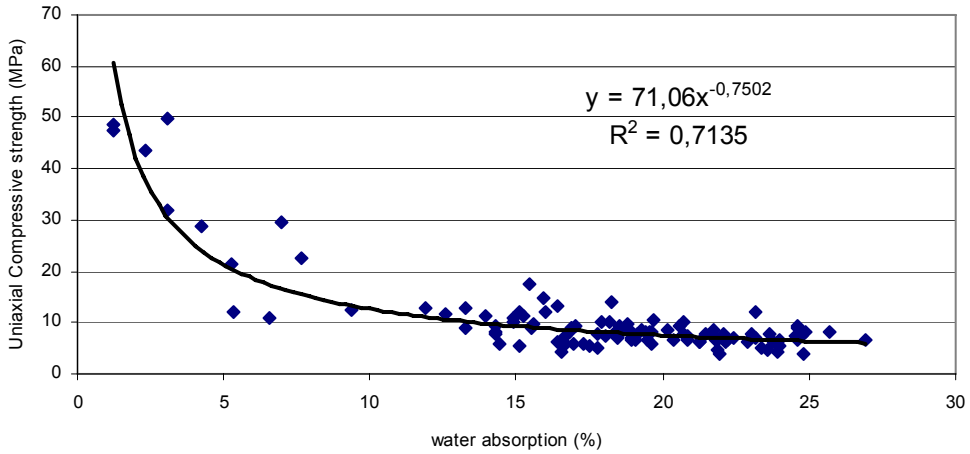

Figure 4.37. Water absorption - Uniaxial Compressive strength diagram

Table 4.38.Equitment and R^2 values for Water absorption - Uniaxial Compressive strength

TRENDLINE TYPE	R^2	EQUATION
LINEAR	R^2 = 0,6077	y = -1,1765x+31,417
POWER	R^2 = 0,7135	$y = 71{,}06x^{-0{,}7502}$
EXPONENTIAL	R^2 = 0,6283	$y = 30{,}826e^{-0{,}0701x}$

Figure 4.37 shows the highest R^2 for test results of the water absorption of limestones versus uniaxial compressive strength. Other trends of correlation are also given in table 4.38. 115 specimens are used to perform this test. It can be seen clearly from figure 4.37, water absorption of limestone decreases as Uniaxial compressive strength increase. Water absorption of limestones reach the maximum value at 49,79 MPa Uniaxial compressive strength and it reaches the minimum value at 3,76 MPa Uniaxial compressive strength . Maximum and minimum water absorption values are 26,89 % and 1,24 %.

Rock samples were selected different from each other much possible. However, rock samples are concentrated between 3,76 MPa and 12,82 MPa Uniaxial compressive strengths. If the rock samples were selected between maximum and minimum Uniaxial compressive strength values equally, it would be seen clearer increase in the figure 4.37. In this graphic the relationship follows a power law with a reasonable squared regression coefficient R-square is 0,7135 and equation is $y = 71{,}06x^{-0{,}7502}$.

4.4.1.11.Porosity versus uniaxial compressive strength

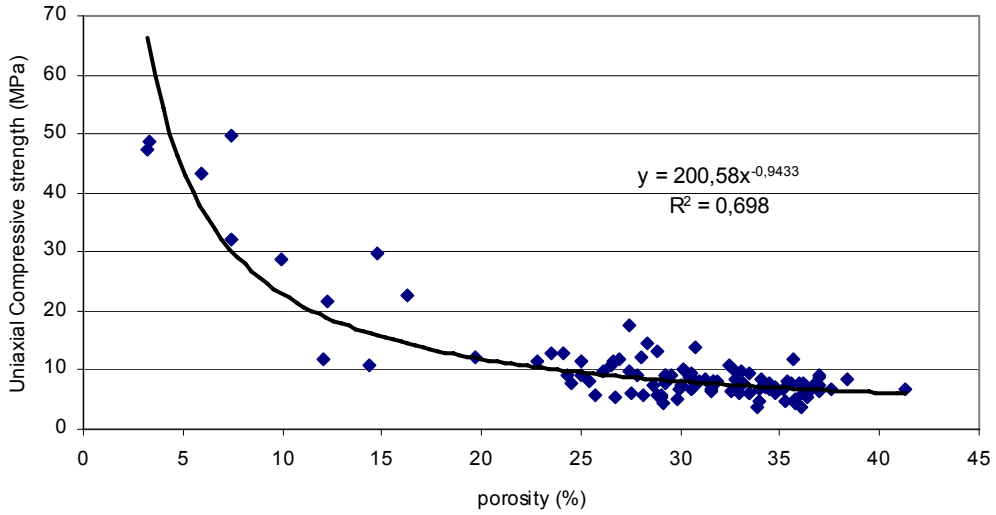

Figure 4.38. Porosity - Uniaxial Compressive strength diagram

Table 4.39.Equitment and R^2 values for porosity - Uniaxial Compressive strength

TRENDLINE TYPE	R^2	EQUATION
LINEAR	$R^2 = 0{,}6940$	$y = -0{,}9317x+37{,}676$
POWER	$R^2 = 0{,}6980$	$y = 200{,}58x^{-0{,}9433}$
EXPONENTIAL	$R^2 = 0{,}6640$	$y = 42{,}088e^{-0{,}0534x}$

Figure 4.38 shows the highest R^2 for test results of the porosity of limestones versus uniaxial compressive strength. Other trends of correlation are also given in table 4.39. 115 specimens are used to perform this test. It can be seen clearly from figure 4.38, porosity of limestone decreases as Uniaxial compressive strength increase. Porosity of limestones reach the maximum value at 49,79 MPa Uniaxial compressive

strength and it reaches the minimum value at 3,76 MPa Uniaxial compressive strength . Maximum and minimum porosity values are 41,29 % and 3,24 %.

Rock samples were selected different from each other much possible. However, rock samples are concentrated between 3,76 MPa and 12,82 MPa Uniaxial compressive strengths. If the rock samples were selected between maximum and minimum Uniaxial compressive strength values equally, it would be seen clearer increase in the figure 4.38. In this graphic the relationship follows a power law with a reasonable squared regression coefficient R-square is 0,6980 and equation is $y = 200{,}58x^{-0{,}9433}$.

4.4.2.Determination of young's modulus

In this part young's modulus of specimens were determined. Result were presented as figures and tables. Limestone specimens were divided into three groups according to their hardness.

- Hard limestone
- Medium limestone
- Soft limestone

4.4.2.1. Hard limestone

Table 4.40. Young's modulus Test Results (sample no: 9)

Sample No: 9					
Δ.L. (mm)	L (mm)	Strain (E-3)	Load (kN)	Diam(cm)	Stress (Mpa)
0,05	158,6	0,315	6,4	6,1	2,191
0,10	158,6	0,631	16,6	6,1	5,683
0,15	158,6	0,946	26,7	6,1	9,141
0,20	158,6	1,261	34,2	6,1	11,708
0,25	158,6	1,576	44,9	6,1	15,372
0,30	158,6	1,892	59	6,1	20,199
0,35	158,6	2,207	74,4	6,1	25,471
0,40	158,6	2,522	92,1	6,1	31,530
0,45	158,6	2,837	98,3	6,1	33,653
0,50	158,6	3,153	113,5	6,1	38,857
0,55	158,6	3,468	122,7	6,1	42,006
0,60	158,6	3,783	132,3	6,1	45,293
0,65	158,6	4,098	138,1	6,1	47,279

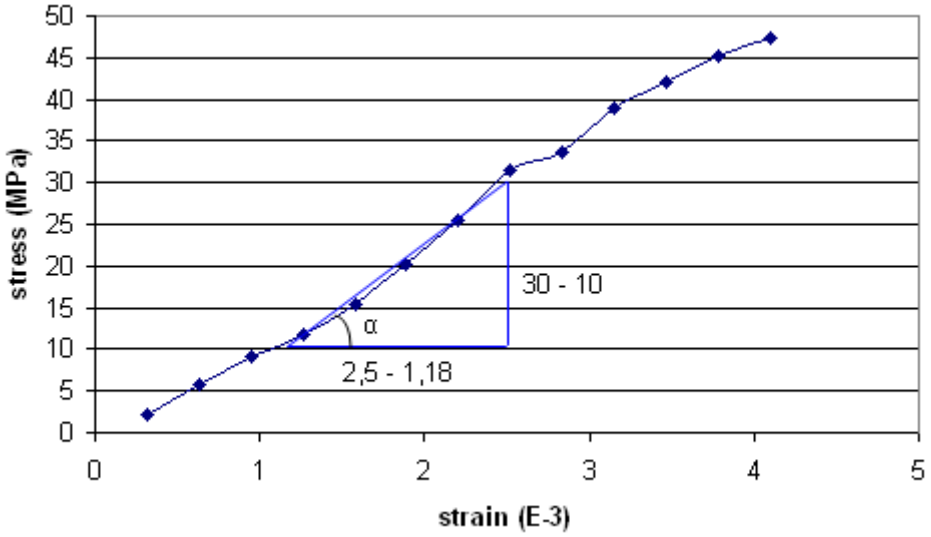

Figure 4.39. Strees-strain diagram (sample no: 9)

Figure 4.39 shows the stress-strain diagram of limestone sample with a number 9. Other values which was obtained from the test is given in table 4.40. As can be seen from figure 4.39, uniaxial compressive stres increases as strain increase. From this figure young's modululus of this sample was determined according to Tangent

modulus measured at a fixed percentage of ultimate strength. The young's modulus of the sample 9 is 15,15 GPa.

Table 4.41. Young's modulus Test Results (sample no: 10)

Sample No: 10					
Δ.L. (mm)	L (mm)	Strain (E-3)	Load (kN)	Diam(cm)	Stress (Mpa)
0,05	146,3	0,342	11,3	6,1	3,869
0,10	146,3	0,684	17,3	6,1	5,923
0,15	146,3	1,025	24,6	6,1	8,422
0,25	146,3	1,709	33,8	6,1	11,571
0,30	146,3	2,051	37,7	6,1	12,907
0,35	146,3	2,392	39,5	6,1	13,523
0,40	146,3	2,734	54,4	6,1	18,624
0,45	146,3	3,076	64,1	6,1	21,945
0,50	146,3	3,418	72,2	6,1	24,718
0,55	146,3	3,759	86,8	6,1	29,716
0,60	146,3	4,101	103,4	6,1	35,399
0,65	146,3	4,443	120	6,1	41,082
0,70	146,3	4,785	133,4	6,1	45,670
0,75	146,3	5,126	138,4	6,1	47,381
0,80	146,3	5,468	142,4	6,1	48,751

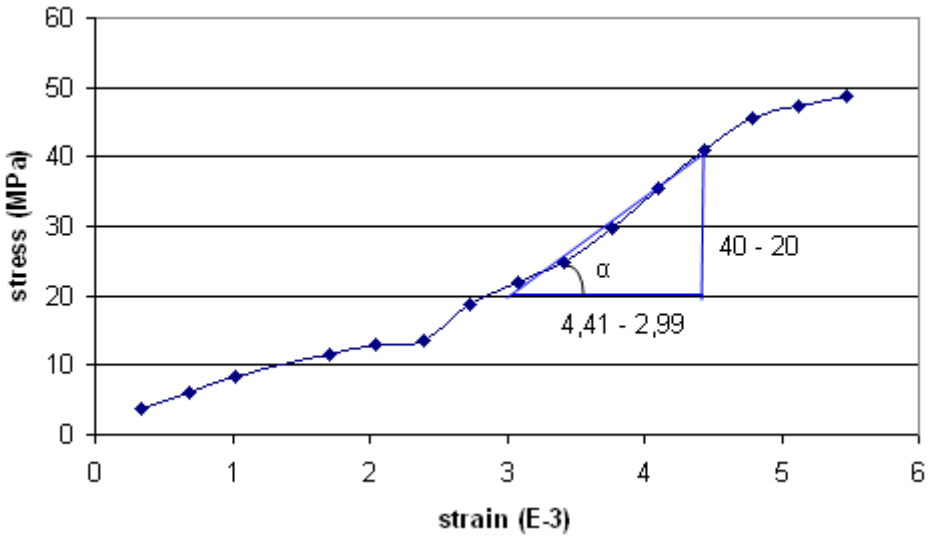

Figure 4.40. Strees-strain diagram (sample no: 10)

Figure 4.40 shows the stress-strain diagram of limestone sample with a number 10. Other values which was obtained from the test is given in table 4.41.As can be seen from figure 4.40, uniaxial compressive stres increases as strain increase. From this figure young's modululus of this sample was determined according to Tangent modulus measured at a fixed percentage of ultimate strength. The young's modulus of the sample 10 is 14,08 GPa.

The same two hard limestones in the above are has an average 14,62 GPa young's modulus.

4.4.2.2. Medium limestone

Table 4.42. Young's modulus Test Results (sample no: 26)

Sample No: 26					
Δ.L. (mm)	L (mm)	Strain (E-3)	Load (kN)	Diam(cm)	Stress (Mpa)
0,05	151,1	0,331	7,8	6,05	2,715
0,10	151,1	0,662	8,9	6,05	3,097
0,15	151,1	0,993	9,3	6,05	3,237
0,20	151,1	1,324	11,4	6,05	3,968
0,25	151,1	1,655	14	6,05	4,872
0,30	151,1	1,985	16,4	6,05	5,708
0,35	151,1	2,316	19,6	6,05	6,821
0,40	151,1	2,647	23,1	6,05	8,040
0,45	151,1	2,978	26,2	6,05	9,118
0,50	151,1	3,309	29,3	6,05	10,197
0,55	151,1	3,640	32,1	6,05	11,172
0,60	151,1	3,971	34,6	6,05	12,042
0,65	151,1	4,302	36,7	6,05	12,773
0,70	151,1	4,633	37,7	6,05	13,121

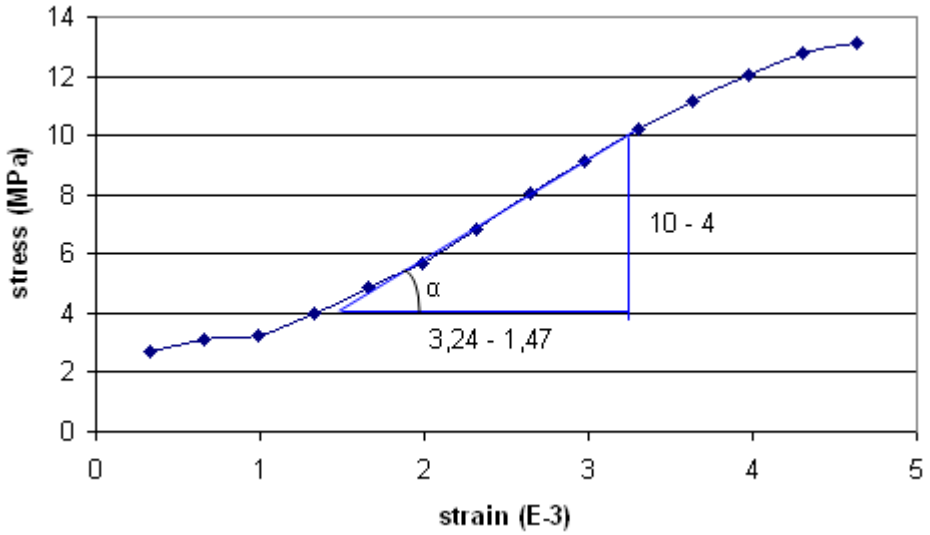

Figure 4.41. Strees-strain diagram (sample no: 26)

Figure 4.41 shows the stress-strain diagram of limestone sample with a number 26. Other values which was obtained from the test is given in table 4.42.As can be seen from figure 4.41, uniaxial compressive stres increases as strain increase. From this figure young's modululus of this sample was determined according to Tangent modulus measured at a fixed percentage of ultimate strength. The young's modulus of the sample 26 is 3,39 GPa.

Table 4.43. Young's modulus Test Results (sample no: 33)

Sample No: 33					
Δ.L. (mm)	L (mm)	Strain (E-3)	Load (kN)	Diam(cm)	Stress (Mpa)
0,05	151,6	0,330	7,9	6,08	2,722
0,10	151,6	0,660	10,6	6,08	3,653
0,15	151,6	0,989	13,6	6,08	4,687
0,20	151,6	1,319	16,8	6,08	5,789
0,25	151,6	1,649	20,5	6,08	7,064
0,30	151,6	1,979	23,9	6,08	8,236
0,35	151,6	2,309	27,1	6,08	9,339
0,40	151,6	2,639	30,1	6,08	10,373
0,45	151,6	2,968	32,8	6,08	11,303
0,50	151,6	3,298	33,8	6,08	11,648
0,55	151,6	3,628	34,2	6,08	11,786

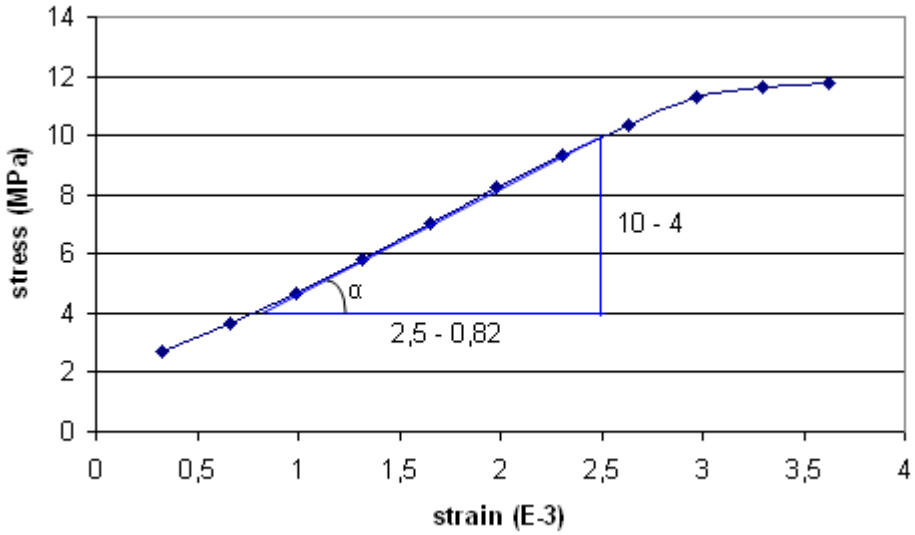

Figure 4.42. Strees-strain diagram (sample no: 33)

Figure 4.42 shows the stress-strain diagram of limestone sample with a number 33. Other values which was obtained from the test is given in table 4.43.As can be seen from figure 4.42, uniaxial compressive stres increases as strain increase. From this figure young's modululus of this sample was determined according to Tangent modulus measured at a fixed percentage of ultimate strength. The young's modulus of the sample 33 is 3,57 GPa.

The same two medium limestones in the above are has an average 3,48 GPa young's modulus.

4.4.2.3. Soft limestone

Table 4.44. Young's modulus Test Results (sample no: 69)

Sample No: 69					
Δ.L. (mm)	L (mm)	Strain (E-3)	Load (kN)	Diam(cm)	Stress (Mpa)
0,05	154	0,325	10,5	6,08	3,618
0,10	154	0,649	11,5	6,08	3,963
0,15	154	0,974	13,5	6,08	4,652
0,20	154	1,299	15,6	6,08	5,376
0,25	154	1,623	17,7	6,08	6,100
0,30	154	1,948	19,4	6,08	6,685
0,35	154	2,273	21,8	6,08	7,512
0,40	154	2,597	22	6,08	7,581

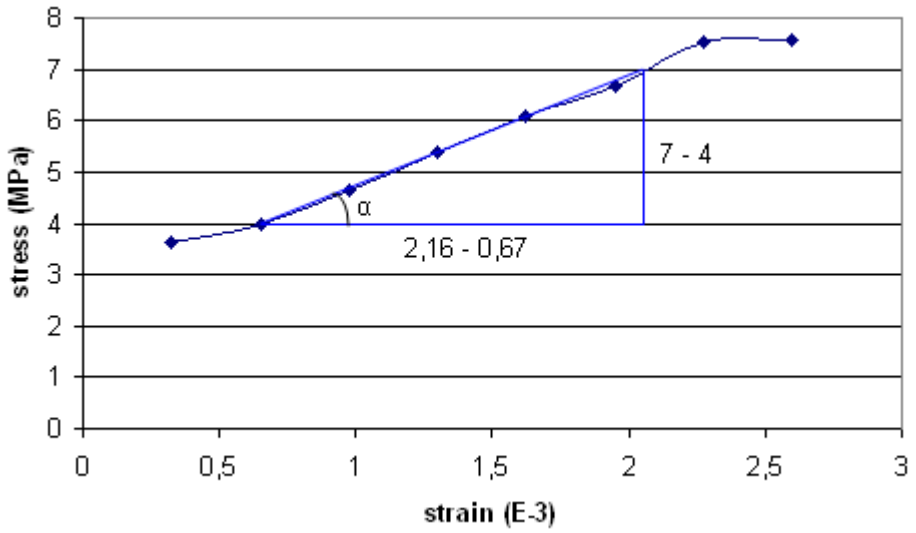

Figure 4.43. Strees-strain diagram (sample no: 69)

Figure 4.43 shows the stress-strain diagram of limestone sample with a number 69. Other values which was obtained from the test is given in table 4.44.As can be seen from figure 4.43, uniaxial compressive stres increases as strain increase. From this figure young's modululus of this sample was determined according to Tangent modulus measured at a fixed percentage of ultimate strength. The young's modulus of the sample 69 is 2,01 GPa.

Table 4.45. Young's modulus Test Results (sample no: 49)

Sample No: 49					
Δ.L. (mm)	L (mm)	Strain (E-3)	Load (kN)	Diam(cm)	Stress (Mpa)
0,05	154,9	0,323	7,6	6,15	2,560
0,10	154,9	0,646	9,1	6,15	3,065
0,15	154,9	0,968	11,1	6,15	3,739
0,20	154,9	1,291	12	6,15	4,042
0,25	154,9	1,614	13,2	6,15	4,446
0,30	154,9	1,937	15,2	6,15	5,119
0,35	154,9	2,260	17,4	6,15	5,860
0,40	154,9	2,582	19,4	6,15	6,534
0,45	154,9	2,905	21,1	6,15	7,107
0,50	154,9	3,228	22,6	6,15	7,612
0,55	154,9	3,551	23,8	6,15	8,016

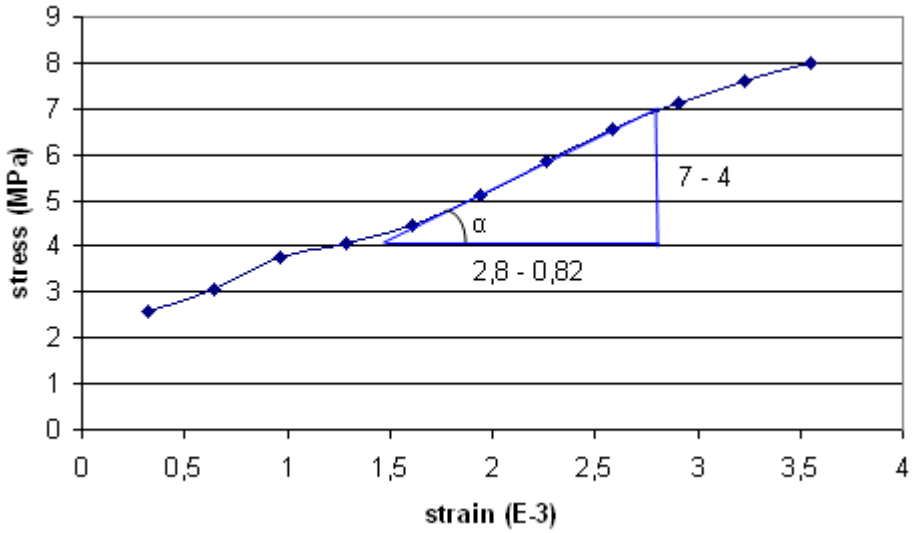

Figure 4.44. Strees-strain diagram (sample no: 49)

Figure 4.44 shows the stress-strain diagram of limestone sample with a number 49. Other values which was obtained from the test is given in table 4.45.As can be seen from figure 4.44, uniaxial compressive stres increases as strain increase. From this figure young's modululus of this sample was determined according to Tangent modulus measured at a fixed percentage of ultimate strength. The young's modulus of the sample 49 is 1,52 GPa.

The same two soft limestones in the above are has an average 1,76 GPa young's modulus.

CHAPTER 5

DISCUSSION

5.1. Introduction

In this chapter obtained values are compared to literature values with their reasons to investigate that they are confidental or not.

5.2. Review The Obtained Results Based on The Literature Survey

In this study; Indirect (Brazillian) tensile strength-, uniaxial compressive strength-, Shear strength- ultrasonic velocity of limestone graphics were found using dry cylindrical specimens with the same orientation. Also, index parameters such as dry density, bulk density, water absorbtion and saturated density were determined.

The soft limestone could have caused scatter of the ultrasonic velocity, varying its velocity in all the samples and causing high scattering. It is observed that, for hard limestone strength values also increase linearly with increasing density [33].

The results of this study also demonstrated that ultrasonic velocity is sensitive to changes in density [38]. The longitudinal velocity under dense conditions was always higher than the velocity under less dense conditions, in all dimensions. It can be easily said that ultrasonic velocity is not dimension dependent

It was established that the uniaxial compressive strength and Brazillian tensile strength in limestone increase with increasing ultrasonic velocity because of the effect of density on the mechanical properties (uniaxial compressive stength,

Brazillian tensile strength and young's modulus) and the physical properties (dry density, saturated density, water absorbtion amd saturated density) [2].

It was also established that the parameters dry and saturated density in limestone increase with increasing ultrasonic velocity. Water absorption is inversely related to ultrasonic velocity. The ultrasonic velocities decreased as the water absorption increased. because of the effect of the density on the physical properties (dry density, saturated density, water absorption) [2].

Bulk density is also increase with increasing ultrasonic velocity. This can be explained by the bulk density changes through changing the amount of air space between the particles of the dry matter and water. Bulk density is increased (greater mass per volume) through compaction (squeezing the particles together as in a bale of hay) or through particle size reduction (allowing smaller particles to fit closer together as in chopping corn) or by increasing the moisture content (filling the air spaces with water). Bulk density is reduced (lesser mass per volume) by adding air space such as fluffing (using a bale buster on the hay) or removing the water through drying [15].

5.3.Comparison Literatur Values With Obtained Values in This Study

In this section literature values of limestone and Gaziantep limestone were compared

5.3.1. Dry density values

In this thesis dry density of Gaziantep limestone's value was obtained as 1,42 g/cm^3 – 2,62 g/cm^3 . To see the results are confidental or not, literature values are search and compared to the our test results.

Literature values:

- Dry density Germany limestone 2,62 g/cm^3 [56].
- Dry density Indiana limestone 2,30 g/cm^3 [56].
- Dry density Tunisian limestone 2,55 g/cm^3 [52].

- Dry density limestone China 2,73 g/cm^3 [42].
- Dry density limestone 2,7 g/cm^3 [53].

5.3.2. Bulk density values

In this thesis bulk density of Gaziantep limestone's value was obtained as 1,42 g/cm^3 – 2,62 g/cm^3 . To see the results are confidental or not, literature values are search and compared to the our test results.

Literature value:

- Bulk density limestone China 1,45 g/cm^3 [42].

5.3.3. Water absorption values

In this thesis water absorption of Gaziantep limestone's value was obtained as 1,24 % – 26,89 %. To see the results are confidental or not, literature values are search and compared to the our test results.

Literature values:

- Water absorption Tunisian limestone 3,86% [52].
- Water absorption limestone China 1,08% [42].

5.3.4. Brazillian tensile strenght values

In this thesis Brazillian tensile strength of Gaziantep limestone's value was obtained as 0,99 MPa – 15,06 MPa. To see the results are confidental or not, literature values are search and compared to the our test results.

Literature values:

- Tensile strenght Germany limestone 4 MPa [56].
- Tensile strenght Indiana limestone 4,1 MPa [56].
- Tensile strenght limestone 5 - 25 MPa [53].

5.3.5.Direct shear strength values

In this thesis direct shear strength of Gaziantep limestone's value was obtained as 1,36 MPa – 6,20 MPa. To see the results are confidental or not, literature values are search and compared to the our test results.

Literature value:

- Shear strength limestone 10-50 MPa [53].

5.3.5.1. Friction angle values (Φ)

In this thesis friction angle of Gaziantep limestone's value was obtained as 40º - 57º. To see the results are confidental or not, literature values are search and compared to the our test results.

Literature values:

- Friction angle of limestone 35° ± 2 [57].
- Friction angle of limestone 35° - 50° [19].

5.3.5.2. Cohesion values (c)

In this thesis cohesion of Gaziantep limestone's value was obtained as 15 MPa – 2,1 MPa. To see the results are confidental or not, literature values are search and compared to the our test results.

Literature value:

- Cohesion of limestone 2,3 ± 0.4 MPa [57].

5.3.5.3. Residual friction angle values

In this thesis residual friction angle of Gaziantep limestone's value was obtained as 38º - 54º. To see the results are confidental or not, literature values are search and compared to the our test results.

Literature value:

- Residual friction angle limestone 33º-37º [44].

5.3.6. Uniaxial compressive strenght values

In this thesis uniaxial compressive strenght of Gaziantep limestone's value was obtained as 3,75 MPa – 49,8 MPa .To see the results are confidental or not, literature values are search and compared to the our test results.

Literature values:

- Uniaxial compressive strenght Germany limestone 64 MPa [56].
- Uniaxial compressive strenght Indiana limestone 53 MPa [56].
- Uniaxial compressive strenght limestone 12 - 294 MPa [20].
- Uniaxial compressive strenght Solenhofen limestone 245 MPa [39].
- Uniaxial compressive strenght Bedford limestone 51MPa [39].
- Uniaxial compressive strenght Tavernalle limestone 97,9 MPa [39].
- Uniaxial compressive strenght limestone 30 - 250 MPa [53].
- Uniaxial compressive strength limestone 248 Mpa [52].
- Uniaxial compressive strenght limestone 54 MPa [52].

5.3.6.1. Young's modulus values

In this thesis young's modulus of Gaziantep limestone's value was obtained as 1,76 GPa – 14,62 GPa.To see the results are confidental or not, literature values are search and compared to the our test results.

Literature values:

- Young's modulus Germany limestone 63,8 GPa [56].
- Young's modulus Indiana limestone 27 GPa [56].

5.3.7. Ultrasonic velocity values

In this thesis ultrasonic velocity of Gaziantep limestone's value was obtained as 1950 m/s – 5910 m/s.To see the results are confidental or not, literature values are search and compared to the our test results.

Literature value:

- Ultrasonic velocity limestone 2500-6000 m/s [53].

CHAPTER 6

CONCLUSIONS

6.1. Conclusions

Indirect (Brazilian) tensile strength, uniaxial compressive strength, Shear strength and ultrasonic velocity of limestone in Gaziantep were studied using dry cylindrical specimens with the same orientation. Also, index parameters such as dry density, bulk density, water absorption and saturated density were determined.

Obtained values for Gaziantep limestone are ;

1) Dry density of Gaziantep limestone's value was obtained as 1,42 g/cm^3 – 2,62 g/cm^3

2) Bulk density of Gaziantep limestone's value was obtained as 1,42 g/cm^3 – 2,62 g/cm^3 .

3) Water absorption of Gaziantep limestone's value was obtained as 1,24 % – 26,89 %.

4) Brazillian tensile strength of Gaziantep limestone's value was obtained as 0,99 MPa – 15,06 MPa.

5) Direct shear strength of Gaziantep limestone's value was obtained as 1,36 MPa – 6,20 MPa.

6) Friction angle of Gaziantep limestone's value was obtained as 40º - 57º.

7) Cohesion of Gaziantep limestone's value was obtained as 15 MPa – 2,1 MPa.

8) Residual friction angle of Gaziantep limestone's value was obtained as 38º - 54º.

9) Uniaxial compressive strenght of Gaziantep limestone's value was obtained as 3,75 MPa – 49,8 MPa .

10) Young's modulus of Gaziantep limestone's value was obtained as 1,76 GPa – 14,62 GPa.

11) Ultrasonic velocity of Gaziantep limestone's value was obtained as 1950 m/s – 5910 m/s.

It was established that the uniaxial compressive strength in limestone increase with increasing ultrasonic velocity, while the same effect of ultrasonic velocity on Brazilian tensile strength was present.

It was also established that the parameters dry and saturated density in limestone increase with increasing ultrasonic velocity.

Water absorption indices are inversely related to ultrasonic velocity. The ultrasonic velocities decreased as the water absorption increased. The coefficient of determination obtained in the graphics allowing us to state that the variation in velocity and water absorption is very well.

The soft limestone could have caused scatter of the ultrasonic velocity, varying its velocity in all the samples and causing high scattering. It is observed that, for hard limestone strength values also increase linearly with increasing density.

It is clear from these correlations that the effect of density on the mechanical properties (uniaxial compressive stength, Brazillian tensile strength and young's modulus) and the physical properties (dry density, saturated density, water absorbtion amd saturated density) is beyond dispute.

The results of this study also demonstrated that ultrasonic velocity is sensitive to changes in density of Gaziantep limestone. The longitudinal velocity under dense conditions was always higher than the velocity under less dense conditions, in all dimensions. It can be easily said that ultrasonic velocity is not dimension dependent .

The results of this study allow us to state that the nondestructive method using ultrasound can be used to reliably evaluate the mechanical properties of limestone with structural dimensions. Hence, this nondestructive method can be employed in the classification of structural and strength properties of limestone.

6.2. Recommendations For Future Work

Furter investigation of this study is detailed correlations for obtained results. Additional to this study experiment will be performed using wet cylindrical specimens with the same orientation to see the effect of the moisture.

REFERENCES

1. Altanhan, H. (2002). *Geotechnical properties of carbonic rocks occurring in Gaziantep- Şanlıurfa region.* M.Sc.Thesis in Civil Engineering University of Gaziantep.

2. Al-Harthi, A.A., Al-Amri, R.M., Shehata,W.M. (23 March 1999) *The porosity and engineering properties of vesicular basalt in Saudi Arabia* .Department of Engineering Geology, Faculty of Earth Sciences, King Abdulaziz University, P.O. Box 1744, Jeddah 21441, Saudi Arabia.

3. Amadei B. and Robinson M. J. (1986). *Strength of rock in multiaxial loading conditions. In Proc*. 27th U.S. Symp. Rock Mech., Tuscaloosa, AL (Edited BY H. L. Hartman), pp. 47-55.

4. Atkinson R. H. and Ko H.-Y. A (1973). *Fluid cushion, multiaxial cell for testing cubical rock specimens.* Int. J. Rock Mech. Min. Sci. & Geomech. Abstr. Pp.10, 351-361.

5. Bieniawski Z. T. (1968). *Propagation of brittle fracture in rock*. In Proc. 10th U.S. Symp. Rock Mech., Austin, TX (Edited by K. E. Gray), pp. 409-427.

6. Brace W. F. and Martin R. J. (1968). *A test of the law of effective stress for crystalline rocks of low porosity.* Int. J. Rock Mech. Min. Sci.pp.5, 415-426.

7. Brown E. T. (1974). *Fracture of rock under uniform biaxial compression*. In Proc. 3rd Int. Congr. Rock Mech., Denver, Vol. 2, pp. 111-117.

8. Brown, E. T. (1981). *Rock characterization testing and monitoring* ISRM suggested methods. Royal School of Mines. Imperial College of Science and technology, London, England.

9. De Freitas, M. H. B.Sc., F.G.S. F. Blyth, G. H. Ph.D., D.I.C., F.G.S. (1979). *A Geology for Engineers.* 6th edition Formerly Reader in Engineering Geology, Imperial College of Science and Technology, London Lecturer in Engineering Geology, Imperial College of Science and Technology, London. pp. 130 – 131, 148 – 149. 171 – 173, 189 – 191.

10. Dusseault M.B., Rothenburg L. and Mraz D. Z. (1987). *The design of openings in salt rock using a multiple mechanism viscoplastic law.* Proc. 28th U.S. symp. Rock Mech., Tuscon, AZ (Edited by I. W. farmer, J.J.K. Daemen, C. S. Desai, C.E. Glass and S. P. Neuman), pp. 633-642.

11. Friedman M., Handin J.,Higgs N.G. and Lantz J. R. (1979). *Strength and ductility of four dry igneous rocks at low pressures and temperatures to partial melting*. In. Proc. 20th U.S. Symp. Rock Mech., Austin, TX, pp. 35 – 43.

12. Freidman M., Handin J. and Bauer S. J. (1982). *Deformation mechanisms in granodiorite at effective pressures to 100 MPa and temperatures to partial melting* .In Proc. 23rd U.S. Symp. Rock Mech., Berkely, CA (Edited by R. E. Goodman and F. E. Heuze), pp. 279 – 290.

13. Garg S. K. and Nur A. (1973). *Effective stress laws for fluid-saturated porous rocks.* J. Geophys. Res.pp. 78, 5911-5921.

14. Goodman R. E. (1980). *Introduction to Rock Mechanics*, pp. 478. Wiley, New York.

15. Herbert L. Brodie. (January-February 1997). *Extension Agricultural Engineer.* Biological Resources Engineering Topics bulk density measurements better compositing school greenhouse barns for dairy housing.

16. Hilsdorf H. K. (1965). *Die Bestimmung der zweiachsigen Festigkeit von Beton*. In Proc. Deutscher A+usschuss fur Stahlbeton, pp. 173.

17. Hoek, E., Marinos, P. and Benissi, M.(1998).*Applicability of the Geological Strength Index (GSI) Classification for Very Weak and Sheared Rock Masses*. The case of the Athens Schist Formation. 3034 Edgemont Boulevard, P.O.Box 75516, North Vancouver, British Columbia,Canada,V7R 4X1.

18. Hoek E. (1983). *Strength of jointed rock masses* – 23rd Rankine Lecture. Geotechnique pp.33, 187-223.

19. Housen, K. (Feb. 7-9, 2003). Effects *of Material Properties on Cratering* The Boeing Co. MS 2T-50 P.O. Box 3999 Seattle, WA 98124 *Bridging the Gap between Modeling and Observation* Lunar & Planetary Institute, Houston, TX pp.33.

20. Hudson, J. A. (Editor-in-Chief). (1993). *Comprehensive Rock Engineering.* Principles, Practice & Projects Imperial College of Science, Technology & Medicine, London, UK Volume 3 Rock Testing and Sıte Characterization Imperial College of Science, Technology & Medicine, London, UK. pp. 73, 79.

21. Hudson J. A., Brown E. T. and Fairhurst C. (1971). *Shape of the complete stress-strain curve of the rock.* In Proc. 13th U.S. Symp. Rock Mech., Urbana, IL (edited by E. J. Cording), pp. 773-795.

22. Hudson J. A., Crouch S. L. and Fairhurst C. (1972). *Soft, stiff and servo-controlled testing machines: a review with reference to rock failure*. Eng. Geol. Amsterdam pp.6, 155 – 189.

23. Hudson J. A., (Editor-in-Chief). (1993). *Comprehensive Rock Engineering.* Principles, Practice & Projects Imperial College of Science, Technology & Medicine, London, UK Volume 1 Rock Testing and Sıte Characterization Imperial College of Science, Technology & Medicine, London, UK.pp.256 - 258.

24. Jaeger J. C. and Cook N. G. W. (1976). *Fundamentals of Rock Mechanics*, 2nd edn., pp.585 Chapman and Hall, London.

25. Johnson B., Freidman M., Hopkins T. W. and Bauer S. J. (1987). *Strength and micro fracturing of Westerly granite extended wet and dry at temperatures to 800^0 and pressures to 200 MPa*. In Proc. 28th U.S.Symp. Rock Mech., Tucson, AZ (Edited by I. W. Farmer, J. J. K. Daemen, C. S. Desai, C. E. Glass and S. P. Neuman), pp. 399 – 412.

26. Kahraman S. (2001) *A correlation between P-wave velocity, number of joints and Schmidt hammer rebound number.* Faculty of Engineering and Architecture, University of Niğde, 5100 Niğde, Turkey.

27. Kantiranis N. a, Filippidis A.a, Tsirambides A. a, Christaras B. b(2005).*Thermal decomposition study of crystalline limestone using P-wave velocity.*a Department of Mineralogy–Petrology–Economic Geology, School of Geology, Aristotle University of Thessaloniki, Thessaloniki GR- 541 24, Greece. b Department of Geology, Laboratory of Engineering Geology and Hydrogeology, School of Geology, Aristotle University of Thessaloniki, GR-541 24, Greece.

28. Kayabasi A., Gökceoğlu C., Ercanoğlu M.(2002).*Estimating the deformation modulus of rock masses : a comparative study.*General Directorate of Electrical Power Researches Survey and Development Administration, Ankara, Turkey.Hacettepe University, Department of Geological Engineering, Applied Geology Division, Beytepe, Ankara 06532, Turkey.

29. Kjellman W. (1936). *Report on an apparatus for consummate investigation of the mechanical properties of soils*. In Proc. 1st Int. Conf. Soil Mech. Found. Eng., Boston, pp. 16-20.

30. Koçkar M.K., Akgün H. (2004).*Design of anchorage and assessment of the stability of openings in silty, sandy limestone a case study in Turkey.* Department of Geological Engineering, Middle East Technical University, 06531 Ankara, Turkey

31. Lama R. D. and Vutukuri V. S. (1978). *Handbook on Mechanical Properties of Rock,* Vol. 2, Trans. Tech., Berlin.

32. Lama R. D. and Vutukuri V. S. (1978). *Handbook on Mechanical Properties of Rock,* Vol. 4, Trans. Tech., Berlin.

33. Lumb, P., 1983. *Engineering properties of fresh and decomposed igneous rocks from Hong Kong.* Eng. Geol. 19,81-94.

34. Maso J. C. and Lerau J. (1980). *Mechanical behavior of Darney sandstone in biaxial compression.* Int. J. Rock Mech. Min. Sci. & Geomech. Abstr. pp.17, 109-115.

35. Nicholson D. T. (13 December 2000). *Pore properties as indicators of breakdown mechanisms ın experimentally weathered limestones.* School of Earth Sciences, University of Leeds, Leeds, LS2 9JT, UK.

36. Nicholson F. H. (15 May 2000). *Physical deterioration of sedimentary rocks subjected to experimental freeze thaw weathering.* School of Biological and Earth Sciences, Liverpool John Moores University.

37. Obert L. and Duvall W. I. (1967).Rock *Mechanics and the design of structures in Rock*, pp. 650. Wiley, Newyork .

38. Oliveira, F. G. R., Candian, M., Francieli F. Lucchette, Salgon, J.L., Sales, A.(Mar. 2005). *Moisture content effect on ultrasonic velocity in Goupia glabra.* University of São Paulo, São Carlos SP, Brazil. Department of Civil Engineering, UFSCar, Federal University of São Carlos, São Carlos - SP, Brazil.

39. Richard E. Goodman. *Introduction to Rock Mechanics.* (1989). Second Edition University of California at Berkeley. pp. 40 – 41, 61.

40. Saliya S. S., Vutukuri V. S. and Lama R. D. (1974). *Handbook on Mechanical Properties of Rocks*, Vol. 1, Trans. Tech., Berlin.

41. Serafim J. L. (1979). Influence *of interstitial water on the behavior of rock masses*. In Rock Mecchanics in Engineering Practice (Edited By K. G. Stagg and O. C. Zienkiewicz), pp. 55-97. Wiley, London.

42. Shaopeng Wu, Yongjie Xue and Wenfeng Yang. *Experimental Evaluation of Stone Matrix Asphalt Mixtures Performance Using Blast Oxygen Furnace Steel Slag as Aggregate* The Key Laboratory of Silicate Materials Science and Engineering of Ministry of Education, Wuhan University of Technology, Wuhan 430070, Hubei, P. R China.

43. Singha M.,Raob K.S.(2004).*Empirical methods to estimate the strength of jointed rock masses.* Department of Civil Engineering, Indian Institute of Technology, Roorkee, Roorkee UA 247667, India. Department of Civil Engineering, Indian Institute of Technology, Delhi, New Delhi 110016, India.

44. Stagg, K. G. and Zienkiewicz, O. C.. *Rock Mechanics in Engineering Practice.*Division of Civil Engineering, School of Engineering, University of Wales, Swansea. pp 113 – 114, 345.

45. Stowe R. L. and Ainsworth D. L. (1968). *Effect of rate of loading on strength and Young's modulus of elasticity of rock*. In. Proc. 10th U.S. Symp. Rock. Mech., Austin, TX (Edited by K. E. Gray), pp 33-34.

46. Songa I., Suha M., Wooa Y.K., Haob T. (2003).*Determination of the elastic modulus set of foliated rocks from ultrasonic velocity measurements.* Department of Geoenvironmental Science, Kongju National University, Kongju, Chungnam 314-701, South Korea. Institute of Geophysics, Chinese Academy of Science, Beijing 100101, China.

47. Sönmez H., Tuncay E., Gokceoğlu C. (2004).*Models to predict the uniaxial compressive strength and the modulus of elasticity for Ankara Agglomerate.* Department of Geological Engineering, Applied Geology Division, Hacettepe University, 06532 Beytepe-Ankara, Turkey

48. Török A. (2003). *Surface strength and mineralogy of weathering crusts on limestone buildings in Budapest.* Department of Construction Materials and Engineering Geology, Budapest University of Technology and Economics,H-1111 Budapest, Sztoczek u. 2, Hungary.

49. Vipulanandan C., Kaulgud S. (2003). *Pulse Velocity of Clay Shale and Limestone.* Center for Innovative Grouting Materials and Technology (CIGMAT) Department of Civil and Environmental Engineering University of Houston, Houston, TX 77204-4003.

50. Vutukuri V. S. and Lama R. D. (1978). *Handbook on Mechanical Properties of Rock,* Vol. 3, Trans. Tech., Berlin.

51. Weibull W. (1951).*A statistical distribution function of wide applicability*. J. Appl. Mech., pp.18, 293-297.

52. http://www.findstone.com/tilimestone.htm.(arrival date:21.05.2005)

53. http://geology.bgsu.edu/Onasch/GEOL_615/Some%20Useful%20Numbers.doc. (arrival date:04.06.2005)

54. http://mta.gov.tr.(arrived date 21.07.2005)

55. http://www.rocscience.com/hoek/pdf/Chapter 4 of Rock Engineering.pdf. (arrival date:28.05.2005)

56. http://www.usace.army.mil/inet/usace-docs/eng-manuals/em1110-2-2901/c-8.pdf (arrival date:12.06.2005)

57. http://users.ntua.gr/marinos/downloads/applicability.pdf.(arrival date:05.04.2005)